PHD

Control of cell proliferation in Saccharomyces cerevisiae.

Lord, Peter Gordon

Award date:
1982

Awarding institution:
University of Bath

CONTROL OF CELL PROLIFERATION IN SACCHAROMYCES CEREVISIAE

submitted by Peter Gordon Lord

for the degree of Ph.D.

of the University of Bath

1982

Peter G. Lord.

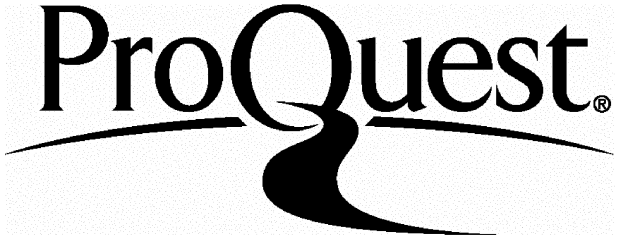

Acknowledgements

It was a pleasure to work under the supervision of Alan Wheals and I heartily thank him for his concomitant guidance and encouragement during the course of this work. I thank the SRC for financial support. I thank Peter Jewell and his assistants, even Mrs Little, for technical support. Many thanks go to Peter Green, Tim Brown, Bernie Silverman and Adrian Bowyer for advice on statistics and computing. Thanks also go to Andrea Marshall for typing this thesis. Finally, I thank the staff and students, past and present in the Microbiology department for the friendship I received during my stay at Bath.

This thesis is dedicated to my parents.

Summary

Cell size and cell cycle time data were obtained from measurements of S.cerevisiae cells growing in batch culture and from time lapse cinephotomicrography measurements of individual S.cerevisiae cells in steady state and perturbed culture conditions. The critical size hypothesis (P.A. Fantes et al. J. theor. Biol. 50: 213-244, 1975) and the transition probability hypothesis (J.A. Smith & L. Martin. Proc. Nat. Acad. Sci. [USA] 70 : 1263-1267) of control of proliferation were evaluated simultaneously with these data. It was concluded that a combination of the two hypotheses is more compatible with the data. Two models which combine the hypotheses and which provide good fits to the data are the Sloppy Size Control model (A.E. Wheals. Molec. cell Biol. in press, 1982) and the Tandem model (B. Shilo et al. Nature 267 : 648-649, 1977), although it is necessary to add to the latter that critical size has mean and variance rather than a fixed value. The difference between the parent and daughter cycle times is explained by both models as being a consequence of unequal division and the operation of a size control mechanism. However, experiments with perturbed cell cultures indicated that some of the difference in cycle times is due to a factor independent of size. Clonal growth rates were measured and shown to vary significantly within a population, suggesting heterogeneity in individual growth rates. It was concluded from the data from both steady state and perturbed cell populations that although variation in growth rates produces variation in cycle times, a probabilistic mechanism (which also produces variation in cycle times) cannot be excluded, as has been suggested (A.L. Koch, Nature 286 : 80-82, 1980).

Contents

CHAPTER ONE

Chapter 1

General Introduction

The cell cycle

A simple definition of the cell cycle is the period between successive divisions of cells undergoing vegetative growth. Howard and Pelc (1953) showed that the eukaryotic cell cycle is comprised of four distinct periods. These are: S phase, which is the DNA synthetic period; G2 phase, which is the interval between S phase and mitosis; M phase, mitosis itself; and G1 phase, which is the interval between mitosis and S phase. Cell division occurs shortly after M phase.

During the cell cycle a cell replicates its nuclear material and organelles and distributes the replicated structures so that when the cell divides, the resulting cells have an equivalent intracellular complement. Throughout most, if not all, of the cell cycle the cell grows in size. Mazia (1978) has put forward the view that the cell cycle is really a 'bicycle'. That is, the cycle has two 'wheels' which run in parallel, the growth wheel being one and the organellar replication or reproductive wheel the other.

The cell cycle as one of several developmental pathways

A cell may follow one of several developmental 'routes' apart from the cell cycle, according to the environmental conditions. The cell may enter irreversibly into a highly differentiated state, as in the case of human erythrocytes. Under starvation conditions, a cell may enter reversibly into a non-cycling state or stationary phase. A diploid cell may undergo meiosis and, depending on the cell type, sporulation. A haploid cell may conjugate with another haploid cell.

When conditions are sufficient to support vegetative growth it is beneficial to cells to maintain the balance between the rate of growth (increase in cellular size) and the rate of proliferation (increase in

cell number). Cells growing slowly but dividing with a high frequency would eventually become so small that they would be unable to contain all the necessary components (organelles etc.) for survival. Alternatively, cells whose growth rate outstrips their rate of cell division would become so large that they would face several problems. For example, with a decreasing surface area to volume ratio,a point would be reached after which the capacity of the cell envelope to transport nutrients would be insufficient to supply the demand of the cytoplasm for those materials. In addition, a limit would be reached where the cell envelope would no longer be strong enough to contain the mass of the cytoplasm, and consequently rupture. Concerning the latter point, it should be noted that temperature-sensitive cytokinesis-defective mutants of S.cerevisiae held at the restrictive temperature continue growing and eventually lyse. The balance between the rate of growth and the rate of proliferation may be achieved by a homeostatic control mechanism in which the rate of proliferation is directly coupled with the rate of growth. Alternatively, the balance may be fortuitous, the rate of cell proliferation changing in parallel to, but independent of, the rate of growth.

It is clear that control mechanisms sensitive to changes in environmental conditions exist in cells, which determine the developmental route and the rate of cell proliferation. What is not clear is how the controls operate. In this thesis I have concentrated on the control of cell proliferation.

S.cerevisiae - its usefulness for cell cycle studies

The yeast S.cerevisiae has been the subject of numerous biological studies for decades. Consequently, a great deal of the organism's biochemistry and genetics is known. It is a free-living unicellular eukaryote which is easy to grow and to manipulate. It does not require a complex set of nutritional requirements and proliferates quickly in comparison to many other eukaryotes. The budding mode of reproduction

leads to asymmetrical division, especially at slow growth rates (Hartwell & Unger 1977). After division, a bud scar, which can be stained with fluorescent dyes (Hayashibe & Katohda 1973, Streiblova & Beran 1963), remains on the parent cell. Parent cells and daughter cells can thus be distinguished using ultraviolet microscopy. The latter points make this organism useful for studying the relationship between cell size and cell division. Another point in favour of the usefulness of S.cerevisiae is the number of cell division cycle (cdc) mutants which have been isolated. These have proved very useful for studying control of, and progress through, the cell cycle. Finally, haploid cells of S.cerevisiae produce mating factors (or sex pheromones) which block cells of opposite mating type at an early stage of the cell cycle (Manney & Meade 1977). This stage of the cell cycle, termed start (Hartwell 1974) is considered to be the rate-limiting step in the cell cycle and therefore, where the control of proliferation acts (Johnston et al. 1977, Shilo et al. 1976, 1977). These factors are thus, valuable probes of cell cycle control.

S.cerevisiae - its disadvantages for cell cycle studies

Although S.cerevisiae is useful for studying the cell cycle it has some disadvantages for such studies such as the following. 1) Synchronization for more than one cycle is difficult to achieve, especially at slow growth rates because daughter cells have longer cycle times than parent cells. 2) The control step of the cycle, start, is not morphologically obvious and so cannot be monitored directly. 3) In liquid culture daughter cells remain attached, by weak bonds, to parent cells after division. This leads to the formation of clumps of cells. Mild sonication is used to disperse clumps but this manipulation can cause problems in some experiments.

The cell cycle of S.cerevisiae

A diagram of the major biochemical and morphological landmark events of the cell cycle is shown in Fig. 1 (from Hartwell and Pringle 1981).

Figure 1

A diagram of the S.cerevisiae cell cycle.

The diagram indicates some of the major landmark events and their temporal order in the cell cycle. However the distances between the events on the diagram are not proportional to the time interval between events. Abbreviations: SPBSF, spindle-pole body satellite formation; SPBD, spindle-pole body duplication; CRF, formation of the chitin ring (shown in the diagram as a heavy line at the parent-bud junction); BE, bud emergence; iDS, initiation of chromosomal DNA synthesis; DS, chromosomal DNA synthesis; SPBS, spindle-pole body separation (and formation of a complete spindle); NM, nuclear migration; mND, medial nuclear division; SE, spindle elongation; lND, late nuclear division; CK, cytokinesis; CS, cell separation; MRF, microfilament ring formation.

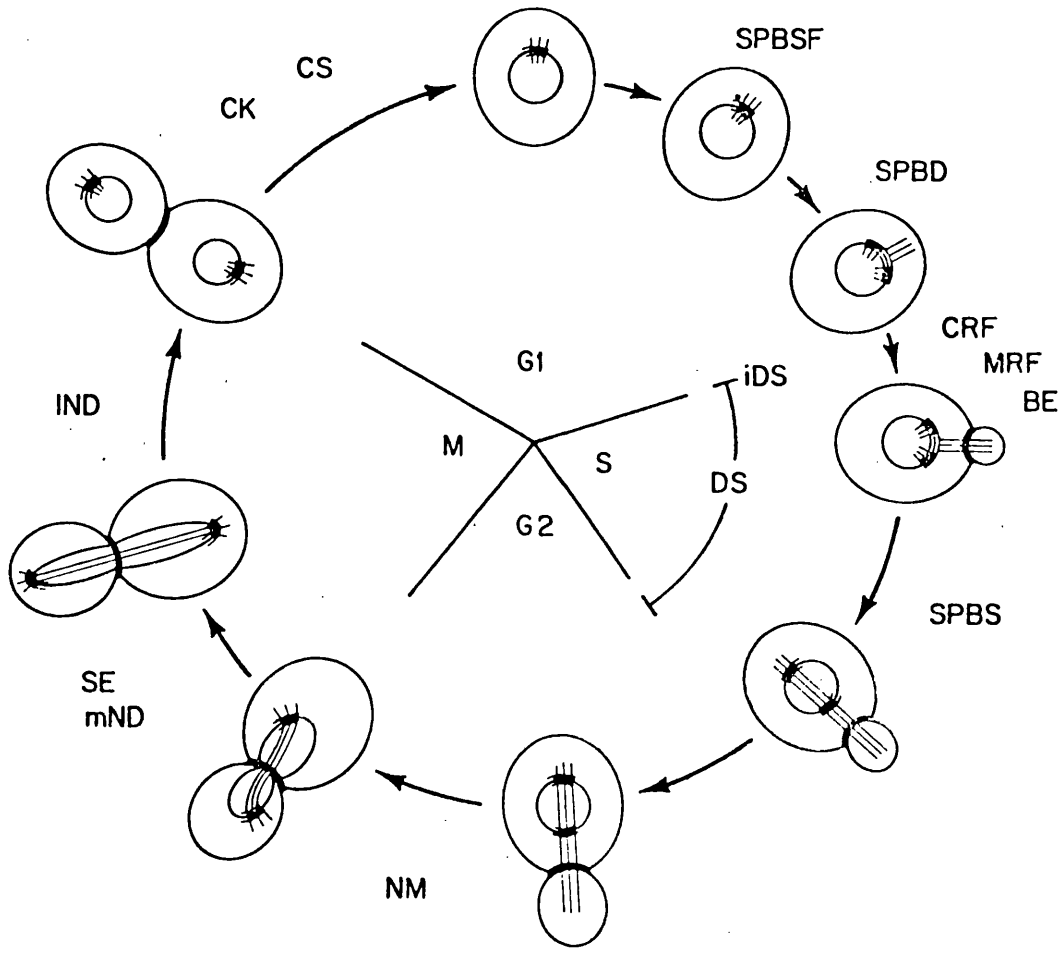
CS
CK
SPBSF
SPBD
CRF
MRF
BE
SPBS
NM
SE
mND
IND
G1
S
G2
M
iDS
DS

The relative order of the events is given but it should be noted that the distance between the events is not proportional to time. In addition, the lengths of the G1, S, G2 and M phases are not in exact proportion. Starting with a cell in the G1 phase the cycle progresses in the following way.

Towards the end of the G1 phase a small satellite structure appears on the spindle-pole body (the microtubule organizing centre in this organism) which is embedded in the nuclear envelope. Shortly afterwards the spindle-pole body duplicates and chromosomal DNA replication begins. At this time, or later, depending on the environmental conditions, a ring of chitin is deposited on the cell wall and the bud emerges from within the ring. A ring of microfilaments also appears in the cytoplasm adjacent to the cell membrane at the parent cell-bud junction (the timing of this event relative to bud emergence is unknown). The spindle-pole body and cytoplasmic microtubules emanating from it are orientated towards the bud site. This orientation may be transient but is maintained through the diagram for simplicity. During the rest of the cycle, the bud increases steadily in size. Near the end of the S phase the spindle-pole bodies separate further and the spindle is formed. Some time later the nucleus migrates to the neck between the bud and the parent cell. The nucleus and the spindle then elongate, with one half of the nucleus in the bud and the other half in the parent cell. In common with many fungi, the nuclear envelope remains intact throughout nuclear division. Finally cell membranes and a septum are produced between the bud and the parent cytoplasms (physiological separation or cytokinesis) and cell separation (physical separation of parent and daughter cells) occurs. Since there is a period of time between the end of nuclear division and cell separation, this period has been termed G1* (Barford and Hall 1976).

Cell cycle controls in S.cerevisiae

Cells in conditions supporting vegetative growth require two types of control to ensure successful mitotic cell cycles. The first type of control is over the order of cell cycle events. Clearly some events must occur in the right order to produce viable daughter cells. For example, cell division must not precede nuclear division. However, the order of some events,e.g. bud emergence relative to initiation of DNA synthesis, is not critical. The second control is over the rate of cell proliferation. Cellular growth must not outstrip cell division nor vice-versa. I will discuss the former briefly, since studies of this have revealed some clues as to how cell proliferation is controlled in S.cerevisiae, before reviewing the literature on the control of cell proliferation itself.

Cell division cycle mutants

Much of our knowledge of the cell cycle of S.cerevisiae has come from studies of cdc mutants (for reviews, see Hartwell 1974, Simchen 1978, Hartwell and Pringle 1981). A cdc mutant is defined as having a mutation which leads to defects in, or failure of, a stage-specific event of the cell cycle (Hartwell 1978). Most of the cdc mutants so far isolated are temperature sensitive.

cdc mutants are classified according to: i) their diagnostic landmark (the first landmark that is blocked); ii) their terminal phenotype (the characteristic morphology attained by most of the mutant cells after prolonged incubation at the restrictive temperature) and iii) whether or not the cells exhibit first cycle arrest after a shift to the restrictive temperature. When cdc mutants showing first cycle arrest are shifted to the restrictive temperature, those cells which are at a stage before the execution point for the particular mutation arrest in the first cycle, and those cells beyond the execution point complete

that cycle and arrest in the next cycle.

Maintenance of the order of cell cycle events

The relative order of events can be achieved in two ways: i) a central timer may sequentially trigger events at appropriate intervals; or ii) there may be functional interrelationships between events such that when, say, event A is completed, event B can begin. From extensive studies using most of the known cdc mutants and stage-specific inhibitors of the cell cycle, enough evidence has been found for functional interrelationships to suggest that it is these which mainly determine the relative order of events (Hartwell & Pringle 1981).

Three types of relationship between events have been found. First there are dependent relationships where one event cannot occur unless another event is completed. An example is the dependency of the CDC 7 step on the CDC 4 step (Hereford & Hartwell 1974). Second there are independent events such as bud emergence and initiation of DNA synthesis since one can occur when the other is blocked. Third there are interdependent events where neither of two (or more) events can occur when either one is blocked. For example, the mating factor-sensitive step is known to be interdependent with the CDC 28 step from reciprocal shift experiments (Hereford and Hartwell 1974).

A picture of the circuitry of the cell cycle (known as a functional sequence map) can be built up from this information. The original functional sequence map published by Hartwell (1974) is shown in Fig. 2. As a result of further studies a much more complicated picture has emerged (Hartwell & Pringle 1981). There now appears to be several parallel, sometimes interbranching, dependent sequences which emanate from a point after the initial complex of events and converge prior to cytokinesis. One important feature of the original map is retained in the updated version. This is the dependence of each parallel sequence on the completion of the mating factor-sensitive/CDC 28 step. This step has

Figure 2

Dependent pathways of events in the *S.cerevisiae* cell cycle.

A functional sequence map of several major landmark events and events defined by *cdc* mutants (after Hartwell *et al.* 1974). Abbreviations as in Fig. 1.

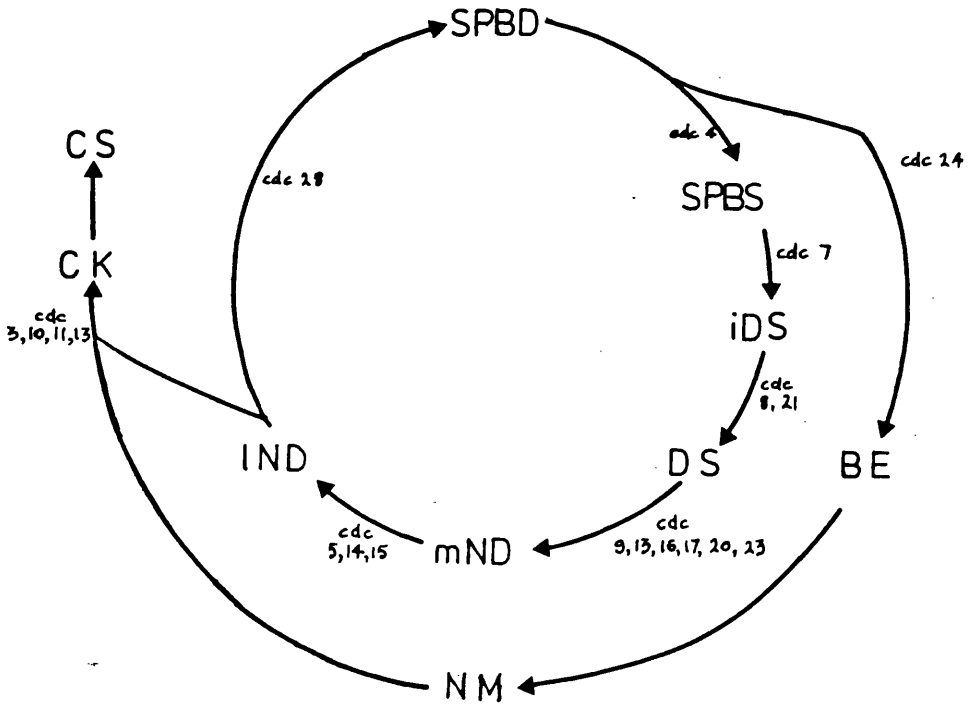
SPBD
cdc 4
SPBS
cdc 7
iDS
cdc 8, 21
DS
cdc 9, 13, 16, 17, 20, 23
mND
cdc 5, 14, 15
IND
cdc 28
CK
cdc 3, 10, 11, 13
CS
cdc 24
BE
NM

been termed start (Hartwell, 1974).

Definition of start

The term has been given to the point, in G1, whose completion commits the cell to a mitotic division (Hartwell, 1974). All the known events of the cell cycle are dependent on the prior occurrence of the start event(s).

Start as a point of control

A great deal of evidence indicates that start is a unique point of control in the cell cycle. First, when cells are deprived of nutrients they arrest uniformly prior to start (Johnston et al. 1977, Lillie & Pringle 1980, Sumrada & Cooper 1978). Second, only (haploid) cells at or before start can undergo conjugation. The only cdc mutants able to conjugate at the restrictive temperature are start mutants (Reid & Hartwell 1977, Reed 1980). In addition, mating pheromones which synchronize the cell cycles of conjugating cells specifically arrest cells at or before start (Hereford & Hartwell 1974, Wilkinson & Pringle 1974, Byers & Goetsch 1975). Finally, when the population doubling time is increased by nutrient limitation,the time from birth to start increases much more than does the time from start to division (Jagadish & Carter 1977).

Thus the completion or non-completion of start, determines whether a cell undergoes a mitotic cell cycle or some other developmental route. When there is a change to starvation conditions cells prior to start enter a stationary state and cells undergoing the mitotic cycle proceed to division and then enter a stationary state. Similarly, cells will only embark on the conjugation pathway once mitotic cycles in progress are completed and further cycles are prevented by the inhibition of start by mating factors. There is, however, an exception to this rule, since cdc 4 mutants arrested at the restrictive temperature can undergo meiosis when shifted to the permissive temperature in sporulation medium whereas

cdc mutants blocked after the CDC 4 step complete mitosis first (Hirschberg & Simchen 1977). The CDC 4 step is thus the commitment point for mitosis. This is not too surprising since CDC gene products are involved in the meiotic pathway (Simchen 1974). Start may be better thought of as a point of commitment to division-orientated events, the latter being either mitotic or meiotic.

Control of the cell cycle via start is further exemplified by the finding that the interval between start and division varies only slightly with growth rate (Jagadish & Carter 1977). This implies that the rate of cell proliferation is governed primarily by the rate of completion of start and that progress through the sequences of events from start to division is not rate-limiting for cell proliferation. However, there is conflicting evidence on this point. The variation in the time from start to division with growth rate has been determined by two other groups of workers by calculating the αfactor execution point at different growth rates. Hartwell and Unger (1977) found, as did Jagadish and Carter (1977), that the start to division period was relatively invariant with growth rate. Whereas Rivin & Fangman (1980) found quite considerable variation in the start to division period with respect to growth rate. Different strains, temperatures and methods of growth rate modulation were used in each of these studies, which could account for the differences in the relative contribution of the rate of traverse of start and the rate of progress through cell cycle events in determining the actual rate of proliferation. Nevertheless, most of the evidence in the literature is in favour of control of cell proliferation via start.

How could start be triggered?

A feature of several current models of cell division control is that the rate of completion of a specific event determines the rate of cell division. The hypothesis of a specific 'control' step has gained much support and is applicable to a variety of cell types (Donachie 1968,

Edmunds & Adams 1981, Fantes 1977, Hartwell 1974, Smith & Martin 1973, Sudbery & Grant 1975). Models which can explain how the control step is triggered can be divided into three categories: i) deterministic models in which the event is triggered by the cell attaining a critical size; ii) stochastic models; and iii) other models.

Critical size models

The essence of a critical size model is that when a cell grows to a certain size the programme of events leading to cell division is initiated. In this case the rate of cell proliferation is determined by the rate at which cells grow to the critical size. A major implication of this model is that in conditions of balanced growth the events of the cell cycle should be more dependendent on cell size than on cell age (the time from 'birth' of a cell). Schaechter et al. (1962) showed that for E.coli the coefficient of variation of cell age at division is approximately twice that of cell length (their measure of size). Other data for E.coli also support the hypothesis (Koch 1977).

The possible ways in which cells 'realize' when they have reached a critical cell size are easily conceived. Donachie (1968) has suggested that a substance produced at a rate proportional to the rate of cell mass increase reaches a critical concentration which triggers cell division cycle events (this is called 'the activator-accumulation' model). Some of the substance is removed in the initiation process thus reducing its concentration. Another round of division events takes place after further mass increase brings the concentration of the substance up to the critical level. Another simple hypothesis was proposed by Pritchard et al. (1969). In their, 'inhibitor-dilution' model, they suggested that at division a quantity of an inhibitory substance is produced. Cell division events are initiated when sufficient cellular growth has occurred to dilute the inhibitor to below a threshold concentration.

The predictions of several size-titration models (including the two above) were rigorously tested by Fantes et al. (1975) using available data. They found that the data were most consistent with what they called the 'unstable inhibitor model'. Unlike the inhibitor in the inhibitor-dilution model the unstable inhibitor is produced continuously, its rate of production being proportional to the number of genome equivalents in the cell. It is unstable, its rate of degradation being proportional to its amount. A further assumption is that there is a rapid turnover of this substance, to ensure a quick response to change. In balanced growth conditions the amount of inhibitor is maintained proportional to the number of genome equivalents. When its concentration drops (due to an increase in cell size) below a critical value, division events are triggered.

Stochastic models

A much quoted example is the stochastic model proposed by Smith & Martin (1973). Their idea is that the cell cycle is comprised of two parts (Fig. 3A). The A state is an indeterminate period from which cells enter an invariant B phase at random but with first order kinetics. Once B phase has been completed cells re-enter the A state. The probability per unit time of exit from the A state (or the 'transition probability') is set by the environmental conditions. The A state occurs in G1 phase. The B phase covers S, G2 and M phases plus the parts of G1 not taken up by the A state. In support of this hypothesis, Smith and Martin took published data on distributions of cycle times in exponentially growing populations of cells and presented the data as α plots. An α plot is constructed by plotting the proportion of cells with a cycle time less than t, on a logarithmic scale, against t, on a linear scale. An ideal α plot is shown in Fig. 3B. The initial plateau represents the B phase. The downward line reflects the distribution of times spent in

Figure 3

Diagram of the cell cycle according to the Transition Probability hypothesis and an 'ideal' $\propto$ plot.

A - in terms of the Transition Probability hypothesis (Smith & Martin 1973) the cell cycle is divided into two major parts, the A state (which is of variable duration) and the B phase (which is of relatively constant duration).

B - an ideal $\propto$ plot (the percentage of cells which are undivided, on a logarithmic scale, versus time) assuming no variance in the duration of the B phase and a constant probability, per unit time, of exit from the A state.

A

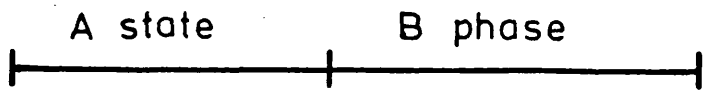

B

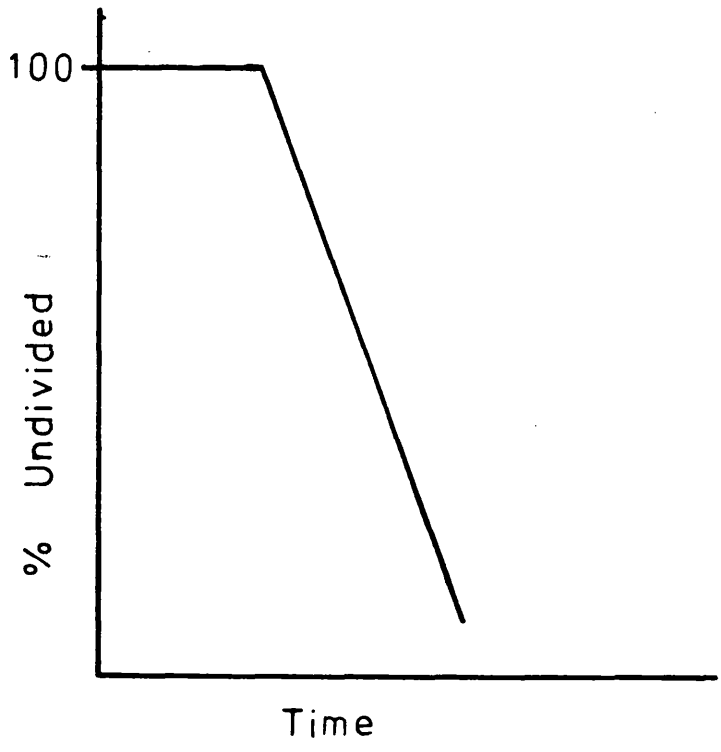

the A state. The slope of the line gives the transition probability. α plots of the data approximated in shape to that expected.

Another stochastic model is that of Klevecz (1976). He proposed a quantal subcycle, G_q, of 3-4 hours duration which integrates to the determinate S+G2+M programme at a point, i. A cell can go through an indefinite number of G_q cycles and in this sense the exit from G_q is probabilistic. His evidence in support of this hypothesis was that the distributions of cycle times he observed in asynchronous cultures were not continuous but quantized in multiples of 3 to 4 hours.

Other models

Some hold the view that oscillatory systems or biological clocks (timing mechanisms) control the cell cycle. Two biochemical oscillators have been hypothesized to explain the mitotic synchrony observed in the syncytial plasmodia of Physarum polycephalum. Sachsenmaier et al. (1972) have proposed a discontinuous relaxation oscillator in which mitotic initiator molecules (or mitogens) form continuously and proportionately to plasmodial mass increase. The molecules are 'counted' by combining stoichiometrically with a number of nuclear receptor sites. At a critical ratio of initiator to nuclei, mitosis occurs, the number of receptor sites doubles and the clock is reset. An alternative model was suggested by Kauffman and Wille (1975). In this model the mechanism is a continuous limit cycle oscillator, in which two or more interacting components fluctuate autonomously. When one of these reaches a threshold level mitosis is triggered. The difference between the two hypotheses is that in the former, mitotic events are essential components of the oscillator system, whereas in the latter, the oscillator functions independently.

Two further models I will mention both suggest that the timing of division of a cell depends on that cell's metabolic rate. Kubitschek

(1971) proposed that cells have a linear rate of growth (increase in cell size) which is determined by the number of activated (nutrient) transport sites in the cell envelope. New sites are activated near to or at division, the number of sites doubling on average. The number of sites activated at division increases with the surface area synthesized during the cycle. His evidence for this was that the generation rates (reciprocals of cycle times) for several cell types were approximately normally distributed. It is not clear in this hypothesis what triggers cell cycle events. In view of the evidence (Cooper & Helmstetter 1968, Jagadish & Carter 1977) it is unlikely that the rate of progress through cell cycle events is directly determined by the growth rate of a cell. A triggering event such as attainment of a critical size could be incorporated into the model but in this case only the reciprocals of the time prior to the triggering event would be expected to be normally distributed. Implicit in the model of Castor (1980) is that the times spent in G1 have a reciprocal-normal distribution and the sums of the times spent in S, G2 and M phases are normally distributed. In this, G1 rate model, constitutive differences amongst cells (thought to be due to variations in their protein-synthetic capacity) in a population lead to variation in the time required to complete an essential (triggering) event in G1 of the cycle. This is similar to Kubitschek's hypothesis but with the inclusion of a triggering event. However, Kubitschek's hypothesis is firmly based on the idea of linear rates of cellular growth, whereas Castor's is not.

How is start triggered?

As discussed above there are several hypothetical ways in which start may be triggered. One approach to the question of what triggers start is to ask which of the current models best explains control of cell proliferation in S.cerevisiae? The approach used in the past has been to select a model and then look for evidence for it. Most of the

experiments used were such that the results could only indicate whether or not the chosen model was applicable. For instance, those who sought evidence for the critical size hypothesis found evidence in its favour (Johnston et al. 1977) and those who sought evidence for the transition probability hypothesis produced evidence in favour of this model (Shilo et al. 1976).

Evidence for the critical size hypothesis

Implicit in a critical size hypothesis is that cellular growth rather than progress through cell division cycle events is rate limiting for cell proliferation. In addition, growth should not be dependent on completion of cell cycle events but at least one event should be dependent on growth.

That growth is not dependent on cell cycle events is evident from several observations. Cellular growth continues when stage-specific cell cycle events are blocked by mating factor (Throm & Duntze 1970, Wilkinson & Pringle 1974), hydroxyurea (Slater 1973) and trenimon (Jaenicke et al. 1970). When cdc mutants are shifted to the restrictive temperature all but the class II start mutants continue growth after cessation of cell division (Johnston et al. 1977, Reed 1980). The latter mutants arrest as unbudded, uninucleate cells whose spindle pole bodies do not bear satellites (B. Byers cited in Johnston et al. 1977) as do cells arrested by starvation (Byers & Goetsch 1975). The primary defect event of these mutants may therefore be in some aspect of growth and as a consequence of this, they arrest prior to start.

It is likely that most cell cycle events can be completed in the absence of growth, since cells deprived of nutrients arrest uniformly in G1 (Johnston et al. 1977). Furthermore, when a population of cells undergoing cell cycle events is selected and resuspended in starvation medium, the cells complete those events without continued growth (Johnston et al. 1977). However, growth may be required for early events. Johnston

et al. (1977) found evidence for this in two ways. Firstly, they showed that when stationary phase cells (99.5% unbudded) were plated onto rich agar medium there was a correlation between the initial size of each cell and the length of time each took to produce a bud. Secondly, they took, for each of four cdc mutants (defective in early events),a population enriched in small, unbudded, nitrogen-starved cells and incubated them in fresh, rich medium at the permissive temperature. They then took samples immediately after resuspension and at intervals (until four hours after resuspension) and plated them on rich agar medium at 36°C. They found that only those cells above a certain size at the time of the shift had completed the early CDC events.

The above experiments suggest that at least cells emerging from stationary phase need to attain a certain size before embarking on cell cycle events. Since start is the earliest event of the cell cycle, and all other events are dependent on its completion, it is likely that the attainment of this size is required only for start.

Is there any evidence for a size control in exponentially growing cells? The potential existence of a size control is evident to the following collection of observations on exponentially growing S.cerevisiae cells. 1) They divide asymmetrically, the parent cell always being larger than the daughter cell at division at all growth rates measured (Beran et al. 1966, Burns 1956, Hartwell & Unger 1977, Kubitschek & Cassle 1966). 2) The difference between the size of daughter cells and the size of parent cells increases as the growth rate decreases (Hartwell & Unger 1977). 3) The unbudded period of daughter cells is longer than that of parent cells and the difference increases with decreasing growth rate (Hartwell & Unger 1977, Carter & Jagadish 1978). 4) Daughter cells increase to a size approaching the size of parent cells before producing a bud (Adams 1977). Evidence that growth is normally rate-limiting for cell proliferation is also provided by observation 1) and the observation that the size of the parent cell portion of the budded cell increases only slightly

during budding (Johnson 1965, Hartwell & Unger 1977) because they imply that parent cells can progress through cell cycle events faster than they can double their size.

Hartwell and Unger (1977) derived the function for the age distribution (the distribution of the frequency of cells at different stages of the cell cycle at any time in an asynchronous culture during exponential growth) for unequally dividing cells based on the findings of Johnston et al.(1977). They obtained mean values for the daughter cycle time (D), and the parent cycle time (P) and the value of the population doubling time (τ) from time lapse photographs of exponentially growing cells. They found good agreement between the observed value of τ and the predicted value using their values of D and P and the equation they derived relating the three parameters. However, a further examination of their model revealed that it could not yield a balanced steady state between cellular growth and cell division. As they suggested, this can be seen in the following way. After division, a daughter cell (call this cell, C1) will attain a mass, m_p, P time units from its subsequent division. The daughter cell (call this cell, C2) produced from this cell's division should attain the same mass, m_p, when it is P time units from its subsequent division. Assuming that cellular mass increases exponentially (for which there is evidence [Elliot & McLaughlin 1978]), that the mass doubling time is equal to the population doubling time, and using their experimentally determined values of D, P and B (the budded period), they found that the value of m_p for cell C2 will be the same as the value of m_p for cell C1 only if all the mass accumulated by cell C1 between time P and division is distributed to its daughter cell C2 at division. This is clearly not consistent with the observation that parent cells increase in volume from one generation to the next (Hartwell & Unger 1977, Lieblova et al. 1964, Mortimer & Johnston 1959) unless, of course, parent cells become progressively less dense in successive generations, Nevertheless,

the Hartwell and Unger age distribution can be used successfully to deduce qualitative properties of the size control (Tyson et al, 1979).

The difference between the sizes of parent and daughter cells at division correlates with the difference between the unbudded periods of parent and daughter cells (see 2 and 3 above). So, much of the daughter cycle time is spent prior to bud emergence (and presumably start). This part of the daughter cycle time could be due to a period of growth required to bring the daughter cell to a critical size or it could be due to the occurrence of necessary G1-specific events. These G1 events would either be completed much more rapidly by parent cells or they may be unnecessary for a successful parent cycle. The idea that most of the unbudded period of daughter cells occurs to fulfil a growth requirement is supported by Singer and Johnston (1981). They grew S.cerevisiae cells in the presence of low concentrations of hydroxyurea in order to lengthen S phase, and consequently the budded period. They found that, as a result of the lengthened budded period, the daughter cells were approximately equal in size to parent cells and that the pre-start part of G1 was reduced. Although they did not determine it directly, this implies that the G1 phase prior to start in daughter cells was reduced because they were born at around about the critical size and thus did not require a period of growth prior to start.

If there is a size control it is reasonable to expect that a mutation in a gene whose product is part of the size-measuring mechanism will lead to the mutated cells' initiating cell cycle events at the same rate as wild type cells, but at a different cell size. For example, if the gene product is an inhibitor then a lesion the gene could yield a less active form of the inhibitor. As a consequence the mutant cells would initiate cell cycle events at a smaller size. Alternatively, if the gene product is an activator then the mutated cells would initiate (or fail to initiate) cell cycle events at a larger size due to the

production of a less active form of activator.

Several small size mutants of Schizosaccharomyces pombe have been isolated and subjected to considerable study. This yeast has a size control which operates in G2, over mitosis (Fantes & Nurse 1977) although work on the small size mutants has revealed a normally cryptic size control in G1 over entry into S phase (Nurse & Thuriaux 1977). Two wee genes have been identified. WEE 1 is thought to produce an inhibitor and WEE 2 (now called CDC 2-1w) is thought to produce a positive control element (Nurse 1977, Nurse & Thuriaux 1980).

Recently, small size mutants of S.cerevisiae have been isolated. whi 1 cells initiate bud emergence at approximately half the size at which the wild type cells do. whi 2 cells continue budding when nutrients are depleted, i.e. in the absence of growth, and consequently produce smaller than normal cells (Sudbery et al. 1980). The isolation procedure for whi 1 cells is interesting because it relies on there being a size control over the α factor-sensitive start event (Carter & Sudbery 1980). The whi 1 mutants originally isolated also had a reduced growth rate but from repeated crossings, whi 1 strains have been derived bearing only the small size phenotype (P.E. Sudbery, personal communication). So the phenotype is not due to a defect in the growth maintaining processes.

Therefore, there is also genetical evidence for a size control. Furthermore, the method used to isolate whi mutants (Carter & Sudbery 1980) indicates that the size control acts over start.

Evidence for a probabilistic traverse of start

One virtue of the transition probability hypothesis (Smith & Martin 1973) is that it can account for the variability of cycle times within an exponentially growing population of cells. This is not as easily accounted for by deterministic models. Since start appears to be the prime rate-determining step in the S.cerevisiae cell cycle a probabilistic control if existent in the organism could operate at start.

To pursue this idea, Shilo et al.(1976) sought evidence that traverse of start shows first order kinetics. They blocked (a) cells carrying a start mutation (cdc 25) at start by incubating them either at the restrictive temperature or in the presence of α factor at the permissive temperature. The kinetics of budding after release from the block was asynchronous and approximately first order. In contrast cells blocked at a stage soon after start, (namely the CDC 24 step) resumed budding,on release, with a high degree of synchrony. These latter cells formed their second buds asynchronously and with similar kinetics as the first buddings, on release, of the start-arrested cells. These results are consistent with a probabilistic traverse of start as long as it is valid to assume that bud emergence occurs shortly after start. The assumption does appear to be valid since the execution point of α factor has been shown to be close to bud emergence in cells grown under similar conditions (Hartwell & Unger 1977, Jagadish & Carter 1977).

To be certain that the rate of bud initiation was simply a consequence of the rate of traverse of start, Shilo et al.(1976) also used a slightly different approach. After releasing cells from a block at start they took samples at intervals and returned each to the restrictive conditions. The rationale behind this was that only those cells which had traversed start by the time of sampling would produce buds after transfer to the restrictive conditions. The kinetics of start traverse as determined in this way were similar to the kinetics of budding following release from start arrest.

Similar experiments using different start mutants (Shilo et al. 1977) and α factor (Samokhin et al. 1981, Shilo et al. 1977) produced similar results and conclusions.

Shilo et al. (1977) also obtained evidence for a probabilistic traverse of start in exponentially growing populations. They plated cells from an exponentially growing population and followed the kinetics of

bud emergence of those cells which were unbudded at the time of plating. They found that the kinetics of budding of these cells was approximately the same as the kinetics of budding of cells released from α factor arrest.

Evidence for other models

Few, if any, attempts have been made to evaluate other models with respect to S.cerevisiae. The type of experiments used to test 'oscillator' models applied to Physarum polycephalum (i.e. fusion of cells at different cell cycle phases [Tyson & Sachsenmaier 1978]) are virtually impossible to perform with S.cerevisiae without introducing perturbations which would make the results difficult to interpret. Until unambiguous tests of these models can be developed for application to S.cerevisiae, their relative merits cannot be determined in this organism.

Kubitschek's (1971) hypothesis is firmly based on the concept of linear cellular growth rate. However, Elliot and McLaughlin (1978) have shown that most macromolecular components are synthesized exponentially throughout the cell cycle so it is likely that cellular growth rate is exponential. There are no data in the literature on S.cerevisiae with which to evaluate the G1 rate model of Castor (1980). Techniques are not available to measure the lengths of G1, S, and G2 and M in individual cells. However, differences in cellular growth rate between individual cells should be taken into consideration when evaluating models in which growth rate is rate-limiting for cell proliferation.

The aims of the work in this thesis.

Of all the models mentioned in the above sections only the critical size hypothesis and the transition probability hypothesis have received significant consideration in studies of the S.cerevisiae cell cycle. This may be due to bias on the part of the investigators. More likely, it is because they can be more readily evaluated with S.cerevisiae. As outlined

above, there is considerable support for the critical size hypothesis and somewhat less, but by no means insignificant, support for the transition probability hypothesis when applied to this organism. The possibility exists that both kinds of mechanism are operative in this yeast. The experiments on S.cerevisiae reported in the literature in support of these models have not provided data with which to simultaniously evaluate the models. The aim of this work was to collect such data, from populations and from individual cells within populations (in steady-state and perturbed culture conditions), and to see how far the current models of cell proliferation in S.cerevisae are compatible with these data.

CHAPTER TWO

Chapter 2

General Materials and Methods

Strains

The following haploid strains of *S.cerevisiae* were used. S288C/1 is a clonal isolate from the stock strain S288C (α) obtained from C.F. Roberts, University of Leicester. A364A (a, ade 1, ade 2, ura 1, tyr 1, his 7, lys 2, gal 1) was provided by L H. Hartwell, University of Washington. S67.3a (a, lys 2, whi 1) and its immediate parent SA (α, lys 2) were obtained from P.E. Sudbery, University of Sheffield. The strains were maintained on YEP Glucose agar (supplemented with adenine for A364A and lysine for S67.3a and SA) slopes and plates stored at $4^{o}C$.

Media

Liquid media. YEPC (where C is the carbon source) contained 20 g carbon source, 20 g bacteriological peptone, 10 g yeast extract and 1 litre distilled water. If supplements (e.g. adenine) were required the distilled water was replaced by 0.05 mg/litre solutions of these. EMMC (C is the carbon source) contained 5 g NH_4Cl, 300 mg NaH_2PO_4, 1 g sodium acetate, 1 g KCl, 500 mg $MgCl_2$, 100 mg Na_2SO_4, 100 mg $CaCl_2$, 10 mg inositol, 10 mg nicotinic acid, 1 mg calcium pantothenate, 1 mg citric acid, 500 ng boric acid, 400 ng $MnSO_4.H_2O$, 400 ng $ZnSO_4.7H_2O$, 200 ng $FeSO_4.7H_2O$, 100 ng Na_2MoO_2, 40 ng $CuSO_4.5H_2O$, 10 ng biotin, 20 g carbon source, in litre distilled water. Both media were sterilized by autoclaving at 15 p.s.i. for 15 min. except the vitamin component of EMMC which was filter sterilized. If necessary, the media were filtered through membrane filters (Oxoid Nuflow N50/45) prior to autoclaving to render them particle-free.

Solid media. YEPD agar was used for slopes and plates. This contains 20 g glucose, 20 g bacteriological peptone, 10 g yeast extract, 20 g agar

and 1 litre distilled water (or 0.05 mg/litre supplement solution as required). Cells were grown on YEPC-PVP agar for time-lapse cinemicrography experiments. This agar contains 30 g carbon source, 30 g bacteriological peptone, 15 g yeast extract, 70 g purified agar, 280-300 g polyvinylpyrrolidone (PVP-40, Sigma) and 1 litre of a 0.05 mg/ml solution of adenine (for A364A) or lysine (for S67.3a and SA). All media were autoclaved at 15 p.s.i. for 15 min.

Powell Chamber media. As for YEPC-PVP solid media but without agar.

Cell counts and volume determination

Samples were fixed by mixing 1 volume sample to 4 volumes of filtered saline-formaldehyde solution (9% NaCl and 4% formaldehyde) and sonicated for 15 s with an MSE 100w ultrasonic disintegrator to separate clumps and divided cells. Cell counts and volume determination were obtained with an Electrozone/Celloscope model 111TS (Particle Data Inc.) using a 60 µm orifice tube at cell densities low enough to avoid coincident counting. Cell volume distributions were obtained using a Nuclear Data 1100 analyser coupled to a Hewlett-Packard X-Y plotter and median cell volumes were obtained from the distributions. The machines were calibrated for volume using 5.7 µm diameter latex balls (Dow Chemical Co.).

Bud scar analysis

Cell suspensions were concentrated by collection on a membrane filter (Oxoid Nuflow 25/45 UP) after which they were resuspended in 0.5 ml of medium. The suspensions were stained with a 2 mg/ml solution of calcofluor (a gift from J. Peberdy, University of Nottingham). Stained cells were observed at 1250 x magnification, using incident UV light on a Leitz Orthoplan microscope. At least 1000 cells were scored from each sample. The number of cells in each of the following categrories was determined: 1) unbudded cells with n bud scars and 2) budded cells with n bud scars, where n took a value from 0 to 17 inclusive.

The method of maximum likelihood was used to estimate from the bud scar analysis data: D, the daughter cycle time; P, the parent cycle time; and B, the length of the budded period. This method uses all the data to estimate the parameters unlike for the estimations using equations A6, A7 and A5 (Appendix) which use only parts of the data. Maximum likelihood estimates of the parameters were obtained from the data by the numerical maximisation of equation A8 (Appendix) using a Fortran program (available from A.E. Wheals, University of Bath). Input for the program comprised: rough estimates of $\frac{P}{\gamma}$ (from equation A7) and $\frac{B}{\gamma}$ (from equation A5) to initiate the program; the number of unbudded daughter cells; the number of unbudded parent cells; the number of budded cells; and the total number of bud scars. The estimates, D', P' and B' obtained by this method are dimensionless. D, P and B were calculated by multiplying D', P' and B' respectively by γ. Maximum likelihood estimation is optimal when D, P and B are of fixed duration. In fact, these parameters are variable (see Chapter 4). However, it is valid to use this method as long as $e^{-\alpha P}$, $e^{-\alpha D}$ and $e^{-\alpha B}$ are normally distributed.

Time-lapse cinephotomicrography

All equipment was situated in a temperature-controlled room. The microscope was a Wild M20 fitted with a long working distance phase condenser. The camera was a Bolex H16 5BM controlled by a Bolex/Wild Variotimer timing system. An electromagnetic shutter, operated by the timer unit, was fitted beneath the condenser, so that cells were not continuously exposed to light. Films were taken at a rate of 1 frame/min on Eastman Ektachrome Commercial 7252 16 mm film. Filming was stopped after all second-generation daughter cells had divided. Films were developed and selected sequences copied by Universal Films Ltd.

Heated slide

The heated slide was made of aluminium with a glass-bottomed well in

the centre for agar. The slide was heated electrically and the temperature maintained by a thermistor regulator. Molten agar (50°C) was added to the well, a coverslip was then placed on top to proved a flat surface, and allowed to solidify. Cells had to be growing exponentially to yield data appropriate for the analysis (Powell 1955). This was achieved by growing cells for several generations prior to filming, at the appropriate temperature, on a slab of agar (under a coverslip) on a microscope slide. Cells were transferred from this to the heated slide with a bent Pasteur pipette. A coverslip was then placed over the cells and secured onto the heated slide with wax (along two sides only, allowing aeration). A suitable field of cells near to the edge of the agar (to ensure adequate aeration) was chosen and filming begun.

Powell Chamber

A detailed description of this is given in Powell (1956). In this, cells are grown on a stretched piece of cellophane and liquid medium is passed underneath. The chamber was set up in the following manner. The cellophane (Cuprophan 150 PM, 11.5 μm thick, Medicell International Ltd.) and its supporting PVC washers were sterilized by soaking them for 10 min in 70% ethanol and then soaked for 5 min. in sterile distilled water. The cellophane was placed in position between the washers on the chamber, the top was screwed on and the vacuum (provided by an electric vacuum pump) applied. Sterile distilled water was pumped (using an LKB Vario-perpex pump) through slowly for c. 30 min. to leach out plasticisers in the cellophane. After that, medium was pumped through at the maximum flow rate. A small drop of cell suspension was placed on the cellophane surface which was then made concave by tightly squeezing the outlet tube and a coverslip placed on top of the cellophane. The pressure on the outlet tube was slowly released. The latter operations ensured firm, even contact between the cellophane and the coverslip. Once the coverslip was

in place the flow rate was reduced to 4 ml/hour. Cells were grown for several generations to ensure that they were growing exponentially, then redistributed prior to filming. Redistribution was accomplished by introducing a small amount of liquid medium underneath the coverslip and then twice raising and lowering the coverslip. The latter was acheived by setting the flow rate to maximum and applying then releasing pressure (by squeezing) on the outlet tube. The coverslip was held in place with forceps to prevent it from falling off. After redistributing the cells, the flow rate was reduced to 4 ml/hour.

Analysis of films

Unless otherwise stated the films were analysed in the following way. Films were projected onto a screen from a Specto MKIII motion analysis projector. All clones in focus and which could be unambiguously scored were followed. The timing of events was scored from the first division of the original cell in each clone. This (the parent) cell was followed for 2 cycles and its first 2 daughter cells were each followed for one cycle, giving 2 parent and 2 daughter cycles for each clone (see Fig. 4). The events scored were: 1) bud emergence; 2) nuclear migration, the time when the nucleus first appeared at the bud isthmus; 3) nuclear division, when the nucleus clearly separated into two; 4) onset of cytokinesis, the time of the appearance of a dark band between the cell and its bud; 5) cell separation, seen as a slight movement of the bud and/or a diminution of the dark band. The volumes of cells at bud emergence and at cell separation were calculated from the lengths of the major (a) and minor (b) axes using the formula for a prolate spheroid of revolution; volume = $(\pi/6).a.b^2$. The population doubling time (τ) was calculated from the semi-logarithmic plot of cell number versus the time from the start of the film. The volume of all cells was measured at intervals to construct a semi-logarithmic plot of total cell volume versus time, to obtain the

Figure 4

The genealogical relationship of cells, used in the analysis of time-lapse films.

The vertical lines represent cell separation. The horizontal lines represent inter-division cycles. P is the parent (original) cell. p_1 and p_2 are the parent cell's first two cycles after time zero. A, B and C are the first three daughter cells of the parent cell, produced after time zero. a and b are the cycles of daughter cells A and B respectively. AA and BA are the daughter cells produced by cells A and B respectively. The size of all these cells was measured at cell separation as was the size at bud emergence of cells P (during p_1 and p_2), A and B.

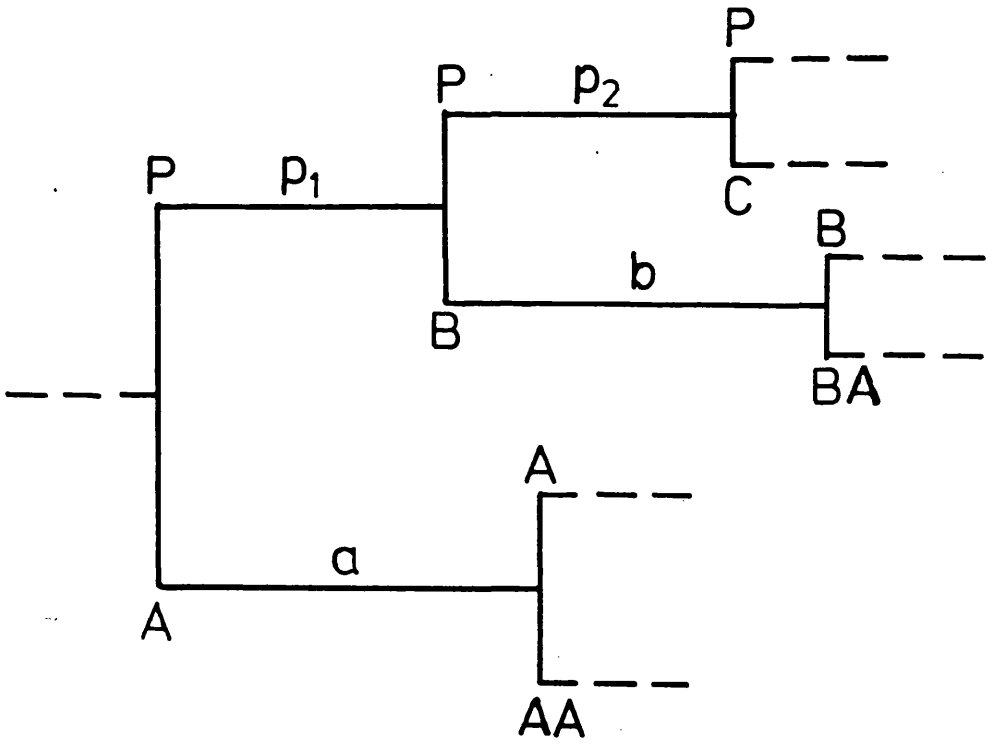
P
P
p_2
P
p_1
C
B
b
B
BA
A
a
A
AA

population volume doubling time (τ_v).

Accuracy of measurements from films

The cycle time of a cell chosen at random was measured on 10 separate occasions and the standard error of measurement found to be 0.66 min. The standard error of measurement for volume was 0.72 μm^3 and was calculated from 10 separate measurements of a randomly chosen cell.

Miscellaneous chemicals

Hydroxyurea was obtained from Sigma. Synthetic α-factor was obtained from The Peptide Institute, Japan.

CHAPTER THREE

Chapter 3

The genealogical age structure of S.cerevisiae cell populations at different growth rates.

Introduction

In an exponentially growing population of S.cerevisiae cells, daughter cells apart from lacking bud scars, differ from parent cells in two obvious respects. Firstly, at division daughter cells are smaller than their parent cells (Beran et al. 1966, Johnson & Gibson 1966, Hartwell & Unger 1977). Secondly, daughter cells have longer cycle times than parent cells (Carter & Jagadish 1978, Hartwell & Unger 1977). Any model of control of cell proliferation in this yeast should be able to explain at least the latter observation.

The formulation of the age distribution function can provide a sound framework upon which a mathematical model of cell proliferation control can be built. Indeed, this has been done in constructing this type of model for bacterial cells (Pritchard et al. 1969). The standard age distribution (Cook & James 1964) does not apply to S.cerevisiae because of the difference between parent and daughter cycle times. It is assumed that the daughter cycle time (D) is longer than the parent cycle time (P) because daughter cells spend a longer time prior to start and that after start daughter cells complete the remaining cell division cycle events in the same time as do parent cells (Hartwell & Unger 1977). This being so, it would be meaningless to say that a particular stage-specific event occurs x minutes after birth, since this value for daughter cells will be different from that for parent cells. Hartwell & Unger (1977) took this into account in deriving the age distribution function for this yeast. In this distribution age is defined in terms of the time prior to division, whereas in the standard age distribution, age is defined in terms of the time since birth. Both distributions are shown in Fig. 5. Note that in the Hartwell

Figure 5

The Hartwell and Unger cell age distribution and the Standard age distribution.

A - the Hartwell and Unger age distribution (redrawn from Hartwell & Unger 1977). D is the age in the cycle of daughter cells immediately after division. P is the age in the cycle of parent cells immediately after division. Age in the cycle, t, is defined as the time prior to division.

B - the Standard age distribution (redrawn from Cook & James 1964). In this case, age in the cycle, t, is defined as the time subsequent to division.

A

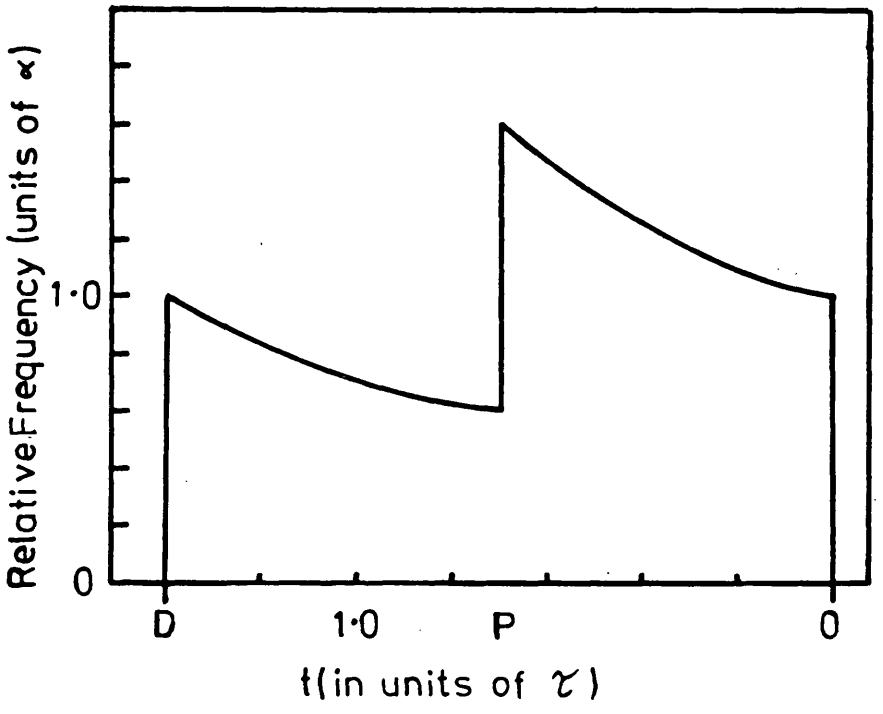
Relative Frequency (units of α)
1·0
0
D
1·0
P
0
t (in units of τ)

B

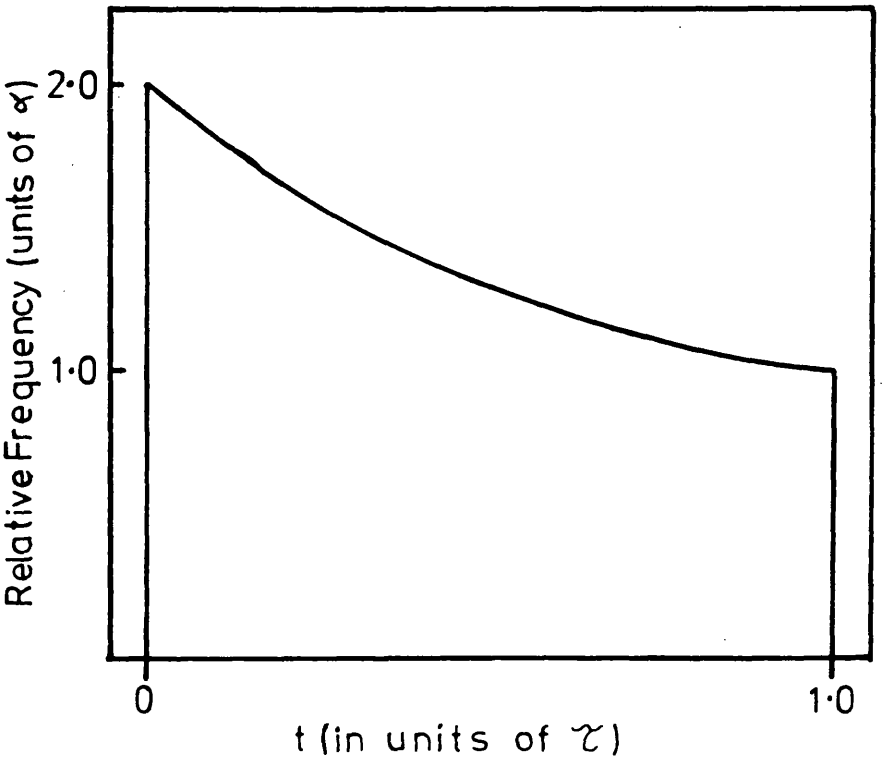
Relative Frequency (units of α)
2·0
1·0
0
1·0
t (in units of τ)

& Unger age distribution t=0 at division, whereas in the standard age distribution t=0 at birth.

To assess the general applicability of the Hartwell & Unger age distribution to studies on the yeast cell cycle, I have determined how the quantitative predictions of the formulation compare with experimental observations. I have used two tests. In the first, I have obtained estimates of D, P and B (the duration of the budded period) from the frequency of budded and unbudded parent and daughter cells and determined whether they fitted the constraints of the formulation. For the second test, I have derived the expressions for the genealogical age distribution to predict from the data the values of the frequency of cells of different genealogical age at different growth rates and compared these with the values found experimentally. I define the genealogical age in terms of the number of cycles a cell has completed. A cell with no bud scars (a daughter cell) has not completed a cycle and is of genealogical age 0. A cell with one bud scar has completed one cycle and is of genealogical age 1, and so on. The general formula for the frequency of cells of genealogical age n from the standard age distribution is $[\frac{1}{2}]^{n+1}$ (where n=0, 1, 2 etc.) (Yanagita 1977). The genealogical age distribution would,in this case, be independent of the growth rate. From the Hartwell & Unger age distribution the frequency of daughter cells is $e^{-\alpha P}$ and the frequency of cells of age n(n=1, 2, 3 etc.) is $[e^{-\alpha P}]^{n-1}\ [1-e^{-\alpha P}]^2$. In this case, the genealogical age distribution varies with the growth rate since $\alpha=\ln 2/\tau$. Only when $D=P=\tau$ will the standard age distribution apply to budding yeast cells (see equation A1).

Results

Cells of S.cerevisiae S288C/1 were grown with shaking at 30°C in 100 ml YEPC or EMMC medium in 250 ml Erlenmeyer flasks. Samples were taken periodically, each was fixed and sonicated. For each experiment

the (prewarmed) medium was inoculated with cells grown exponentially for at least ten times the doubling time in medium of the same composition so that the genealogical age distribution was truly representative of cells in that medium. Growth was determined by total cell count. Bud scar analysis was carried out on samples of cells which were in the mid-exponential phase of growth. Tables 1 and 2 summarize the media used, the doubling times achieved in these media and the data collected from the bud scar analyses. The median cell volume was also measured in each experiment.

Substituting equations A6 and A7 into equation A2 yields

$$F_{DB} \cdot F_{PB} = F_B^2 \qquad [1]$$

where F_{DB}, F_{PB} and F_B are the fraction of daughter cells which are budded, the fraction of parent cells which are budded, and the fraction of budded cells respectively. Equation [1] provides a test for a number of assumptions made in formulating the Hartwell & Unger age distribution (see Discussion below). Experimental values of F_{DB}, F_{PB} and F_B (calculated from the data in Table 1) were substituted into equation [1] and excellent agreement was found with the equation at all growth rates; the mean departure from the expected value was 0.003.

The relationships between D, P and B (from maximum likelihood estimates) respectively against τ are shown in Fig. 6. Each parameter increases linearly with τ. The empirical relationships between each parameter and τ were determined by linear regression (Table 3). The curves of D versus τ and P versus τ are very good fits to the data as is obvious from the coefficients of determination.

By extrapolation, the curves of D versus τ and P versus τ intercept when D=P=65.1 min. and τ =65.9 min. Therefore, the population will be distributed according to the standard age distribution when τ is about

TABLE 1. Numbers of budded and unbudded parent and daughter cells at different doubling times.

Medium*	Doubling time, τ (min.)	Unbudded Daughters	Budded Daughters	Unbudded Parents	Budded Parents	Bud scars
YEP + Glucose	76.3	247	408	160	407	1,264
YEP + Glucose	79.6	224	306	140	377	1,095
YEP + Glucose	84.1	279	302	118	348	1,006
YEP + Fructose	86.6	304	327	132	264	908
YEP + Mannose	91.2	266	268	192	324	1,015
YEP + Mannose	92.9	354	296	119	308	942
YEP + Raffinose	114.1	264	298	160	307	911
YEP + Cellobiose	114.6	351	260	119	320	932
YEP + Raffinose	122.5	410	196	167	259	953
YEP + Galactose	127.3	537	201	201	207	897
YEP + Glycerol	128.9	387	235	170	301	1,049
YEP + Glycerol	153.6	478	181	164	225	896
YEP + Glycerol	156.7	418	183	155	276	984

TABLE 1. - continued

YEP + Sorbitol	156.9	424	204	166	241	869
YEP + Mannitol	162.7	439	172	206	218	979
YEP + Mannitol	193.3	512	154	172	208	847
EMM + Galactose	203.9	538	125	201	208	875
YEP + Mannitol	222.6	507	155	211	177	934
EMM + Galactose	242.3	590	86	244	167	925

* YEP: Yeast extract, peptone; EMM: Edinburgh minimal medium.

TABLE 2. Percentages of cells of different genealogical ages at each doubling time.

Doubling time, τ (min.)	Genealogical age[4]						$\chi^4 \neq$
	0	1	2	3	4	>4	
76.3	53.60	20.54	11.29	6.47	3.47	4.26	—
79.6	50.62	20.73	13.28	9.55	2.87	2.96	+++
84.1	55.49	19.68	12.51	5.73	3.15	3.44	—
86.6	61.44	15.68	10.42	5.84	3.51	3.12	+++
91.2	50.86	23.52	14.38	6.00	2.67	2.57	—
92.9	60.35	16.81	10.77	5.57	3.16	3.34	—
114.1	54.62	22.64	12.44	5.05	2.82	2.43	—
114.6	58.19	17.71	13.33	4.57	3.05	3.14	++
122.5	58.72	17.73	8.43	5.04	3.78	4.36	—
127.3	64.40	15.18	9.69	5.32	2.36	3.05	+++
128.9	56.91	18.21	11.99	5.58	3.39	3.93	—
153.6	62.88	14.50	9.92	6.87	2.77	3.05	++
156.7	58.33	16.47	11.82	5.81	3.78	3.49	—

TABLE 2. - continued

156.9	60.68	17.49	10.82	5.89	2.71	2.42	+
162.7	59.61	17.27	9.85	6.83	3.12	4.29	——
193.3	63.67	15.39	9.85	4.78	3.06	3.25	+
203.9	61.85	16.14	11.29	5.04	3.17	2.52	++
222.6	63.05	15.52	9.05	5.33	2.95	4.10	——
242.3	62.19	17.02	8.28	6.16	3.04	3.31	+

≠ Genealogical age, n, is equal to the number of bud scars. At least 1,000 cells were scored for each growth rate.

≠ χ^2 test of goodness of fit of the data. The null hypothesis was that there was no significant difference between the observed frequency of cells of each of the six genealogical age classes above (as numbers) and the expected frequency (as numbers) based on P = 0.62γ+ 24 and equations A9 and A14. ——, no significant difference; +, ++, +++, significant difference at the 5%, 1%, and 0.1% levels respectively.

TABLE 3. Empirical relationships of cell cycle parameters in two strains of S.cerevisiae.

Period	Strains	
	S288C/1*	C276≠
D	1.48τ - 32 (r^2= 0.99)≠	1.41τ - 28
P	0.62τ + 24 (r^2= 0.98)	0.53τ + 45
B	0.18τ + 46 (r^2= 0.66)	0.17τ + 87
P - B	0.44τ - 22 (r^2= 0.94)	0.36τ - 42
D - B	1.30τ - 78 (r^2= 0.97)	1.24τ - 115

All values are in minutes. * From bud scar analysis, 30°C, batch culture. ≠ From time lapse photomicroscopy measurements, 24°C, batch culture (Hartwell & Unger 1977). ≠ r^2= coefficient of determination.

65 min. The interval from the birth of a parent cell to bud emergence (the P-B period) also has a linear relationship to γ .

The predicted variation in the percentages of cells of different genealogical age with γ , using equations [A9] and [A14] and $P=0.62\gamma+24$ (Table 3), are shown in Fig. 7. The experimental values for the percentages of cells of different genealogical ages are given in Table 2. Fig. 8 shows the variation in the percentage of cells of genealogical age 1 with γ . The data do not fit the predicted values using the standard age distribution, at any growth rate, but they are in good qualitative agreement with the curve predicted from the Hartwell & Unger age distribution. The fraction of cells of genealogical age 1 decreases as increases. Similar plots for cells of each genealogical age class show equally good qualitative fits to the predicted values (data not shown). However, a chi-square analysis was performed on the data at each growth rate, and a significant difference from the expected series of values was found in half the experiments (Table 2). To determine whether this was a random effect or whether the frequencies of some age classes showed a systematic departure from expectation, a 'box and whiskers' plot (Tukey 1977) for each age class was constructed (Fig. 9).

This method of analysis revealed information which otherwise would not have been evident using conventional statistical procedures. Two conclusions are apparent from the plot. First, although there is obvious scatter, the data do follow the general trend predicted from the Hartwell & Unger age distribution extremely well (the median values are close to zero). Second, there is an excess of daughter cells and fewer cells of genealogical age greater than 4.

The formation of buds in a regular spiral sequence from one pole of the cell to the other has been described previously (Streiblova 1970) for most haploid strains. I noted that at slower growth rates a small

Figure 7

The theoretical relative frequency of cells of different genealogical ages as a function of τ.

The curves are based on equations A9 and A 14 and $P=0.62\tau+24$ min. D, frequency of daughter cells; P_1, frequency of parent cells of genealogical age 1, etc.

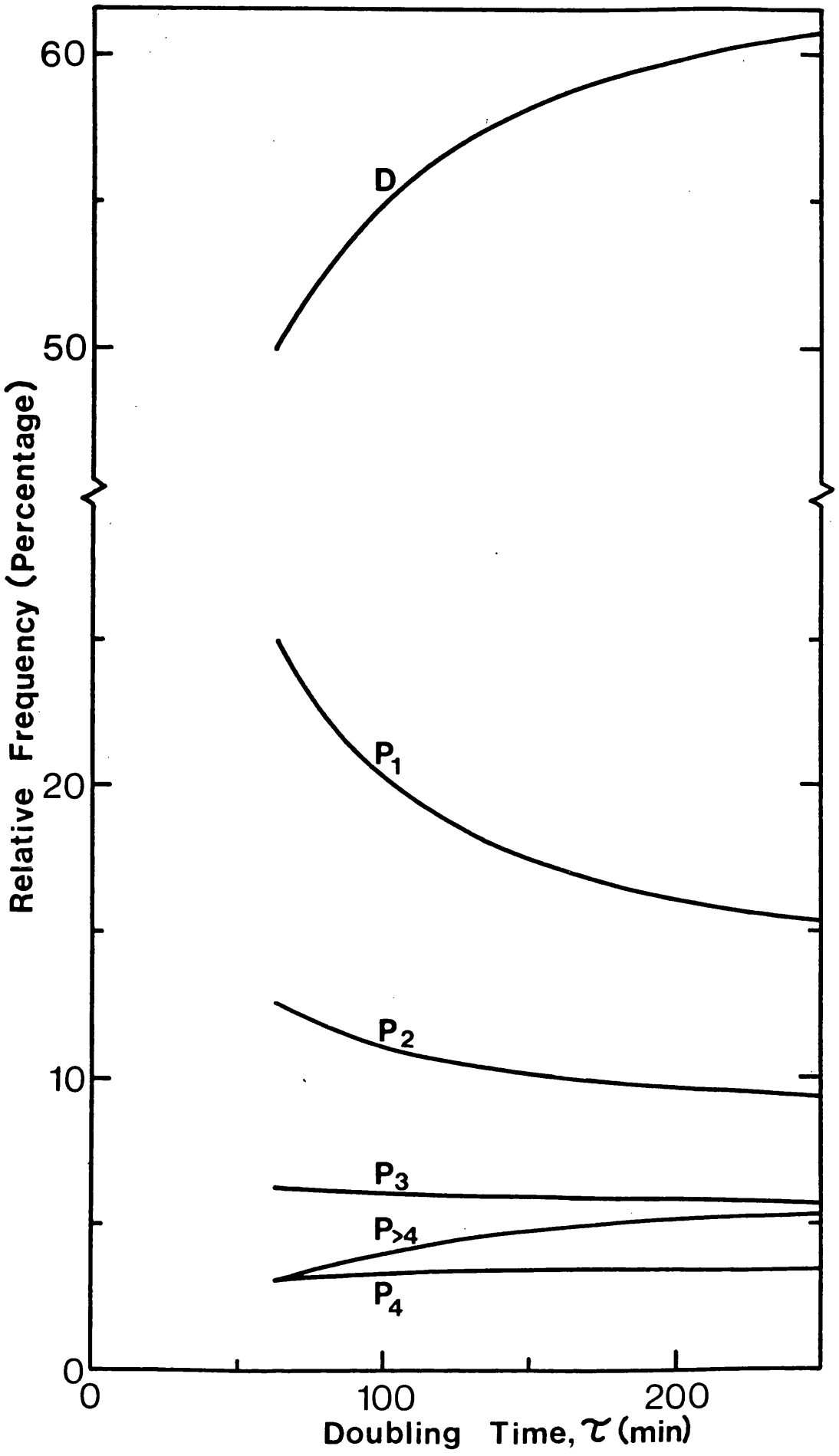
60
50
20
10
0
0
100
200
Relative Frequency (Percentage)
Doubling Time, τ (min)
D
P1
P2
P3
P>4
P4

Figure 9

The relationship of observed to expected frequencies of cells of different genealogical ages over a range of growth rates.

A value of $P=0.62\tau + 24$ min. and equations A9 and A14 were used to calculate the expected number of cells of different genealogical ages at each growth rate. The observed values (as numbers) were taken from Table 2. Since the relative frequency of cells declines with genealogical age, a normalising procedure was performed; this was done by taking square roots of both observed (O) and expected (E) values in order to make the differences of comparable magnitude. The difference between the square roots of the observed and expected frequencies at each of 19 growth rates is presented in the form of a box enclosing the central 50% of the data points (the median is indicated by a cross-bar) and 'whiskers' extend to the extreme values. A difference of $\pm$ 0.5 on the ordinate indicates a departure from the expected value of $\pm$ 16 when the number counted was 250.

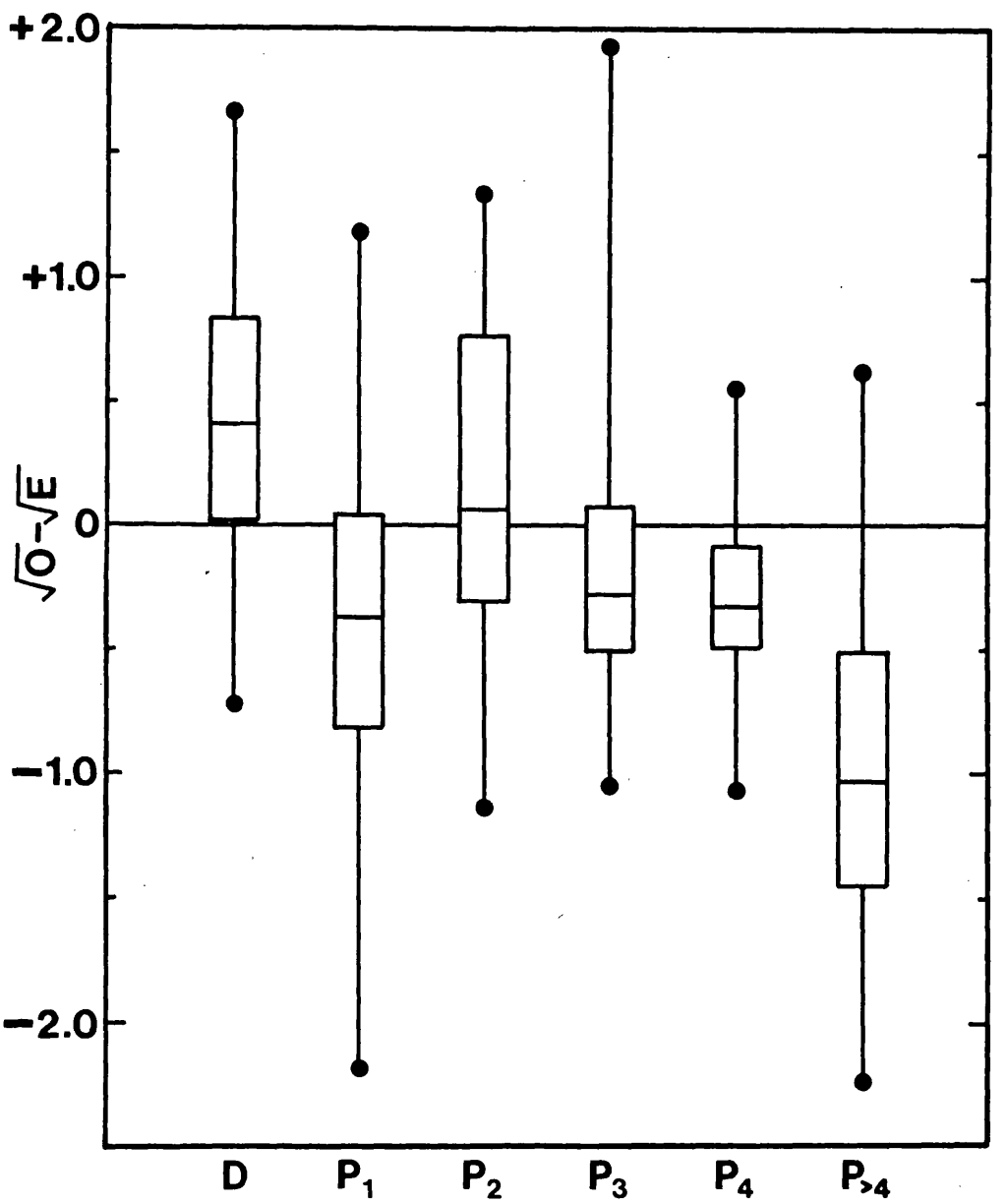
+2.0
+1.0
0
−1.0
−2.0
√O−√E
D
P1
P2
P3
P4
P>4

fraction of cells do not form buds in a spiral arrangement. There is a gap in the sequence of bud scars on some of these cells, and on others,bud scars occur at opposite poles. The fraction of cells with these bud scar patterns increased from 0.3% at τ=120 min. to 1.5% at τ=200 min. In a similar study in which growth rate was altered by glucose limitation in a chemostat, the majority of cells had this irregular pattern at the lower growth rates, i.e. at τ >400 min. (Thompson & Wheals 1980).

The median cell volume increased with increasing growth rate (Fig. 10), the largest increases occurring at the faster growth rates. A curve of increasing slope (from slow to fast growth rates) gave the best fit to the data.

Discussion

In formulating the age distribution for budding yeasts, Hartwell & Unger (1977) made the following assumptions: i) all parent cells have the same cycle time, P; ii) all daughter cells have the same cycle time, D; and iii) D > P. Implicitly, it was also assumed that: iv) the budded period, B, is the same duration for all cells; v) P > B; and vi) all cells are immortal.

Age distribution functions apply only to exponentially growing cells. In these experiments the cells were growing exponentially, as judged by increases in cell number, both before and after sampling for bud scar analysis. So the data are appropriate for testing the Hartwell & Unger formulation.

Assumptions i and ii are clearly false, since considerable cycle time variability has been found for both parent and daughter cells (Hartwell & Unger 1977, this thesis, Chapter 4). Nevertheless, Hartwell & Unger have shown that the mean values of D and P can be used successfully as approximations. More importantly, it is necessary to ascertain whether

Figure 10

The median cell volume, the volume at bud emergence and the volume at P, as a function of τ.

The data points are median cell volume measurements determined by a size analyser. The solid line is a curve, fitted by eye through the data points, of the median cell volume as a function of τ. The long dashes represent the curve of the volume at P as a function of τ and was calculated from equation A16, $P=0.62\tau + 24$ min. and values of V_m taken from the curve fitted through the data points. The short dashes represent the curve of the volume at bud emergence as a function of τ and was calculated from equation A15, $B= 0.18\tau + 46$ min. and values of V_p from the curve of V_p versus τ.

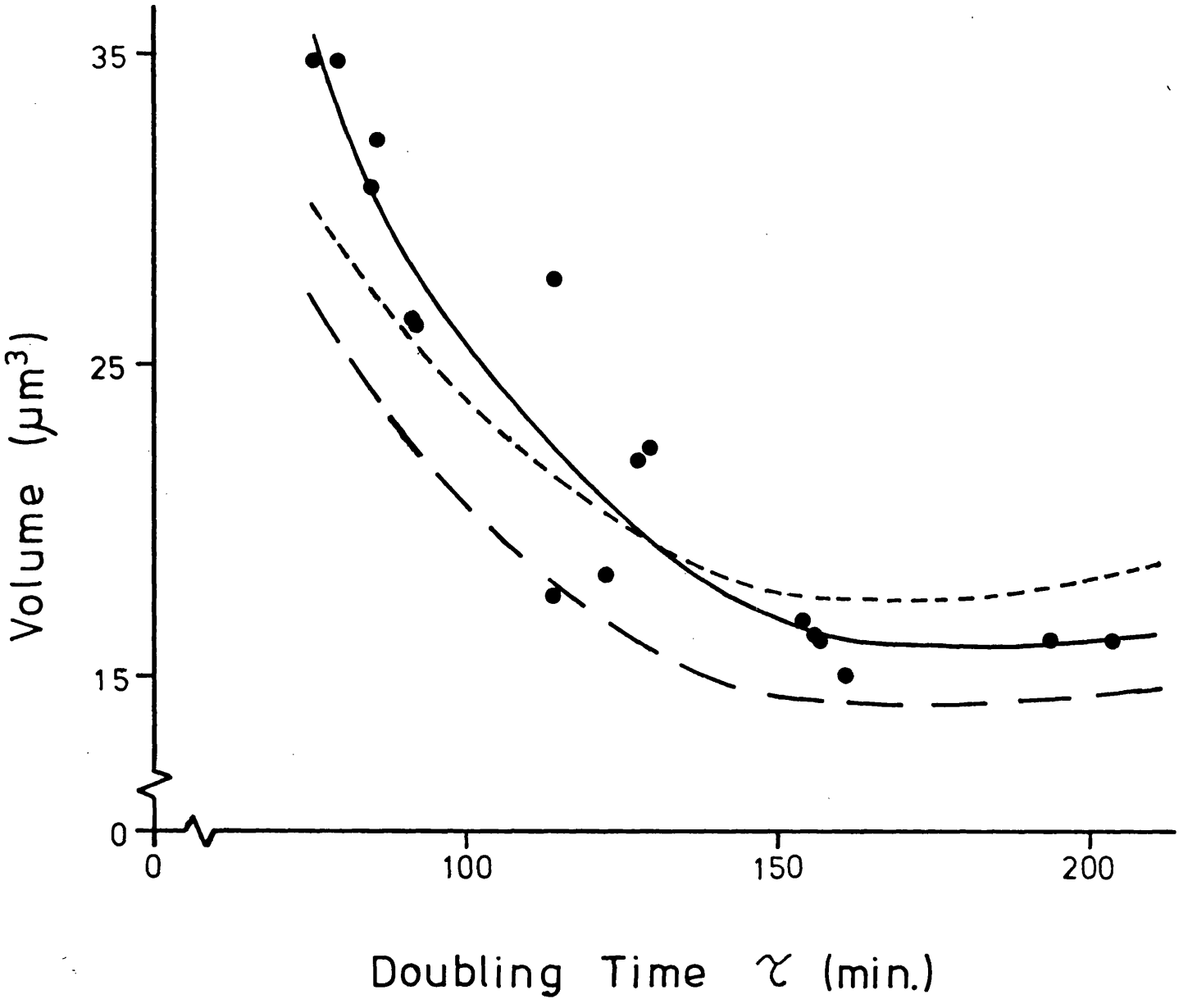
35
25
15
0
0
100
150
200
Volume (μm^3)
Doubling Time τ (min.)

the mean P value is different for parent cells of different genealogical ages. Fig. 9 reveals that this is not so. The observed frequency of P_1 to P_4 cells is close to the predicted value, assuming a constant P. Since the rate of entry of parent cells into age category n+1 is determined by the rate of exit of parent cells of age n, a departure from expected values could occur only if cells spent longer or shorter times at each age. There was little departure from expected values, so it can be concluded that $\bar{P}$ is constant for at least cells of ages 1 to 4. Cells of age greater than 4 could have shorter (or longer) cycle times but this is not the cause of the shortage of cells of age >4. Since the frequency of $P_{>4}$ cells is the sum of the frequencies of all older age groups, the total frequency should be as expected, whatever the duration of the cycle times of cells in this age group. The cause of the shortage is discussed below.

It is also important to know whether daughter cells born from parent cells of different genealogical age have different cycle times. Information on this point is not available from these results. However, there was little difference between the mean cycle times of first and second generation daughter cells on the films described in Chapter 4, so it is reasonable to assume that all daughter cells have cycle times distributed around the same mean value and this is independent of their parent cells' genealogical age.

Assumption iii is supported by a large body of evidence and is confirmed in this study since F_D is always greater than F_P.

Direct measurements of the length of the budded phase, B, have revealed that the mean B value of daughter cells is slightly longer than that of parent cells for one strain (A364A, see Chapter 4) but are the same for two other strains (SA and S67.3a, see Chapter 5). For all three strains, the mean B value of the parent cell's first cycle (the first cycle measured

on the film) was the same as that of their second cycle. In the present study, there is evidence that P is constant for cells of different genealogical age. If B is also constant for these cells, then the fraction of budded cells should be the same in each age group. I calculated the fraction of budded cells in each parental age group for each growth rate (F_{PBn}) and subtracted this value from the mean value ($\bar{F}_{PB}$) of the five age groups, P_1 to P_4 and $P_{>4}$, at that growth rate. Table 4 shows the median difference for each age group for all 19 growth rates. There was no evidence that this fraction changed systematically with genealogical age. So it is reasonable to assume that the length of the budded period is constant for parent cells of different genealogical age. Assumption iv therefore, appears to be valid, although daughter cells may have a slightly longer budded period than parent cells depending on the strain.

Assumption v is satisfied by numerous observations of the presence of unbudded parent cells in exponentially growing populations of yeast cells.

Micro-manipulation of yeast cells has shown them to be capable of completing up to 46 cycles; a mean value of 30 was obtained in one study (Muller 1971), hence they are practically immortal (assumption vi). However, the shortage of $P_{>4}$ cells is most easily explained on the basis of cell loss from this class, since entry into this class was at the appropriate rate. I did notice several highly fluorescent moribund cells in all the experiments, so an increasing probability of death with increasing genealogical age is possible in batch cultures. Since immortality is assumed, death of older cells has the effect of decreasing F_D and increasing F_D above its expected value, as was observed (Fig. 9). In this sense, F_D is an unreliable value on which to base estimates of cell cycle parameters, and equation A7 was used rather than $P=-\ln F_D/\alpha$ (from equation A9) to calculate P.

Finally, I substituted experimental values of F_{DB}, F_{PB} and F_B into

TABLE 4. Median value of $(\bar{F}_{PB} - F_{PBn})^*$ for each parental age group.

	Genealogical age				
	1	2	3	4	>4
Median value of $(\bar{F}_{PB} - F_{PBn})$	0.0058	0.0107	-0.0231	0.0012	0.0109

*F_{PBn} = the fraction, budded cells/total cells for parental age group, n ; $\bar{F}_{PB}$ = mean value of F_{PBn}, where n = 1, 2, 3, 4 and >4.

equation 1 for all the growth rates and found good agreement. Equation 1 is derived from equations A2, A6 and A7. Since equation A2 is based on assumptions i, ii, iii and vi, and since equations A6 and A7 are in addition based on assumptions iv and v, equation 1 simultaneously tests all six assumptions. This confirms that although the assumptions are often simplifications, they are not a gross distortion of reality. The other important solution for equation 1 is when assumption iv does not hold but instead $F_{DB}=F_{PB}$. This would occur only when D=P.

Fig. 6 clearly shows direct linear relationships of D,P and B to τ. A similar conclusion was reached previously on the basis of a more limited sample analysed by time-lapse photomicroscopy (Hartwell & Unger 1977). There is good quantitative agreement between the two sets of data, even though different strains, temperatures and methods of varying the growth rate were used (Table 3). Qualitatively similar results have also been obtained from bud scar analyses of chemostat-grown cells (Carter & Jagadish 1978, Thompson & Wheals 1980).

Having derived the age distribution for budding yeasts and having found evidence for its validity, Hartwell & Unger (1977) used it to examine the model for the coordination of growth and cell division proposed by Johnston et al.(1977). In this model, growth is rate-limiting for cell proliferation and the attainment of a critical cell size is a prerequisite for start. As described in Chapter 1, Hartwell & Unger showed that if exponential cellular mass increase was assumed, a daughter cell would reach the same mass at the same reference point, P, in the cycle that its parent cell had at that point only if all the mass accumulated by the parent cell during the parent cycle was distributed to the daughter cell at division. This is clearly not true of S.cerevisiae cells, since at division P_n cells are larger than P_{n-1} cells (Hartwell & Unger 1977, Lieblova et al. 1964, Mortimer & Johnston 1959). However, the critical

size hypothesis is qualitatively consistent with the age distribution since this yeast divides asymmetrically (Beran et al. 1966, Johnson & Gibson 1966, Hartwell & Unger 1977). Parent cells are at or above the critical size after division and are free to traverse start immediately, whereas daughter cells after division are less than this size and are free to traverse start only after they have grown to the critical size.

Taking the critical size hypothesis at its simplest and assuming that traverse of start cannot occur until after division, start should occur immediately a cell attains the critical size after division. If this were true, parent cells would traverse start immediately after division, at P in the cycle, and P would be the point at which daughter cells attain the critical size. It is thought that bud emergence occurs shortly after start (Hartwell 1974). If start does occur at P then Table 3 suggests that the time from start to bud emergence varies substantially with the growth rate, from 13 min. at τ =80 min. to 66 min. at τ =200 min. (from the data for S288C/1).

The evidence in the literature for an increasing interval between start and bud emergence with increasing τ, is contradictory. Rivin & Fangman (1980), by varying the growth rate using different nitrogen sources, found that this interval increased from 11 min. at τ =80 min. to 63 min. at τ =200 min. (comparable to the increase in the P-B interval of S288C/1). However, this interval was found to be approximately constant by Hartwell & Unger (1977) who used different concentrations of cycloheximide to vary the growth rate. In the latter reference the data (their Table IV) were incorrectly calculated and presented, but the conclusion remains the same (L.H. Hartwell, personal communication).

The discrepancy between the two sets of evidence may be due to differences between the strains and/or the growth conditions used. Nevertheless, these pieces of evidence and the observations that the P-B interval varies substantially with the growth rate (Table 3) raise questions

about cell cycle controls and particularly about the proposed size control in this yeast.

If, as suggested above, start occurs at P then the observation of an increasing P-B interval with increasing γ implies the presence of an additional, temporal control over the timing of bud emergence apart from the prerequisite completion of start. For example, the rate of those reactions initiated upon completion of start which are necessary for bud emergence, may be modulated by the growth conditions.

The implication of a pre start period after P, which would be present if there is a constant interval between start and bud emergence, and which increases with increasing γ, is that the attainment of a critical size is insufficient for cells to traverse start. Execution point determinations of the α factor sensitive step (Hartwell & Unger 1977) give estimates of the timing of the completion of start. Attainment of a critical size then, may initiate start, but the rate of completion of start may vary with the growth rate.

Assuming that there is a critical cell size, cell size will have least effect on the rate of cell proliferation when daughter cells are born at or above the critical size. When this occurs the daughter cycle time will equal the parent cycle time. Extrapolating from the data in Fig. 6, this situation will arise when γ =65 min.

Several authors have noted that in populations of budding yeasts, as the growth rate decreases, the fraction of daughter cells increases (Beran 1968, Beran et al. 1967, Beran et al. 1966, Carter & Jagadish 1978, Hayashibe & Sando 1970). Beran and his colleagues also found that the fractions of cells of different genealogical ages vary with the growth rate, although they did not give a satisfactory explanation for this finding. My analysis, using the Hartwell & Unger age distribution, provides a simple quantitative explanation. There were only two discrepancies. First, there was a shortage of cells of genealogical age greater than 4 and a

corresponding excess of daughter cells, the reason for which could well be increased mortality of older cells. Second, at nearly half of the growth rates the observed frequencies were significantly different from those expected, as tested by a chi-square test (Table 2). Part of the reason for the differences was undoubtedly due to the first feature above. In addition, it must be noted that the Hartwell & Unger age distribution does not take into account the variability in both daughter and parent cycle times. The variability in D and P increases the total variance beyond that due to sampling error, and hence a chi-square test gives a false indication that the results are significantly different from the expected values.

Buds on haploid cells of most S.cerevisiae strains are formed in a highly ordered sequence. The first bud forms next to the birth scar (Freifelder 1960, Streiblova 1970), and successive buds form adjacently in rows, rings or spirals (Streiblova 1970). The cells used in these experiments formed buds predominantly in a precise spiral sequence (evident on cells with many bud scars). It is not known how this pattern is determined. However, the spindle pole body (SPB) may be involved. Around the time of bud emergence the duplicated SPB is orientated towards the emerging bud, and cytoplasmic microtubules extend from the SPB to the base of the emerging bud (Byers & Goetsch 1975). After nuclear division each SPB is orientated towards the opposite pole from the site of budding (Matile et al. 1969). If the site of budding is determined by the position of the SPB and assuming that the SPB maintains its orientation after nuclear division then buds should appear alternately (from one cycle to the next) at opposite poles of the cells. If, after nuclear division, the SPB has no stable orientation, then the pattern of bud formation should be random. To produce the spiral pattern of bud formation, the SPB must reorientate after nuclear division in a precisely controlled manner to become aligned

adjacent to the previous site of budding. Factors which affect the precision of the budding pattern are i) growth rate; slow growing cells have a less precise pattern (Thompson & Wheals 1980, and Results, this chapter); ii) zygosity of the mating type locus; cells heterozygous for mating type have a random pattern of bud formation (Streiblova 1970).

The median cell size varied with the growth rate (Fig. 10) as was observed previously (Tyson et al. 1979), although in the present study the variation in size was not as dramatic. Using equations A15 and A16 and values taken from the curve drawn through the data of median volume versus growth rate, the volumes at P and B were calculated for each growth rate. Both the volume at P and the volume at B increase with growth rate (Fig. 10). Direct measurements of cells which had small buds have shown that the volume of a cell at bud emergence does, in fact, increase with increasing growth rate (Johnston et al. 1979). If there is a size control and if V_p is the critical cell size then this size must be nutrient modulated. A similar conclusion has been made for a proposed size control in Schizosaccharomyces pombe (Fantes & Nurse 1977).

A comparison of strain S288C/1 with the parent strain studied previously (Tyson et al. 1979) shows that i) the duration of B has a different relationship with γ, and ii) the median cell size is smaller at all growth rates. Clearly the strain has changed in some respects. Nevertheless, the changes are quantitative rather than qualitative.

These results show that the theoretical age distribution derived by Hartwell & Unger (1977) is a good approximation to the true age distribution of S.cerevisiae cells. The results also emphasize the need to treat populations of S.cerevisiae cells as comprising two distinct sub-populations (i.e. parent and daughter cells). The derivation should subsequently prove to be useful in developing models of cell proliferation for this organism.

CHAPTER FOUR

Chapter 4

Variability in individual cell cycles of Saccharomyces cerevisiae.

Introduction

The two currently favoured hypotheses to describe the control of cell proliferation in S.cerevisiae are somewhat contradictory. The critical size hypothesis suggests a deterministic, size control mechanism (Fantes et al. 1975, Johnston et al. 1977). A stochastic, 'timing' mechanism is suggested by the transition probability hypothesis (Smith & Martin 1973, Shilo et al. 1976). Although much of the evidence for both hypotheses comes from observations of perturbed cell populations, there is some evidence for both from studies of steady state populations (Johnston et al. 1977, Hartwell & Unger 1977, Shilo et al. 1976, 1977). Neither hypothesis, however, fully explains all the observations.

The critical size hypothesis accounts for the observation of a size requirement for the traverse of start (Johnston et al. 1977) and explains the difference between the parent and daughter cycle times. It cannot account for variation in cycle times unless, for example, it is postulated that there is variation in birth size. Even so, parent cells (all of which are born above the critical size) should still show negligible variability in cycle time. In addition, this hypothesis predicts that cells released from start-arrest should show quasi-synchronous entry into the post-start sequence of events (the division sequence), which they do not (Shilo et al. 1976).

The transition probability hypothesis can explain variability in cycle time and can account for the asynchronous entry into the division sequence observed in cells released from start-arrest (Shilo et al. 1976). It cannot account for the size requirement for start or for the difference

between parent and daughter cycle times.

Shilo et al.(1977) admitted that a probabilistic mechanism alone is insufficient to explain control of cell proliferation in S.cerevisiae and consequently, taking the evidence for a size control, suggested that cells do not enter the A state until they have attained a minimum cell size. Their view then, is that the mechanisms act in tandem and this will be referred to as the Tandem model. In terms of this model, daughter cells require a period of growth after birth to attain a critical size, after which they enter the A state and from this they enter the B phase (i.e. post-start events) probabilistically. Parent cells are above the critical size and so enter the A state directly after division. An alternative model has been proposed which also combines the deterministic and probabilistic elements but in a different way (Wheals 1982). In this, 'sloppy' size control (SSC) model, the probability of entering the division sequence (B phase) increases with size such that small cells have a low probability and large cells a high probability. The probabilistic element is in this case an integral part of the sizing mechanism.

In order to evaluate the two models it is necessary to obtain simultaneous measurements of the size and cycle times of individual cells in steady state populations. Such data, from time lapse cine films, has been obtained previously but the analysis was limited by the microscopical technique used (Wheals 1982). In that study the only morphological event whose timing could be unambiguously measured was bud emergence. Cell size was measured at bud emergence and the interval between successive bud emergence events was taken as a measure of the cycle time. A satisfactory evaluation of the models requires data of cell sizes at birth and of the timing of both division and start.

The phase contrast image of S.cerevisiae cells can be improved to a remarkable degree by raising the refractive index of the growth medium

to an appropriate value (Robinow 1975). When the refractive index of the surrounding medium is close to that of the cell contents, much intracellular detail is discernible (see Fig. 11). I have used this technique and time lapse cinephotomicrography to measure the size of cells at division (as well as at bud emergence) and to measure the timing of the following events in the cell cycle: bud emergence, nuclear migration, nuclear division and septum formation. I have filmed cell populations growing on four different carbon sources (supporting four different growth rates) to see how the timing of events varies with the growth rate. With these data I have compared the relative merits of the Tandem and SSC models.

Results

Populations of A364A cells were filmed growing on YEPC-PVP agar media at 30°C, where C, the carbon source was either glucose, raffinose, sorbitol or galactose. The procedures for making and analysing the films are fully described in Chapter 2.

In order to test the predictions of the models, it is necessary that the data be collected from exponentially growing cells under balanced, steady state growth conditions (Powell, 1955). The criteria used to establish this (data not shown) were i) exponential increase in cell number, ii) exponential increase in total cell volume, iii) population doubling time from i) equal to population volume doubling time from ii), iv) mean duration of first and second parent cycles equal, and v) mean cycle times of first and second generation daughters equal. All criteria except number iii) were achieved. τ_v was found to be 6-15% longer than τ. This may be because during the course of the film an increasing proportions of the cells are slightly out of the focal plane and/or the cells change in their orientation. Consequently, cell volume would be underestimated for an increasing proportion of the population during filming. However, a

Figure 11

Photographs of a yeast cell growing on YEP-PVP-glucose-agar, taken at intervals, to show the different stages in the cell cycle.

The cell is from a culture of S.cerevisiae, A364A. A - medial nuclear divisicn. B - late nuclear division. C - onset of cytokinesis. D - late septum formation. Vacuole (V), nucleus (N), septum (S). The bar represents 5 μm.

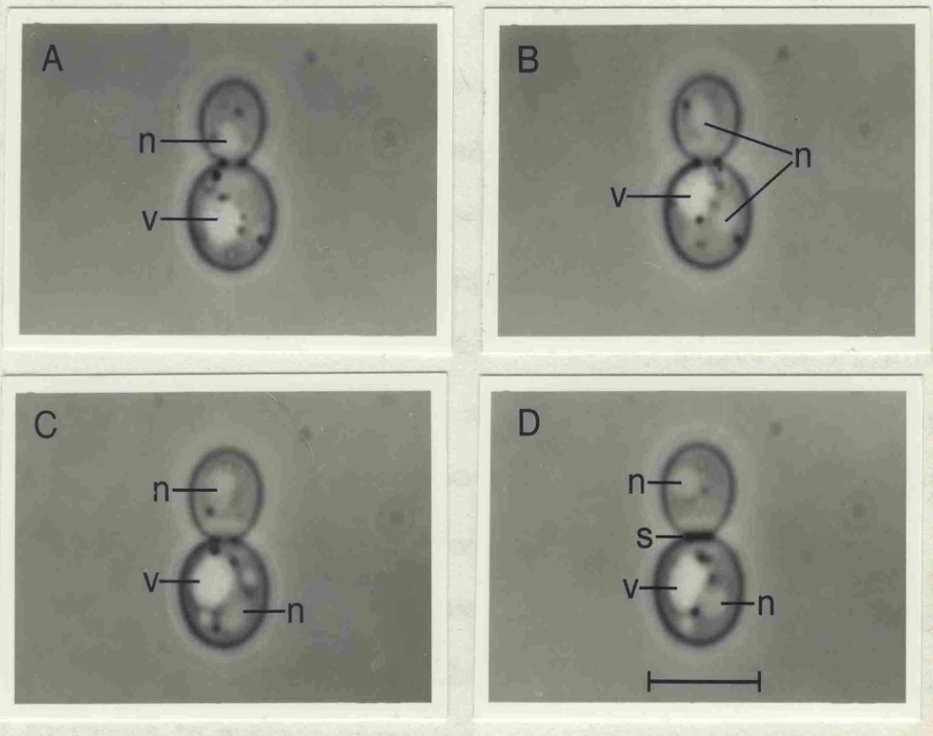
A
n
v
B
n
v
C
n
v
n
D
n
s
v
n

discrepancy between γ and γ_v was not found in a similar, previous study (Wheals 1982). The only difference between the studies is that in these experiments PVP-40 is present in the medium. This substance may, in some way, cause the discrepancy. Even though the average cell size may be slightly decreasing during the course of the experiments, it is reasonable to conclude that the conditions approximate to a steady state, so the data are appropriate to testing the models.

The mean duration and variability of various periods in the cell cycle are shown in Table 5 for parent and daughter cells at each growth rate. The major conclusions from these data are as follows. i) The mean daughter cycle time is always longer than the mean parent cycle time, this difference being mostly due to the longer unbudded period of daughter cells. ii) The variability of daughter cycle times is much greater than that of parent cycle times, the difference being attributable to the more variable unbudded period of daughter cells. iii) The budded period is 5-8 minutes longer for daughter cells compared to parent cells, this increase being accounted for by the time from bud emergence to nuclear migration. iv) There is a tendency for all periods to increase in length with increasing population doubling time. This feature is most evident for the unbudded period (especially for daughter cells), the budded period and the period from bud emergence to nuclear migration.

The distributions of cycle times of parent and daughter cells are shown in Figure 12. The data are presented as α plots, the percentage of undivided cells on a logarithmic scale against cycle time (Smith & Martin 1973). A straight line would indicate a constant probability of division per unit time, as is suggested by the transition probability hypothesis. The data present a homogeneous series showing the following features. i) The minimum cycle time for both parent and daughter cells increases with increasing population doubling time. ii) The shortest 30%

TABLE 5. The duration and variability of cell cycle phases at different growth rates.

Period	Doubling time	Parent cells		Daughter cells	
		Mean	SD[a]	Mean	SD
Cycle time	96.9[b]	72.6	6.4	117.7	27.8
	121.5[c]	87.2	10.3	140.9	29.3
	142.0[d]	98.4	9.3	174.8	35.1
	160.0[e]	108.9	14.7	205.1	56.7
Unbudded period	96.9	8.6	3.7	47.5	25.3
	121.5	13.2	4.5	62.6	27.1
	142.0	11.5	3.5	80.5	31.0
	160.0	15.1	8.3	103.9	53.1
Budded period	96.9	64.0	6.0	69.9	7.6
	121.5	73.9	9.4	78.6	8.2
	142.0	86.9	8.4	94.6	12.3
	160.0	93.8	12.1	101.2	15.3

TABLE 5. - continued.

Bud emergence to	96.9	36.1	5.8	41.5	6.4
nuclear migration	121.5	44.9	5.8	48.8	7.2
	142.0	53.3	7.7	58.9	10.7
	160.0	58.7	9.2	66.0	13.6
Nuclear migration	96.9	8.8	2.2	8.1	1.7
to nuclear division	121.5	8.5	1.9	9.2	2.0
	142.0	8.9	1.8	9.0	1.9
	160.0	9.8	2.1	9.8	2.3
Nuclear division to	96.9	9.7	4.1	11.1	3.8
onset of cytokinesis	121.5	8.1	3.1	9.0	2.2
	142.0	12.4	3.2	16.0	4.7
	160.0	10.2	3.6	10.8	2.9

TABLE 5. - continued.

Onset of cytokinesis	96.9	9.7	2.2	9.0	1.6
to cell separation	121.5	12.6	5.1	11.5	3.9
	142.0	11.9	3.7	11.5	2.4
	160.0	15.0	4.1	14.6	4.5

All values are in minutes. The number of cycles measured were: [b] 32 parent and 32 daughter cycles; [c] 34 parent and 33 daughter cycles; [d] 40 parent and 40 daughter cycles; and [e] 38 parent and 37 daughter cycles. [a] SD is the standard deviation. Data from parent cells first and second cycles were pooled since Student's t-tests showed that there was no significant difference between the mean values of any parameter for first and second parent cycles. Similarly, Student's t-tests showed that it was permissible to pool the data from first and second generation daughter cells.

Figure 12

$\propto$ plots of parent and daughter cycle times at four different growth rates.

An $\propto$ plot is the percentage of cells with cycle times (t_{ct}) greater than or equal to t (on a logarithmic scale) versus t. Glucose-grown cells (○,●); raffinose-grown cells (□,■); sorbitol-grown cells (△,▲); galactose-grown cells (▽,▼); open symbols, parent cells; closed symbols, daughter cells.

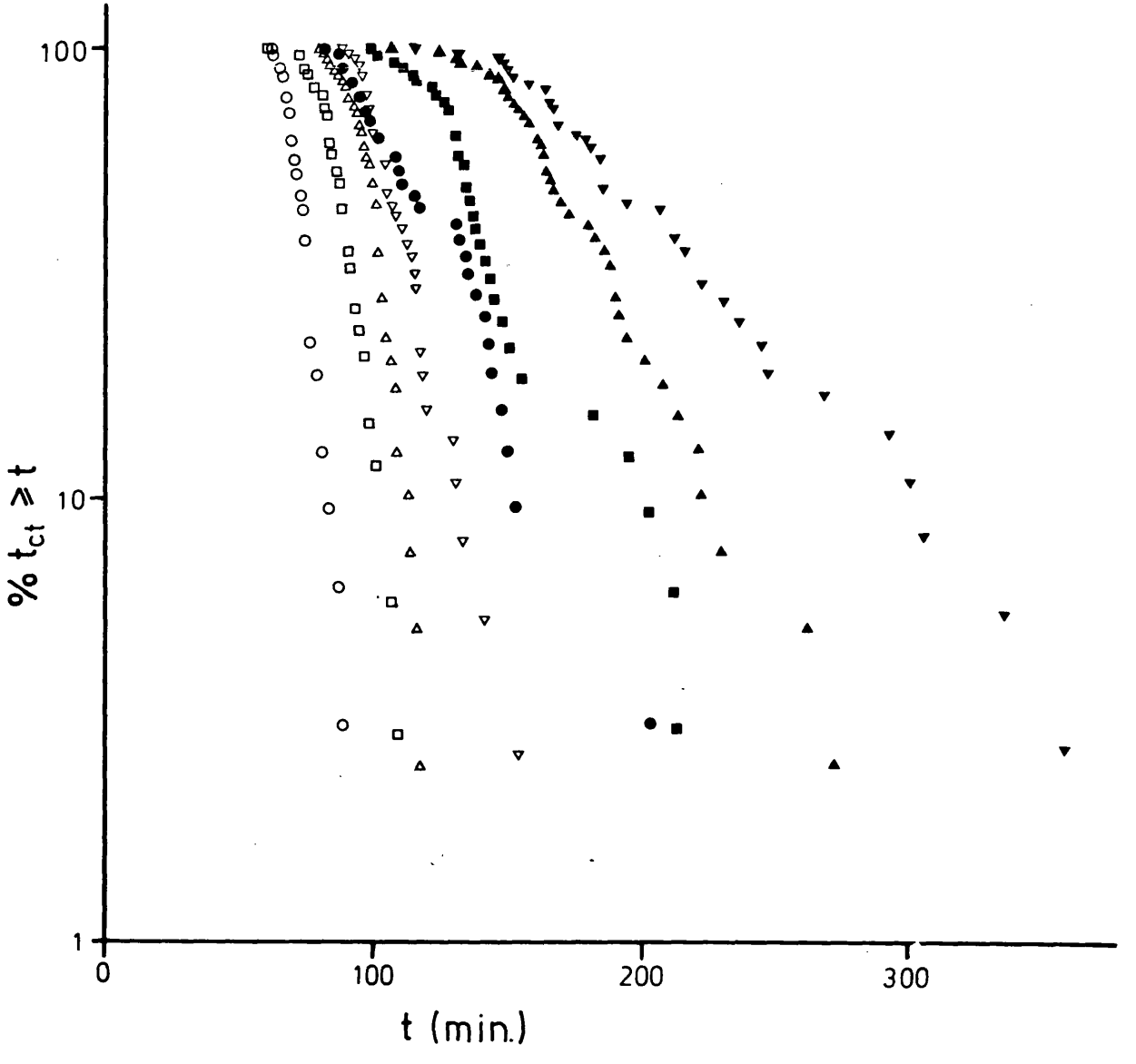
100
10
1
% $t_{ct} \geq t$
0
100
200
300
t (min.)

of cycle times of parent and daughter cells show substantial downward curvature. iii) The longest 50% of parent and daughter cycle times show an approximately exponential distribution. iv) The slopes of the straight line portions tend to decrease with increasing population doubling time (especially those of daughter cycle time plots). v) For each population doubling time the minimum cycle time is less, the initial curvature less pronounced and the slope steeper for parent cells than for daughter cells. In addition, no daughter cell had a cycle time less than that of its sibling parent (i.e. $a > p_1$, $b > p_2$ in Fig. 4). An examination of the distributions of the budded (not shown) and unbudded (Fig. 13) periods of parent and daughter cells indicates that both periods contribute to the slope and initial curvature of the α plots. However, as was inferred in Table 5, it was the unbudded period that determined the overall shape of the daughter cycle time α plots.

In order to see whether there was any evidence of homeostatic regulation during the budded period, or whether this was a constant sequential process with small standard deviation, the following test was done. If no regulation occurred, the sum of the variances of the individual intervals of the budded period should equal the variance of the budded period. If regulation did occur then the variance of the budded period should be less than the sum of the individual variances. Within the limits of experimental error the variances were equal suggesting that there is no additional control at division as has been shown for Schizosaccharomyces pombe (Fantes,1977).

The volumes of daughter cells at cell separation were always smaller than their sibling parent cells (data not shown). There was wide variation in the birth size of daughter cells and similar variation in their size at bud emergence, with some overlap between the distributions (Figure 14). Since bud emergence occurs shortly after start (Hartwell & Unger, 1977;

Figure 13

<u>χ plots of the durations of the unbudded period of parent and daughter cells at four different growth rates.</u>

The percentage of cells with unbudded periods of duration, t_{ub}, greater than or equal to t (on a logarithmic scale) versus t. Glucose-grown cells (○,●); raffinose-grown cells (□,■); sorbitol-grown cells (△,▲); galactose-grown cells (▽,▼); open symbols, parent cells; closed symbols, daughter cells.

% $t_{ub} \geq t$
1
10
100
0
100
200
t (min.)

Figure 14

The distributions of the sizes of daughter cells at two stages of the cell cycle.

Histograms of the sizes of daughter cells (A and B in Fig. 4) at birth (solid line) and at bud emergence (broken line). A - glucose-grown cells; B - raffinose-grown cells; C - sorbitol-grown cells; D - galactose-grown cells.

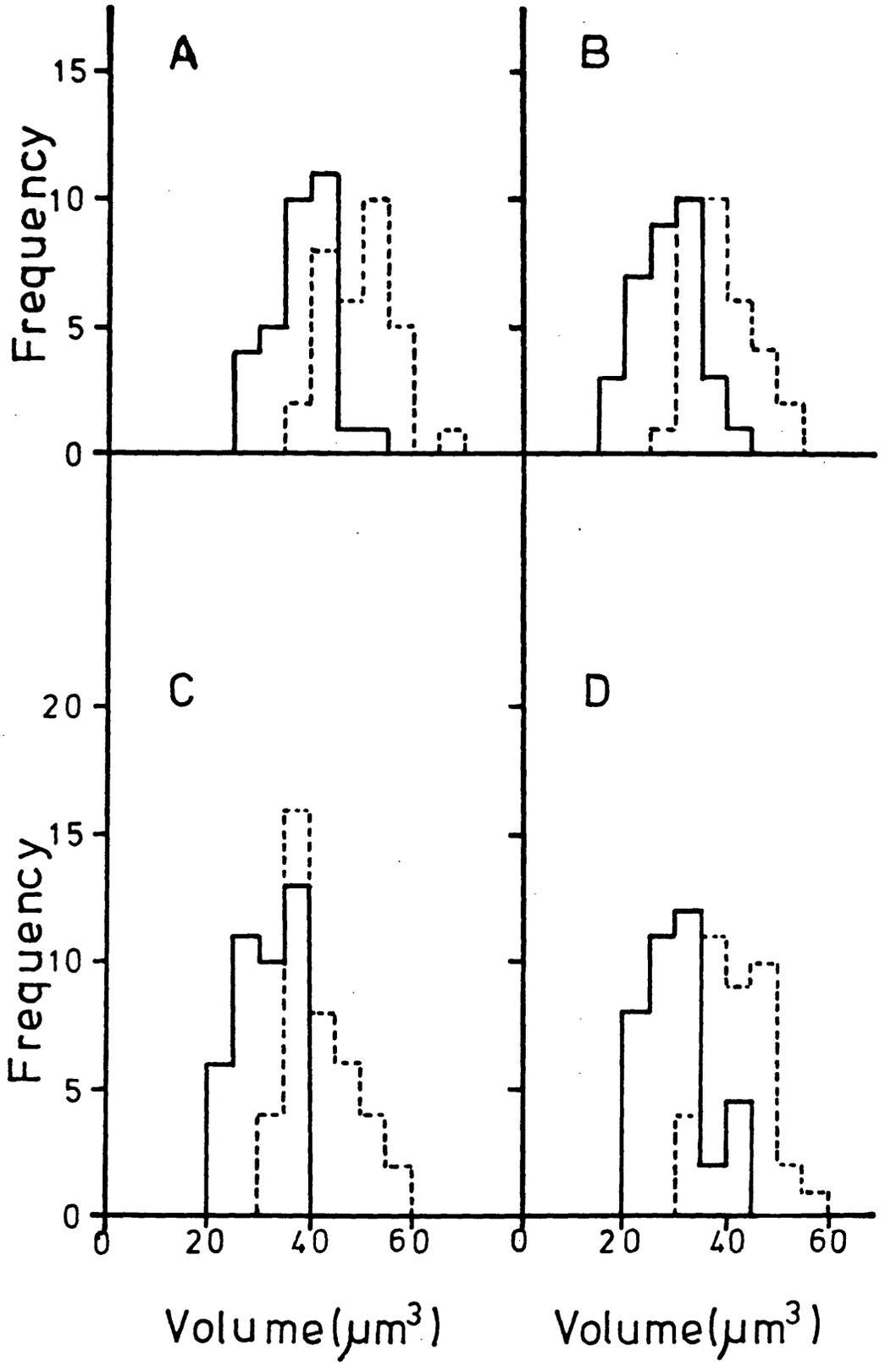
A
B
C
D
Frequency
Frequency
15
10
5
0
20
15
10
5
0
0
20
40
60
0
20
40
60
Volume(μm³)
Volume(μm³)

Hereford & Hartwell 1974; Shilo et al. 1976) the size at bud emergence is taken as an approximate measure of the size at start. There was no correlation between the size at birth and the size at bud emergence for individual cells. This suggests that cells do not grow a constant increment from birth to bud emergence (data not shown).

Table 6 shows that the mean size of daughter cells born from parent cells (i.e. P in Fig. 4) was approximately 3-4 μm^3 larger than those born from first generation parent cells (i.e. A and B in Fig. 4). Daughter cells from older parent cells were born at the same size at each generation (i.e. A=B=C in Fig. 4) except for raffinose grown cells where the third generation daughter cells were smaller. Although cells from the fastest growing populations were larger than cells from the slowest growing populations as expected, raffinose grown cells were the smallest of all. A plot was made (for each growth rate) of the size of daughter cells at birth versus size at bud emergence of the parent cell from which it was produced (data not shown). There was a trend for larger parent cells to produce larger daughter cells but the correlation was very weak ($t < 0.5$ in all cases).

The duration of the unbudded period is approximately equal to the pre-start period. A plot of size at cell separation (birth) against the duration of the unbudded period will reveal whether the birth size is important in determining when start occurs.

These parameters are plotted in Fig. 15 for each experiment. In each case birth size is not important in determining the length of the unbudded period of parent cells. Birth size is important for daughter cells. However, the size effect is only a loose one since the correlation coefficients are low (see legend to Fig. 15).

Wiemken et al. (1970) have reported on the dynamic behaviour of the vacuole during the cell cycle of S.cerevisiae. I have seen this behaviour

TABLE 6. Mean birth size of daughter cells.

Medium	Doubling time (min.)	Mean birth size (μm^3)				
		A*	B	C	AA	BA
YEP Glucose	96.9	37.9	37.4	35.5	34.4	31.3
YEP Raffinose	121.5	28.1	28.3	23.3	25.4	26.0
YEP Sorbitol	142.0	30.9	31.7	29.6	27.0	25.8
YEP Galactose	160.0	30.5	29.2	29.7	27.3	25.4

* A, B, C, AA and BA refer to daughter cells in Fig. 4.

Figure 15

Cell size at cell separation versus the duration of the subsequent unbudded period.

A - glucose-grown cells; B - raffinose-grown cells; C - sorbitol-grown cells; D - galactose-grown cells; (O), parent cells; (⊙), daughter cells. The correlation coefficients of daughter cell size at cell separation versus the duration of the unbudded period are: A, - 0.4110; B, - 0.5462; C, - 0.6210; D, - 0.4819.

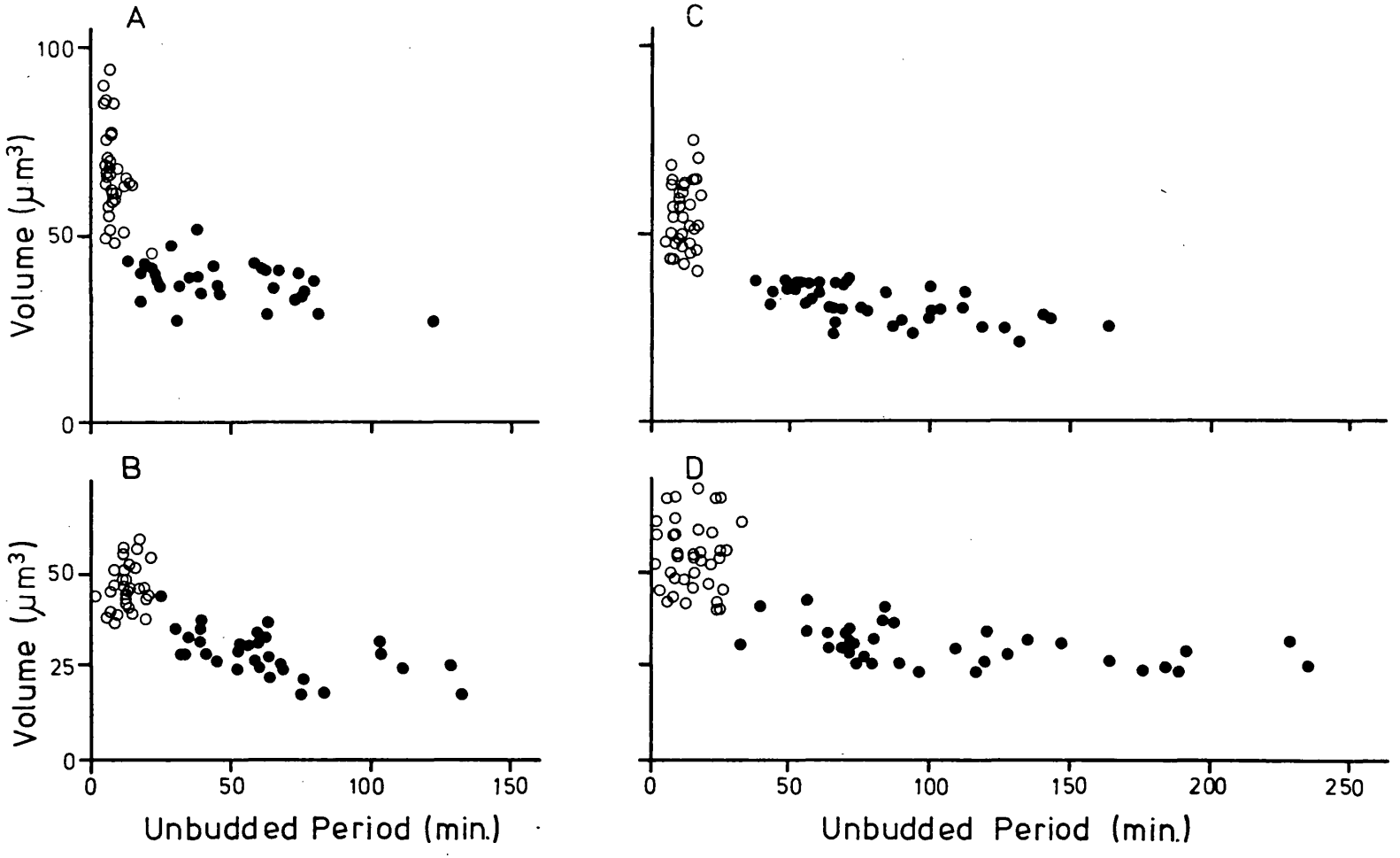
A
B
C
D
Volume (μm³)
Volume (μm³)
100
50
0
50
25
0
0
50
100
150
0
50
100
150
200
250
Unbudded Period (min.)
Unbudded Period (min.)

only in glucose grown cells. Small vacuoles appeared at about the time the nucleus divided. The small vacuoles fused to form a large vacuole which after a few minutes broke down into several small vacuoles. Shortly afterwards, these vacuoles disappeared. The length of time between appearance and disappearance of the vacuoles seemed to depend on the geneal-logical age of the cell. The vacuoles of cells budding for the first time (A and B in Figure 4) disappeared about eight minutes before cell separation. Disappearance of the vacuoles occurred at about the same time as cell separation in the older, parent cells. Unlike Wiemken et al. (1970) I did not see vacuoles in the buds.

Discussion

The refractive index technique significantly increases the amount of information which is obtainable from time lapse cinephotomicrographic studies. In previous time lapse studies of mammalian as well as of yeast cell populations only one reference point in the cell cycle was monitored (Absher et al. 1974, Hartwell & Unger 1977, Wheals 1982) whereas in these studies no less than five reference points were monitored. The two most important reference points in this study are division and bud emergence. The basis of all proliferation control models for S.cerevisiae is that start is the rate limiting event in the cell cycle (Johnston et al. 1977, Shilo et al. 1976, Wheals 1982). The major implication of this is that the pre-start period is subject to greater variation than is the post-start period. It would be ideal to be able to monitor division and start directly. Indirect evidence suggests that the period between start and bud emergence is small and relatively invariant (Hartwell & Unger 1977, Hereford & Hartwell 1974, Shilo et al. 1976). The unbudded period (which was measured in this study) thus serves as a good approximate measure of the pre-start period. That start is the rate-limiting event in the daughter cycle is supported not only by the greater expansion of the unbudded period in

comparison to the budded period with increasing cycle time, but also by the considerably larger variance in the unbudded period than in the budded period at each growth rate (Table 5). In the case of parent cells, the expansion of the cycle time (with decreasing growth rate) is mainly due to the expansion of the budded period (Table 5). It is difficult to establish for parent cells whether or not the variability of the unbudded period is greater than that of the budded period at each growth rate since the variance of the unbudded period is, to a significant degree, produced by experimental error in measuring such a short interval.

The lengths of the parental unbudded periods are approximately exponential which supports the view of a probabilistic feature of start (Fig. 13). Fig. 15 indicates the presence of a size control over start, certainly for daughter cells. Models which incorporate both the probabilistic and deterministic features of start are therefore more plausible for application to S.cerevisiae than are the individual probabilistic or deterministic models. Two 'hybrid' models have been proposed, namely the Tandem model (Shilo et al. 1977) and the SSC model (Wheals 1982). The important differences between these and the deterministic and probabilistic models are illustrated in Fig. 16 which gives the theoretical relationship between the probability of traversing start and cell size. For the deterministic model (Fig. 16a) all cells below critical size have zero probability and all cells at or above critical size have a probability of one. For the probabilistic model (Fig. 16b) all cells have the same probability, regardless of size. For the Tandem model (Fig. 16c) all cells below critical size have zero probability and all cells at or above critical size have a high probability (not unity). In the case of the SSC model (Fig. 16d) the probability increases smoothly with size to a high plateau value.

How then do the hybrid models compare in accounting for the results

Figure 16

The theoretical relationship between the probability of traversing start, and cell size.

A - the simple deterministic model; B - the simple probabilistic model; C - the Tandem model; D - the Sloppy Size Control model.

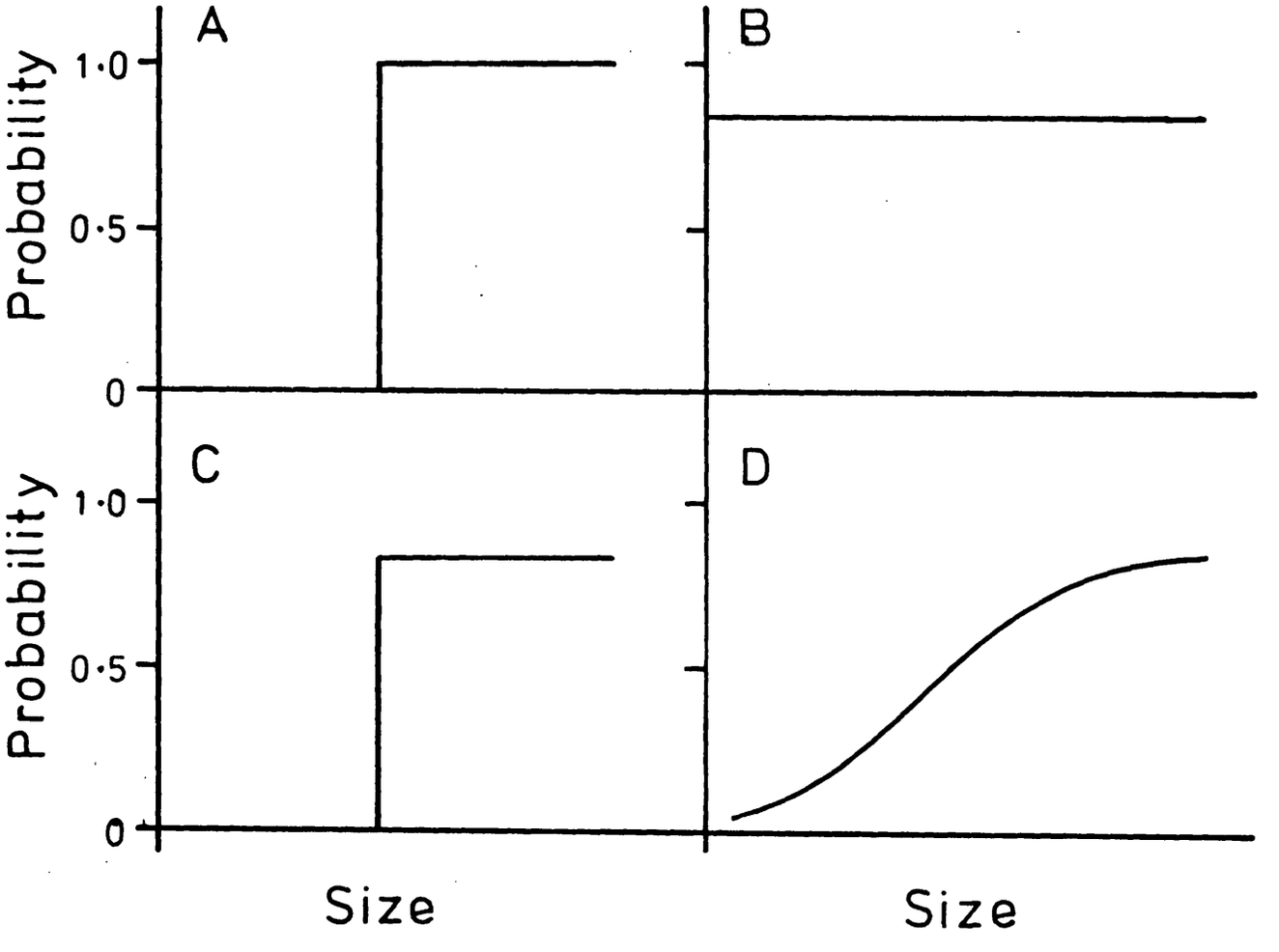
A
B
C
D
Probability
1·0
0·5
0
Probability
1·0
0·5
0
Size
Size

of these experiments? Consider first the Tandem model. The difference between the length of the parent and daughter unbudded periods (Table 5) is accounted for by the asymmetry of division and the critical size requirement suggested by the model. The greater variance of the daughter unbudded period in comparison to the parental unbudded period (Table 5) is explained again by the critical size requirement and also by the variation in the birth size of daughter cells. The approximately exponential distribution of the lengths of the parental unbudded periods is consistent with the model. However, according to the model daughter cells after having attained the critical size should exhibit the same kinetics of entry into the division sequence as parent cells. Hence the latter portions of the α curves for parent and daughter cells in Figs. 12 and 13 should become parallel, which they clearly do not. This result could be explained in terms of the model if it was further assumed that the transition probability value was different between parent and daughter cells. If, as implied by the model, after daughter cells attain the critical size they have a constant probability of traversing start, then their sizes at start (and consequently at bud emergence) should be exponentially-distributed. A plot of the percentage of unbudded daughter cells (on a log. scale) against cell size (a Υ-plot, Wheals 1982) should thus fit a straight line of negative slope after an initial plateau. A representative Υ plot, for galactose-grown cells, is shown in Fig. 17. A curve of increasing (negative) slope gives the better fit to the data, which could be accommodated in the Tandem model by the additional assumption of variance in the critical size. Therefore, whilst there is agreement with some of the results, to fully account for the observations the Tandem model requires further modification.

As for the SSC model, the difference between the lengths of the parent and daughter unbudded periods is explained since daughter cells would on average have a lower transition probability value than parent

Figure 17

Ψ plot of data from galactose-grown cells.

A Ψ plot is the percentage of daughter cells remaining unbudded (on a logarithmic scale) plotted against size.

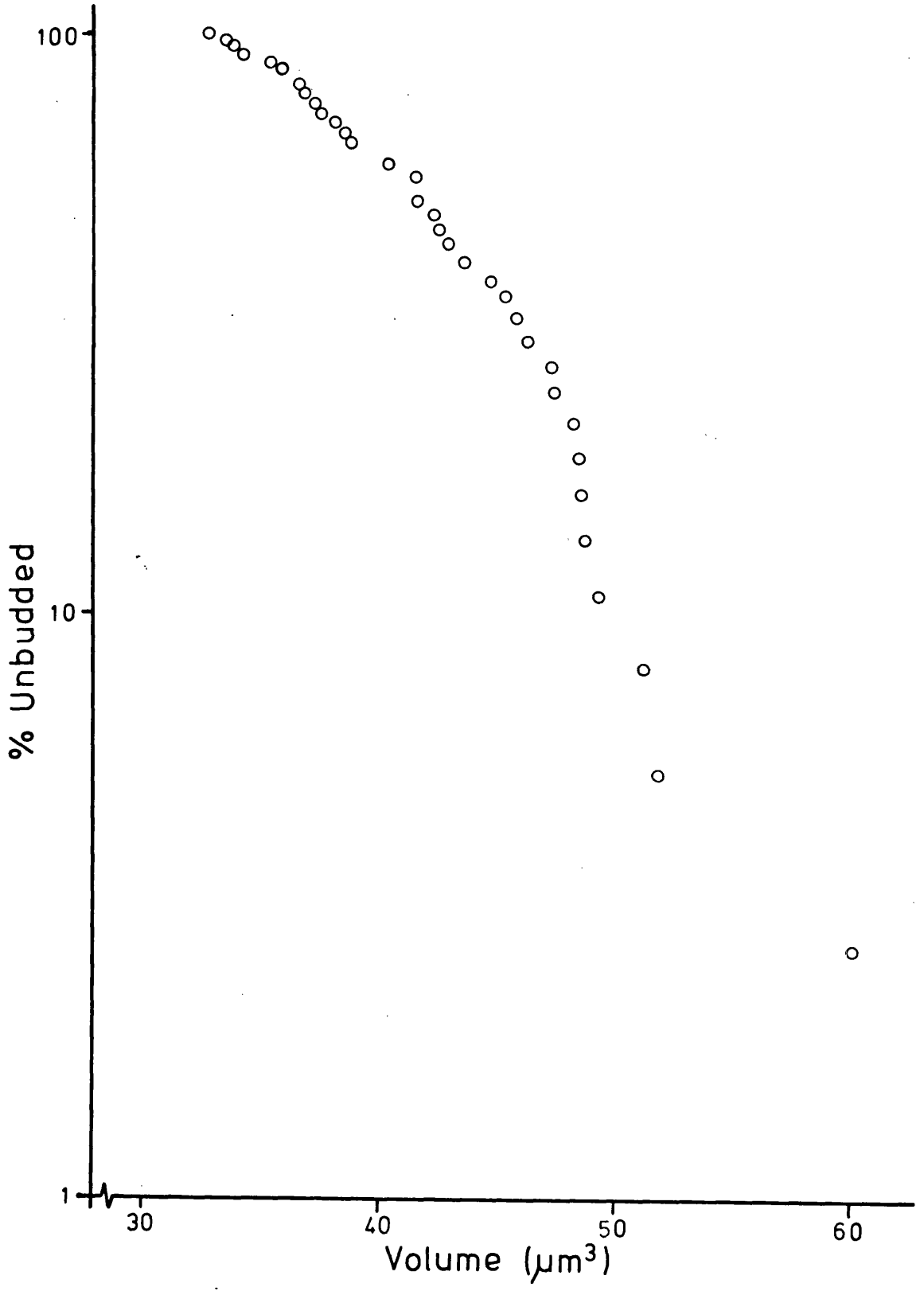
100
10
1
% Unbudded
30
40
50
60
Volume (μm³)

cells. This also accounts for the greater variance in the duration of the daughter unbudded period in comparison to the duration of the parental unbudded period. The complex shape of the α curves of the unbudded period of daughter cells is consistent with the model because of the heterogeneity in transition probability values in the daughter cell population. These α curves are different from the corresponding α curves for parent cells since the prediction of the model is that the transition probability values are more homogeneous in the parent cell population. The increasing slope of each α curve is also consistent with the SSC model since it proposes that the transition probability increases with size. Therefore, no modification of the SSC model is apparently necessary for it to account for these results.

One feature of the results, however, is not readily explained by either model, and is the observation that the minimum unbudded period of daughter cells is greater than the minimum parental unbudded period even though some daughter cells are born at about the same size as the smallest parent cells (Fig. 15). This suggests that whereas the parental unbudded period is virtually fully compressible, the daughter unbudded period is incompressible below a minimum duration. This may represent an additional period in the unbudded period of daughter cells which is not determined by their size. The possibility that a difference exists between the unbudded periods of parent and daughter cells which is not due to the difference in cell size at division is investigated in Chapter 6.

It has generally been assumed that the budded period is the same duration in parent and daughter cycles (Hartwell & Unger 1977, Wheals 1982). This study clearly shows a shorter parental budded period (Table 5). Since the time from nuclear migration through to cell separation is identical for both parent and daughter cells, this indicates that bud emergence is delayed in parent cells. The delay may occur because the

previous bud has to separate from the parent cell before a new one can emerge. The signal to form a bud may have occurred but the timing is dependent on the completion of previous events. Further to this, it is perhaps unreasonable to suppose that the time from start to bud emergence could be as little as one minute (the shortest unbudded period of galactose grown cells). Rather, a parent cell is competent to traverse start when it has physiologically separated from the daughter cell (directly analogous to the situation in Schizosaccharomyces pombe (Nasmyth et al. 1979, Nurse and Thuriaux 1977). Since the onset of cytokinesis occurs about 10 minutes before cell separation, and membrane separation has occurred by this stage (Cabib, 1975), traverse of start could be occurring 10-20 minutes before bud emergence.

Cell cycle kinetics of S.cerevisiae are well described in terms of the SSC model or a modified Tandem model. For the latter it is proposed that the critical size is variable. In this respect both models could be described as having a 'sloppy' size control. The addition of variation in critical size would mean that the relationship between the probability (or frequency) of entering the division sequence and cell size for the Tandem model would be similar to that for the SSC model (Fig. 16). The 'phenotypes' of the SSC and modified Tandem models are therefore very similar. The difference between the two lies at the conceptual level. The SSC model suggests one mechanism and includes a minimum of assumptions. The modified Tandem model suggests two mechanisms (for two transition points) and includes relatively more assumptions than does the SSC model. Although the SSC model is lower in complexity, this cannot be taken as confirmation of its validity. Neither should the modified tandem model be rejected on the basis of its higher complexity.

CHAPTER FIVE

Chapter 5

A comparison of the kinetics of cell proliferation of whi 1 and wild type S.cerevisiae cells.

Introduction

Mutants of Schizosaccharomyces pombe have been isolated which divide at a smaller cell size than wild type cells. These, wee, mutants have proved to be very useful for studying proliferation control in that organism. In contrast to S.cerevisiae, control of cell proliferation in Schizpombe occurs in G2. Evidence from wild type cells suggests that mitosis is initiated when cells attain a critical cell size (Fantes 1977). Studies of the wee mutants revealed a second control step which i) is cryptic for wild type cells at fast growth rates (Nurse & Thuriaux 1977), ii) occurs in G1, and iii) controls the initiation of DNA synthesis via a 'sizing' mechanism. Only when the mitotic control mechanism is defective or lost (as in wee mutants) or when cells are born small (i.e. at slow growth rates or upon germination from spores) does the G1 control become rate-limiting for cell proliferation (Nurse & Thuriaux 1977, Nasmyth 1979). It has been suggested that the WEE 1 gene product is an inhibitor of mitosis and that WEE 2 is a positive regulator of mitosis (Nurse & Thuriaux 1980).

Similar small size mutants of S.cerevisiae have only recently been isolated. whi 1 cells produce buds at a smaller cell size than wild type cells and whi 2 cells continue budding when nutrients are depleted, producing very small cells (Sudbery et al. 1980). The purpose of this study was to find out what controls exist over cell proliferation in cells with a defective (or absent) size control mechanism. The kinetics of cell proliferation of a whi 1 mutant have been compared to those of its immediate (WHI 1) parent strain.

Results

Time lapse cine films were made of growing cells of strain S67.3a (whi 1) and of strain SA (WHI 1). Both strains were grown at 25°C on YEP Glucose-PVP agar supplemented with lysine. The mean cycle times of first and second generation daughter cells were equivalent as were the mean cycle times of parent cells in their first and in their second cycles after time 0. Both cell number and total cellular volume increased exponentially with time from time 0. The data are therefore appropriate for the analysis. The values of γ and γ_v for S67.3a were greater than those for SA and for both strains γ was less than γ_v (Table 7).

The mean durations of the cell cycle and constituent periods are given in Table 8 for parent and daughter cells of each strain. The general features common to both strains, which are apparent from the table are as follows: i) the mean daughter cycle time is longer than the mean parent cycle time; ii) there is more variation in daughter cycle times than in parent cycle times; iii) the difference between the means of the daughter and parent cycle times is accounted for entirely by the difference in the mean duration of the unbudded periods; iv) the large variation in the daughter cycle time is mainly due to the large variation in the duration of the unbudded period of daughter cells; v) the mean lengths of each period between bud emergence and division are equivalent for parent and daughter cells.

All periods, except the period between nuclear division and cytokinesis, during the cycle of S67.3a cells were longer than those of SA cells. This is probably due to the difference in the growth rates of the strains. The cycle times of S67.3a cells were much more variable than those of SA cells, particularly the daughter cycle times. The coefficients of variation of the daughter cycle times of SA and S67.3a cells were 28% and 44% respectively. The difference in the variability of daughter cycle times is mainly due to the difference in the variability of the unbudded

TABLE 7. The population, and the total cell volume, doubling times of strains SA and S67.3a.

Strain	τ (min.)	τ_v (min.)
SA	119.1	136.5
S67.3a	161.8	169.5

TABLE 8. The mean durations of cell cycle periods of parent and daughter cells of strains SA and S67.3a.

Period	SA		S67.3a	
	Parent cells	Daughter cells	Parent cells	Daughter cells
Cycle time	92.7 (10.3)*	136.6 (37.8)	133.1 (24.4)	198.1 (87.3)
Unbudded period	8.2 (6.2)	52.9 (38.2)	24.5 (18.4)	89.2 (87.9)
Budded period	84.5 (10.0)	83.7 (7.6)	108.5 (16.2)	108.8 (17.4)
Bud emergence to nuclear migration	46.1 (9.3)	45.4 (8.3)	68.4 (15.6)	70.4 (15.8)

TABLE 8. continued.

Nuclear migration to nuclear division	9.6 (1.7)	9.0 (1.3)	11.0 (3.0)	9.8 (1.8)
Nuclear division to cytokinesis	17.3 (3.7)	17.8 (4.1)	15.7 (4.2)	16.2 (5.3)
Cytokinesis to cell separation	11.5 (2.8)	11.4 (2.3)	13.0 (3.8)	12.4 (3.5)

All values are in minutes. * standard deviations are given in brackets. 36 parent and 36 daughter cycles were monitored for SA cells. 32 parent and 32 daughter cycles were monitored for S67.3a cells. Data were pooled as in Table 5.

periods between the strains. The coefficients of variation of the daughter unbudded periods of SA and S67.3a were 72% and 99% respectively.

The distributions of the parent and daughter cycles times of both strains are presented as α plots in Fig. 18. For both strains the α plot of parent cycle times is 'steeper' than that of daughter cycle times. As was the case for A364A cells (Chapter 4) the shape of the α plot of daughter cycle times was determined mainly by the distribution of the lengths of the unbudded period (Fig. 19).

Fig. 20 shows the distributions of daughter cell sizes at birth and at bud emergence. The distribution of birth sizes overlaps with the distribution of bud emergence sizes for both strains although more so for S67.3a. The mean values of the size of daughter cells at 3 cell cycle stages are given in Table 9. The mean size of S67.3a cells are less than half the size of SA cells at the corresponding stages.

In Chapter 4 the plots of size at cell separation (birth) against the duration of the subsequent unbudded period revealed the relative importance of size in determining the length of the unbudded period (the latter being taken as an approximate measure of the pre-start period). The data for both strains, plotted in this way are shown in Fig. 21. The graph for SA cells is similar to those obtained for A364A cells (Chapter 4), except that some of the points for the daughter cells are clustered directly beneath the points for the parent cells. As was concluded for A364A cells, birth size of parent SA cells is not important in determining the length of the unbudded period but, since daughter cell size at birth is loosely correlated with the length of the unbudded period ($r=0.54$), birth size is important for daughter cells.

The graph for S67.3a cells is different in several ways. There is a higher correlation between the birth size of daughter cells and the duration of the unbudded period ($r=0.70$). Size does not appear to be important in

Figure 18

∝ plots of parent and daughter cycle times of strains SA and S67.3a.

The percentage of cells with cycle times (t_{ct}) greater than or equal to t (on a logarithmic scale) versus t. SA cells (○,●); S67.3a cells (□,■); open symbols; parent cells; closed symbols, daughter cells.

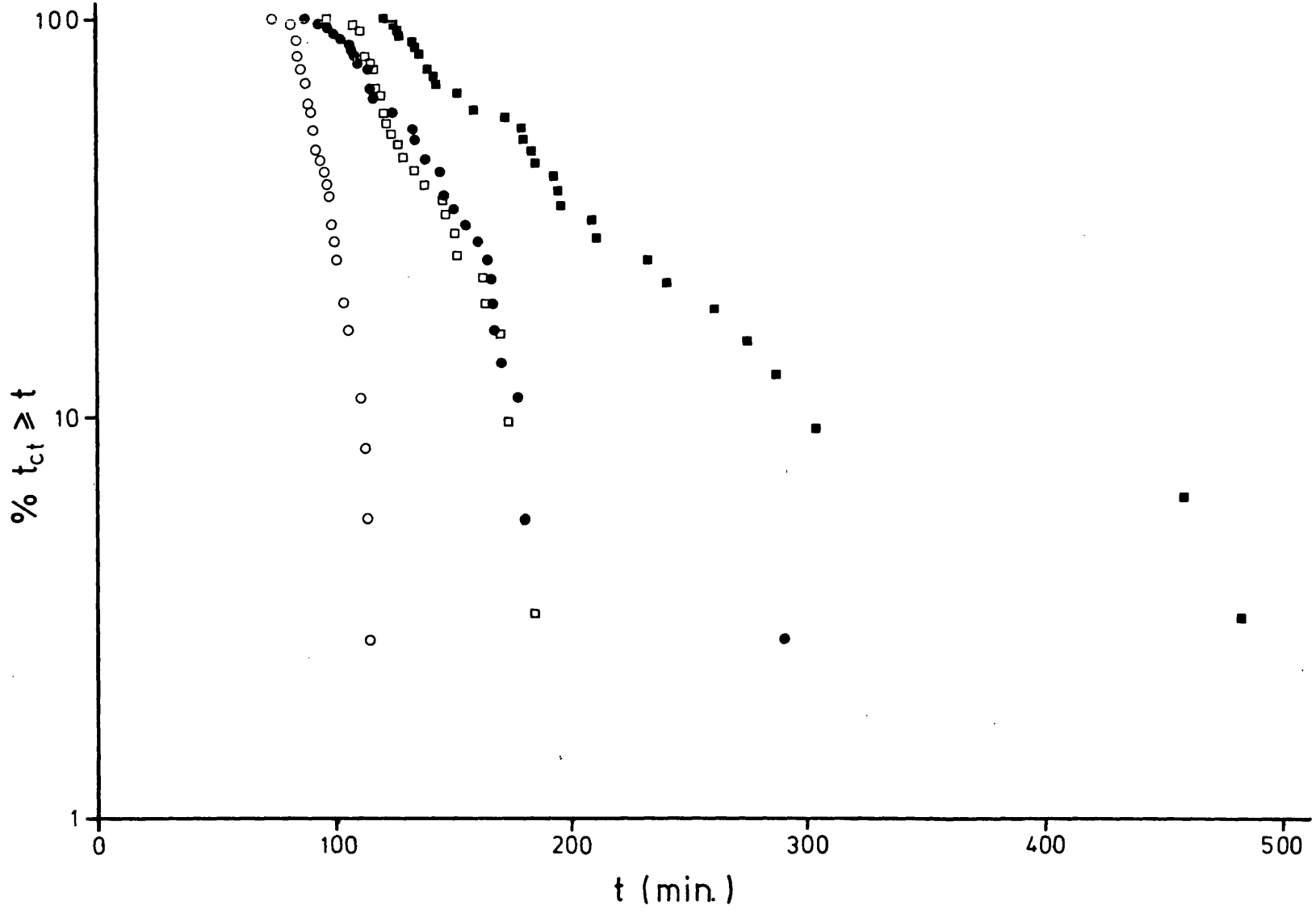
100
10
1
% $t_{ct} \geq t$
0
100
200
300
400
500
t (min.)

Figure 19

∝ plots of the unbudded periods of parent and daughter cells of strains SA and S67.3a.

The percentage of cells with unbudded periods of duration, t_{ub}, greater than or equal to t (on a logarithmic scale) versus t. SA cells (o,●); S67.3a cells (□,■); open symbols, parent cells; closed symbols, daughter cells.

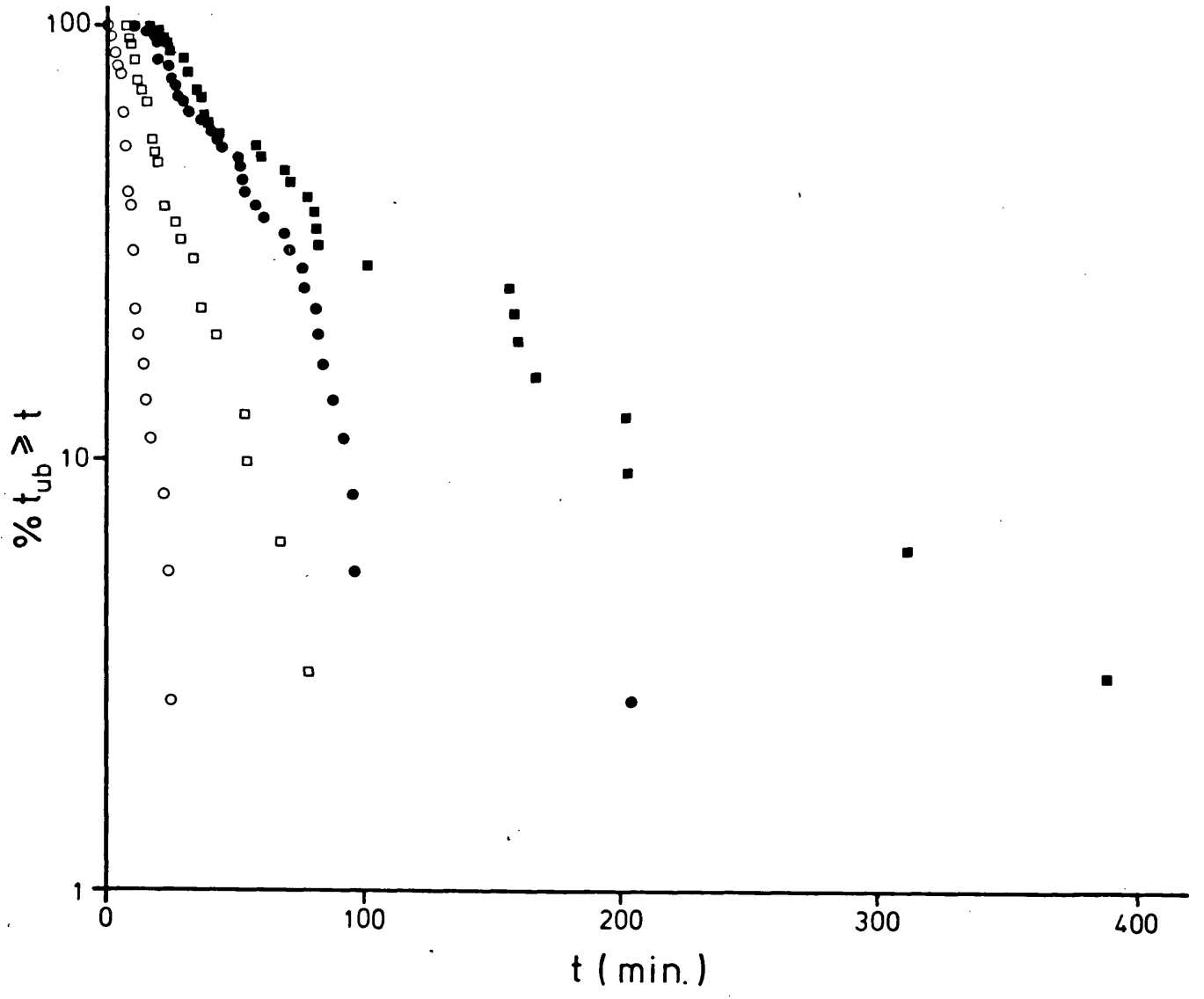
100
10
1
% $t_{ub} \geq t$
0
100
200
300
400
t (min.)

Figure 20

The distributions of the size of daughter cells of strains SA and S67.3a at two stages of the cell cycle.

Histograms of the size of daughter cells at birth (solid line) and at bud emergence (broken line). A - SA cells; B - S67.3a cells.

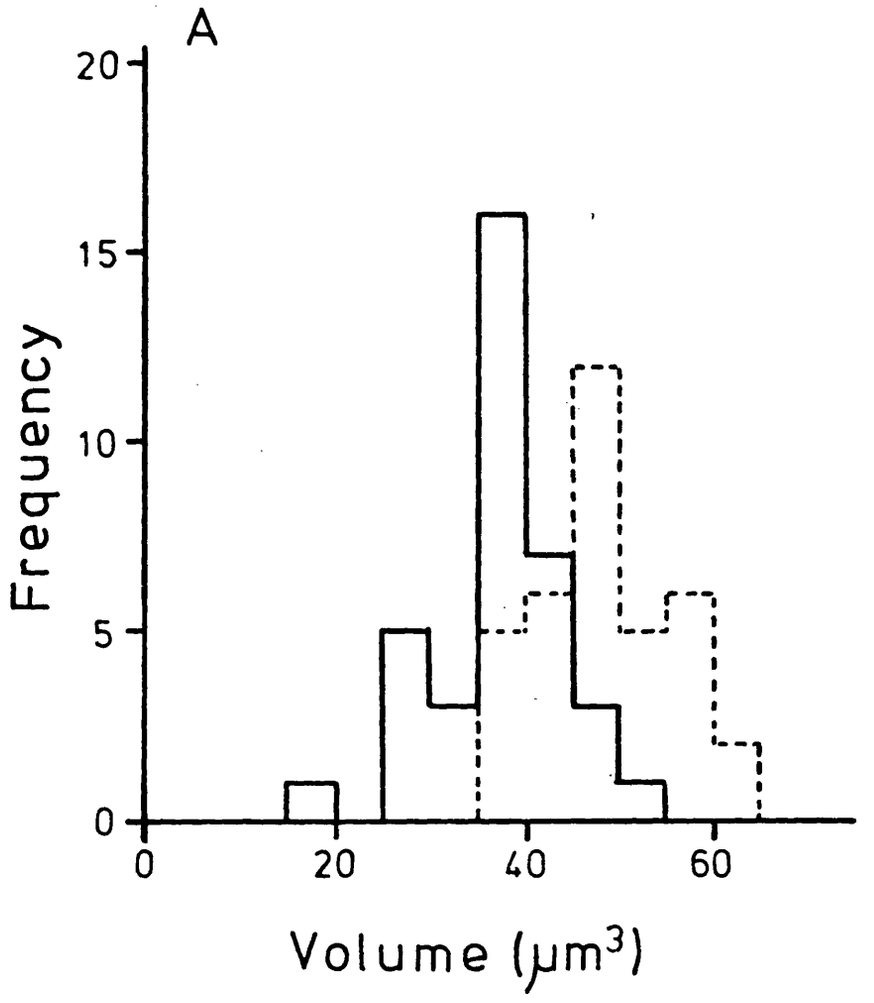
A
20
15
10
5
0
Frequency
0
20
40
60
Volume (μm³)

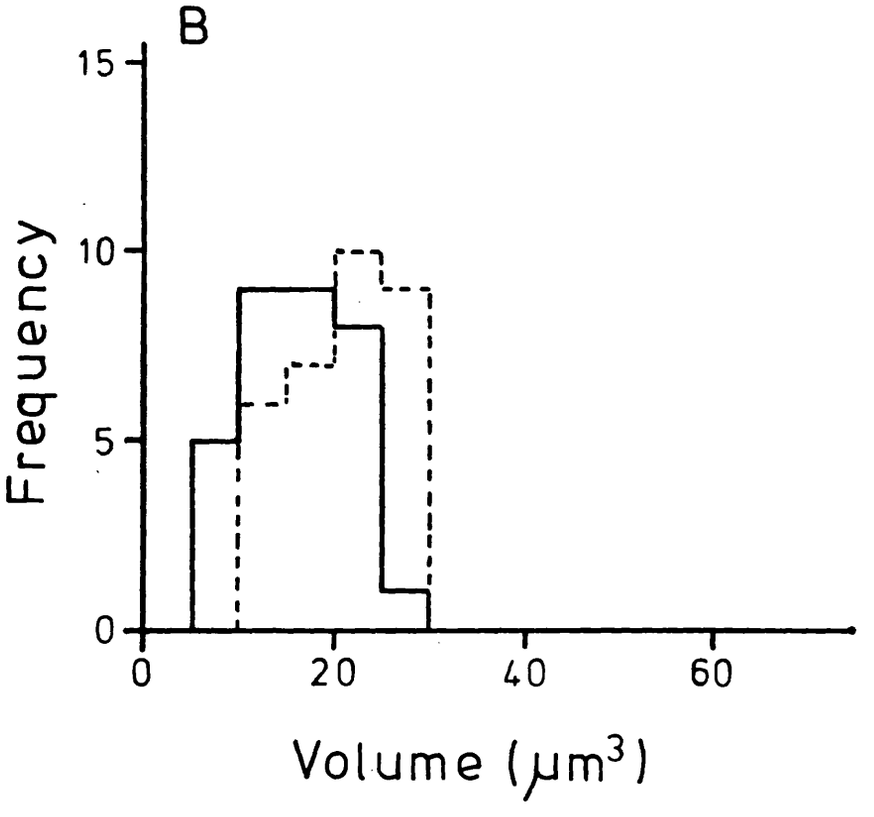
B
15
10
5
0
Frequency
0
20
40
60
Volume (μm³)

TABLE 9. The mean volumes of daughter cells of strains SA and S67.3a at three stages of the cell cycle.

Strain	Mean volume (μm^3)		
	Birth	Bud emergence	Cell separation
SA	37.2 (6.9)*	48.3 (7.5)	53.0 (7.6)
S67.3a	16.3 (5.3)	20.2 (5.4)	21.7 (5.0)

* standard deviations in brackets.

Figure 21

Cell size at cell separation versus the duration of the subsequent unbudded period.

A - SA cells; B - S67.3a cells; (▲), parent cells; (△), daughter cells. The correlation coefficients of daughter cell size at cell separation versus the duration of the unbudded period are: A,-0.54; B,-0.70.

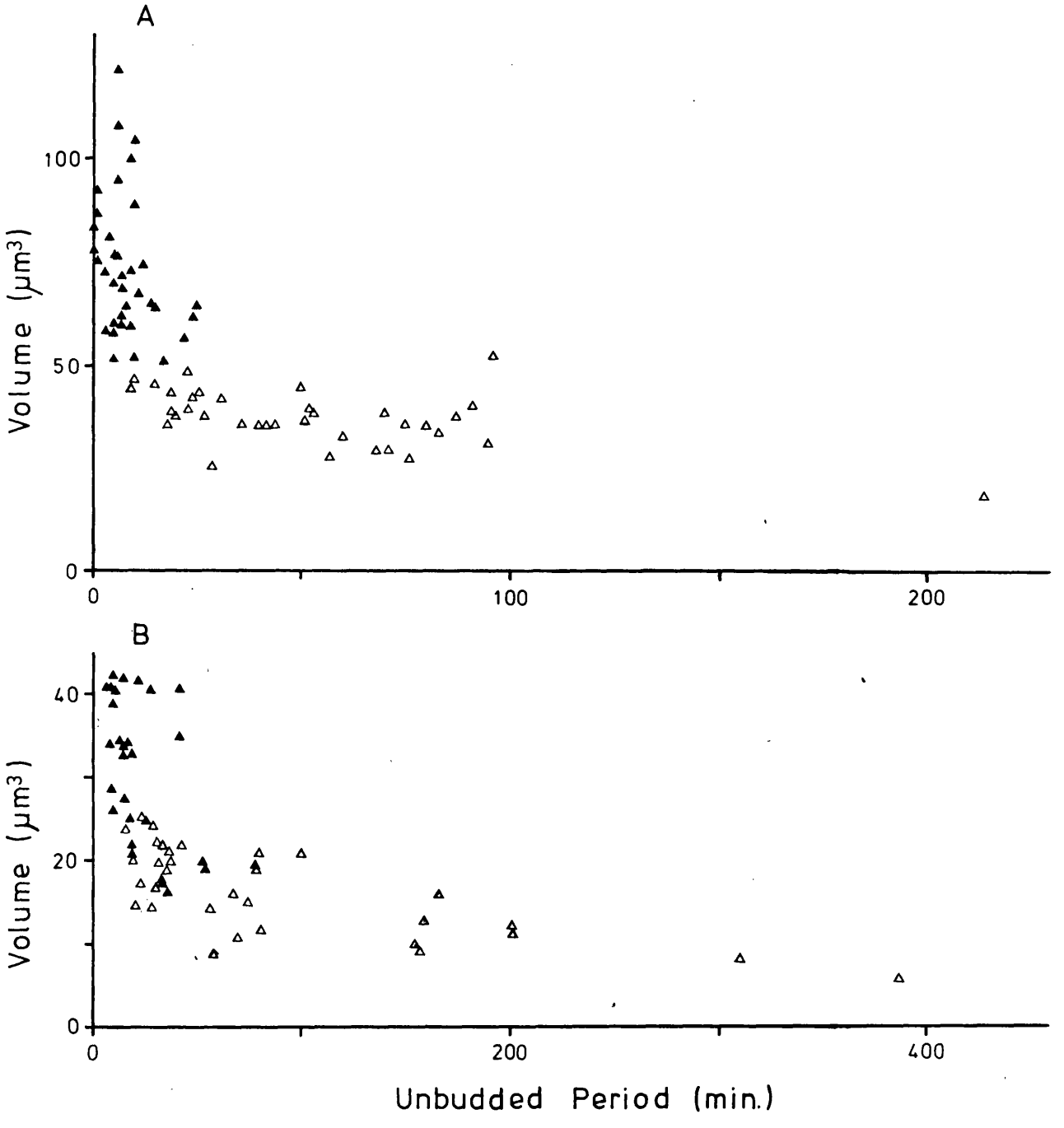
A
B
Volume (μm³)
Volume (μm³)
0
50
100
0
100
200
0
20
40
0
200
400
Unbudded Period (min.)

determining the length of the unbudded period for parent cells although some of the parent cells whose birth size is less than 20 μm^3 do have longer unbudded periods than the other parent cells. This suggests that the size of these parent cells has some influence over the length of their unbudded periods. In comparison to SA parent cells the larger S67.3a parent cells have a broader distribution of times spent in the unbudded period. Whereas for SA cells the data points for parent and daughter cells form discrete clusters, the points for S67.3a cells interdigitate.

The size of daughter cells at bud emergence is correlated with their size at birth in the case of S67.3a cells ($r=0.69$) whereas there is negligible correlation between these parameters in the case of SA cells ($r=0.21$). This may indicate that S67.3a daughter cells must increase in size by a 'constant' amount before they can produce a bud.

Discussion

The comparison of these strains is rendered difficult because of the difference in the growth rates under equivalent environmental conditions. It is well known that the size at bud emergence (and by inference the size at start) decreases as the growth rate decreases (Johnston *et al*. 1979, Tyson *et al*. 1979). Howevever, the magnitude of the difference in size at bud emergence between these strains is too great to be simply due to the modest difference in the growth rates.

It is clear from Table 8 that the rate limiting step in the cell cycle of *whi 1* cells occurs during the unbudded period, as it does for wild type cells, since the variability in cycle times is largely due to the variability in the duration of the unbudded period. The predominant effects of the *whi 1* mutation are that *whi 1* cells produce buds at a smaller size than do wild type cells and that the duration of the unbudded period (particularly of daughter cells) is more variable in *whi 1* cells than in wild type cells.

The budded period of whi 1 cells is of more variable duration but this is more likely a consequence of the slower growth rate (see Chapter 4) than a direct consequence of the whi 1 mutation.

The question is, 'what determines the rate of proliferation of whi 1 cells?'. If the size control is completly absent in whi 1 cells as a result of the mutation then entry into the cell division sequence should be solely probabilistic, the exponential rate constant being the same for both parent and daughter cells. This would be due to the elimination of the C period (period of growth between division and attainment of a critical size) according to the Tandem model (Shilo et al. 1976, 1977) or due to loss of modulation (by size) of the probability of entering the cell division sequence according to the SSC model (Wheals 1982). The results indicate, however, that this is not the case. If whi 1 cells were under solely probabilistic 'control', then: 1) the mean parent cycle time would be the same as the mean daughter cycle time; 2) the variances of the parent and daughter cycle times would be equal; 3) there would be no correlation between the size of daughter cells at birth and the duration of their subsequent unbudded period; and 4) there would be a correlation between the size of daughter cells at birth and at bud emergence. Only 4) is true of whi 1 cells.

The difference between the parent and daughter cycle times (Table 8), the difference between the sizes at division of parent and daughter cells (not shown),and the correlation between the birth size of daughter cells and the duration of their subsequent unbudded period (Fig. 21), together suggest that whi 1 cells have some element of size control. This control may be the same, although defective, size control mechanism as operates in wild type cells. Alternatively a size related factor not evident in wild type cells may account for the dependancy of duration of the unbudded daughter cells on their size at birth. For example, the correlation between the size at birth and the size at bud emergence may imply that

whi 1 daughter cells must increase in size by a constant amount before they can initiate the cell division sequence. However, it would be necessary to assume that small cells take longer to increase in size by this amount than large cells to account for the correlation between birth size and the duration of the unbudded period. This assumption cannot be satisfactorally tested with the data but it is worth noting than a clone showing the fastest rate of growth (in size) was comprised of some of the smallest cells (see Chapter 7). It would also be necessary to assume that the size increment is not a prerequisite for whi 1 parent cells to initiate the cell division sequence since parent cells show little increase in size between division and bud emergence (data not shown).

The same size control as in wild type cells may be operative in whi 1 cells, certainly the α plots of cycle times of whi 1 cells (Fig. 18) could be accounted for by both the SSC model (Wheals 1982) and the modified Tandem model (Shilo et al. 1976, 1977 and Chapter 4). However, in terms of these models some parameters, including cell size, are different in whi 1 cells than in wild type cells. This is evident since i) the unbudded periods of both parent and daughter whi 1 cells are much more variable in duration than expected solely from their slower growth rate and ii) in Fig. 21B the parent and daughter cell data points of whi 1 cells interdigitate to a large extent, whereas there is little or no interdigitation of these data points for wild type cells (Fig 21A, see also Fig. 15, Chapter 4).

To account for these results the parameters of the modified Tandem

model must be different for whi 1 cells than for wild type cells in the following ways. 1) The mean critical size, $\bar{V}_c$, must be smaller. 2) The transition probability value must be lower. 3) The variation around $\bar{V}_c$ must be larger. The reason for 1) is obvious from the results. 2) provides an explanation for the larger variance of the duration of the parental unbudded period. Assumption 3) helps to explain the interdigitation of the data points in Fig. 21B. If 3) holds, then those daughter cells which produce buds at the smallest sizes would, after division, tend to be smaller than $\bar{V}_c$. Consequently these, now parent cells would be more likely to require a period of growth (C period) before entering the A state than parent cells whose post-division size is above $\bar{V}_c$. A broad distribution of $\bar{V}_c$ would also lead to a larger overlap between the distribution of daughter cell sizes at bud emergence and the distribution of their sizes at their subsequent division. Indeed, the distributions for whi 1 cells do overlap to a greater extent than do the distributions for wild type cells (Table 9). It follows from this that more parent cells are born of a smaller size than the larger of the daughter cells in a population of whi 1 cells. The interdigitation of the data points in Fig. 21B is thus explained by the presence of parent cells which are smaller than some of the daughter cells and these parent cells will have unbudded periods of equivalent durations to those of the larger daughter cells.

In terms of the SSC model, the differences in the parameters between

whi 1 and wild type cells are likely to be as follows. 1) The plateau probability value must be attained at roughly half the cell size that wild type cells attain the plateau value since whi 1 cells are smaller at bud emergence. 2) The plateau value must be lower for whi 1 cells to account for the larger variability in the duration of the unbudded period (especially of the larger parent cells). 3) The coefficient of variation of the daughter cell sizes at bud emergence is larger for whi 1 cells (26.7% as opposed to 15.5% for SA cells) which suggests that the difference in transition probability between the smallest and the largest daughter cells is not as great as it is for SA (wild type) cells. This implies a shallower sigmoidal relationship between transition probability and cell size. These differences in the parameters are illustrated in Fig. 22.

The interdigitation of parent and daughter cell data points in Fig. 21B can be explained as a consequence of i) the broader distribution of daughter cell sizes at bud emergence (and by inference at start) since this would lead to the production of parent cells which are smaller than some (but not their sibling) daughter cells, and ii) the volume accumulated during the budded period which is retained by the parent cells (see Table 9) would not be sufficient for the smaller of the parent cells to raise their transition probabilities above those of the larger of the daughter cells, as it would in the case of wild type cells.

The correlation observed between the sizes at birth and at bud emergence of whi 1 daughter cells can be explained as a consequence of the altered parameters of either of the two models. With both models V_c is variable, although the cause of the variability is different. If the parameters are altered as above, the variability of V_c is larger for whi 1 cells than for wild type cells. This leads to a lower correlation between the size accumulated during the unbudded period and the size at birth of whi 1 daughter cells (which was observed). Consequently, there will be

Figure 22

The theoretical relationship between transition probability and cell size of strains SA and S67.3a.

A - SA cells; B - S67.3a cells.

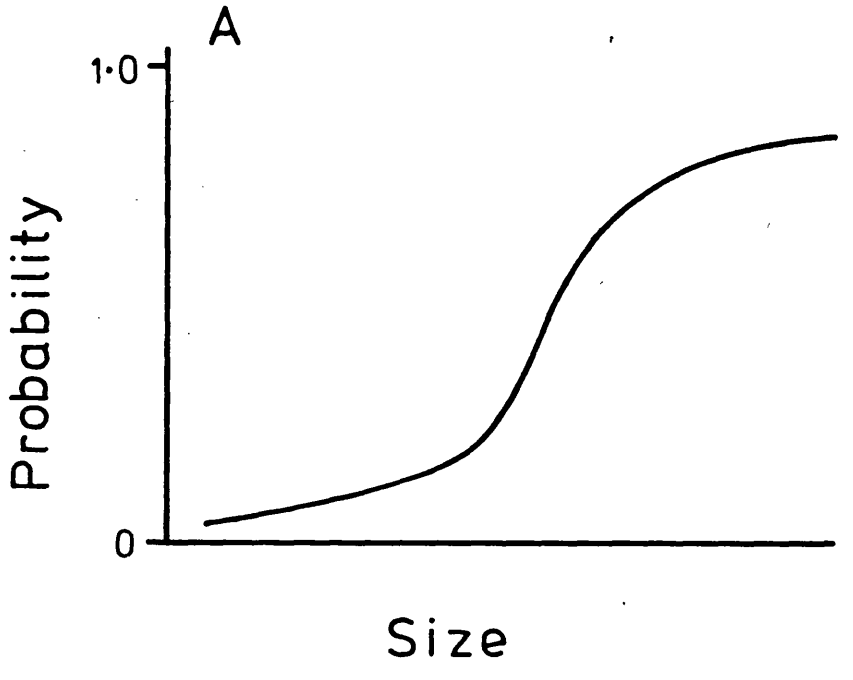
A
1·0
Probability
0
Size

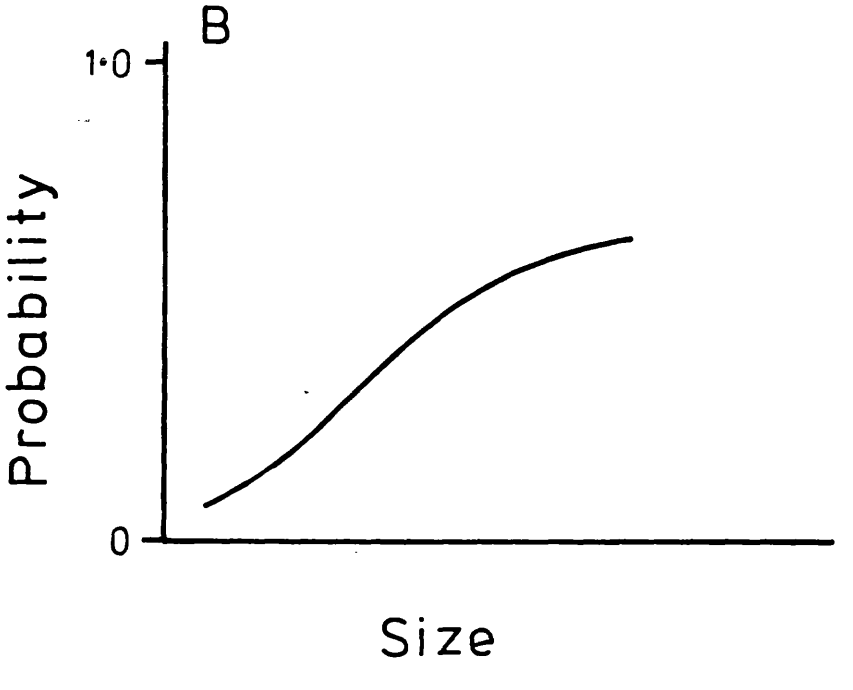
B
1·0
Probability
0
Size

a larger correlation between the sizes at birth and at bud emergence for whi 1 daughter cells.

As with the wee mutants of Schiz. pombe, the whi 1 mutant of S.cerevisiae retains a size control. In this respect the small size mutants of these organisms are analogous. The fact that wee mutants possess a functional size control is simply explained by the existence in Schiz. pombe of two independent size controls over two temporally distinct cell cycle events. The wee mutants have defects in the size control expressed in G2 over mitosis, but are subject to a size control expressed in G1 over the initiation of DNA synthesis (Nurse & Thuriaux 1977, Nasmyth 1979). An analogous explanation for the size control of whi 1 mutants is not as tenable. There is no known event prior to start over which a 'cryptic' size control could occur. Start is by definition the earliest cell cycle specific event (Hartwell 1974). Since post-start events occur in two or more independent pathways (Hartwell and Pringle, 1981) it is highly unlikely that there is a size control over a post-start (but pre-bud emergence) event which would not affect the timing (and the variability in the timing) of post-start functions in whi 1 cells.

Clearly the only event over which the size control of whi 1 cells can reasonably affect is start. Sudbery et al. (1980) found that the mean size (of budded parent cells) of whi 1 haploids, whi 1/whi 1 diploids, WHI 1 haploids, whi 1/WHI 1 diploids and WHI 1/WHI 1 diploids are roughly in the ratio of 1:2:2:3:4. This observation led Sudbery et al. to suggest that the small size of whi 1 cells is due to a gene dosage effect. They hypothesized that there are two genes (whi 1 mutants defining one of them) whose products act in parallel, the cell size at bud emergence (and by inference, at start) being proportional to the combined number of the two genes (call this the 2-gene hypothesis). However, the two genes need not necessarily be different. An alternative hypothesis to explain

the gene dosage effect is that the WHI 1 gene is present in two copies per haploid complement (duplicate gene hypothesis). In this hypothesis a whi 1 mutant would contain one defective and one functional copy of the WHI 1 gene.

The properties of the size control are similar in wild type and in whi 1 cells. For example, the (daughter) cell size at bud emergence is growth rate-modulated in both whi 1 and wild type strains (B.L.A. Carter, personal communication). This is to be expected by the duplicate copy hypothesis but in the case of the 2-gene hypothesis it is necessary to assume that the unidentified gene is also subject to this modulation. That the size control of whi 1 cells is slightly different from that of wild type cells (e.g. cell size at bud emergence is more variable for whi 1 daughter cells) lends some support to the 2-gene hypothesis. It is reasonable to expect that there are small differences in the behaviour of two non-identical gene products even if they do have the same function. However, there may be some physical constraints imposed on whi 1 cells (which affect the size control) simply because they are small. The clonal growth rates of whi 1 cells are more variable than those of wild type, SA, cells (see Chapter 7) and this may be a consequence of the small size of whi 1 cells. So the duplicate copy hypothesis is still plausible in spite of the slight difference in the size control of whi 1 cells. Clearly more direct evidence is required to distinguish between the two hypotheses.

CHAPTER SIX

Chapter 6

Alterations in the timing of start in response to perturbations

Introduction

The difference between the parent and daughter cycle times in exponentially growing populations of S.cerevisiae can be broadly explained by the existence of a size control over start and the asymmetrical mode of division (Hartwell and Unger 1977), although the data in Chapter 4 suggest that there may be an additional factor involved which is independent of cell size. To examine further the importance of size in determining the cycle time difference I have compared the timing of start in parent and in daughter cells in conditions where daughter cells are large enough to prevent size being rate-limiting for start. I have used two methods of obviating the effect of cell size for this comparison.

Singer and Johnston (1981) have reported that the G_1 period of S.cerevisiae cells is shortened when S phase is lengthened by incorporating a low concentration of hydroxyurea (HU) in the growth medium. Their formal explanation for this is that daughter cells are born at a larger size due to the extended budded period (which is due to the lengthened S phase) and therefore need less time to attain a 'critical size' for start than daughter cells grown in the same medium but without HU. They further showed that it was that part of G_1 between cytokinesis and start which was reduced. In addition, they reported that there was a tendency for daughter cells to produce buds at the same time as their sibling parent cells, in the presence of HU. The predictions of both the modified Tandem and the SSC models are that not only should the mean daughter cycle time approach the mean parent cycle time in length but the rate of traverse of

start should also be the same for parent and daughter cells in low concentrations of HU. I have filmed cells growing in steady state in low concentrations of HU to see if the predictions of the models are fulfilled.

Shilo et al. (1976, 1977) obtained evidence that cells released from start arrest traverse start with the same kinetics as exponentially-growing cells. They did not measure the size of cells, so they could not conclude unambiguously that a size control was not exerting an effect. Neither did they distinguish between parent and daughter cells, so they could not determine whether or not the kinetics of traverse of start were different for parent and daughter cells following release from arrest at start. α factor inhibits start in a strains but does not inhibit growth (Hereford & Hartwell 1974, Throm & Duntze 1970). Using α factor I have accumulated cells at start and released them after sufficient time for daughter cells to attain a size at which they should be as competent as parent cells to traverse start. The Tandem and SSC models predict that after release from start arrest, parent and daughter cells should traverse start with the same kinetics. I have compared the kinetics of the traverse of start following release, of parent and daughter cells by following the kinetics of bud emergence using time-lapse cinephotomicrography. Shilo et al. (1976) showed that the rate of bud emergence provides a good estimate of the rate of emergence from start.

Results

A. The kinetics of cell proliferation in low concentrations of hydroxyurea.

Time-lapse cine films were made of A364A cells growing on YEP Galactose-PVP medium with and without HU, in a Powell chamber at 30°C. This medium was chosen because there is a large difference between the cycle times of parent and daughter cells growing on this medium (see Chapter 4). Three films were analysed; of cells growing in the absence

of HU, and in the presence of 1.5 mg/ml and 2.5 mg/ml HU. In each case the cells were judged to be in exponential growth by some or all the criteria referred to in Chapters 4 and 5. The values of τ and τ_v are given in Table 10. As in the previous analyses $\tau < \tau_v$.

The mean durations of the cell cycle and its constituent periods for parent and daughter cells are listed in Table 11. Cells grown in the presence of HU have longer budded periods than cells grown in the absence of HU. There was little increase in the duration of the periods from nuclear migration to cell separation with increasing concentrations of HU. These results are consistent with S phase being lengthened by the addition of HU to the medium (Singer & Johnston 1981). Nuclear division and consequently cytokinesis and cell separation are thus delayed since nuclear division is dependent on the completion of DNA synthesis (Hartwell 1974). Nuclear migration is also delayed so there may be some dependency for this event on the completion of DNA synthesis. The parent cycle time increases with increasing concentrations of HU due to the expansion of the budded period. The parental unbudded period is unaffected by the presence of HU. The increased variance of the parent cycle times in the presence of HU is due to the increased variance of the budded period. The mean parent cycle time is less than the mean daughter cycle time in the presence or in the absence of HU, although the difference between the means is less for cells grown in the presence of HU. In the absence of HU and in the presence of 1.5 mg/ml HU, all daughter cells had a longer unbudded period than their sibling parent cells whereas in the presence of 2.5 mg/ml HU all except 6 daughter cells had longer unbudded periods than their sibling parent cells (data not shown). The mean daughter cycle time in the presence of 1.5 mg/ml HU is slightly less than that in the absence of HU. There was a marked increase in the mean length of the daughter cycle time in the presence of 2.5 mg/ml HU. The mean duration of the unbudded period of daughter cells decreased with increasing

TABLE 10. Values of τ and τ_v in different concentrations of hydroxyurea.

Concentration of hydroxyurea (mg/ml)	τ (min.)	τ_v (min.)
0	103.4	135.2
1.5	118.0	141.3
2.5	138.1	NM*

* NM - not measured.

TABLE 11. The mean durations of the cell cycle and constituent periods for parent and daughter cells in each concentration of hydroxyurea.

Period	Concentration of HU (mg/ml)					
	0		1.5		2.5	
	P[a]	D[a]	P	D	P	D
Cycle time	78.2	133.2	107.1	128.8	122.1	147.3
	(9.1)[b]	(21.2)	(18.3)	(21.6)	(17.7)	(24.2)
Unbudded period	8.0	59.1	6.6	26.8	6.2	17.9
	(4.6)	(18.5)	(7.2)	(14.1)	(5.6)	(12.3)
Budded period	70.2	74.2	100.5	102.1	115.9	128.5
	(7.7)	(6.7)	(13.9)	(12.6)	(16.9)	(17.5)

TABLE 11. - continued.

Bud emergence to nuclear migration	44.7 (7.1)	49.3 (6.2)	71.1 (11.8)	73.3 (11.0)	81.0 (15.9)	90.7 (16.5)
Nuclear migration to nuclear division	8.1 (1.5)	7.8 (1.2)	11.2 (4.3)	10.9 (3.3)	13.2 (4.8)	16.8 (6.1)
Nuclear division to cytokinesis	8.3 (2.2)	8.2 (2.3)	9.4 (2.3)	9.0 (2.3)	9.7 (3.4)	12.0 (4.3)
Cytokinesis to cell separation	9.1 (2.0)	8.9 (1.6)	8.9 (1.6)	8.9 (1.6)	12.0 (3.8)	10.0 (2.5)

All values in minutes. 40 parent and 40 daughter cycles were monitored in each case.

[a] P - parent cells, D - daughter cells; [b] values in brackets are standard deviations. Data were pooled as in Table 5.

concentrations of HU. The variability of the unbudded period gave an increasing contribution to the variability of the daughter cycle time with increasing concentrations of HU.

The rationale behind these experiments was to increase the size of daughter cells at birth so that they are born of a size either above a 'critical size' (in terms of the Tandem model) or with a transition probability as high as parent cells (in terms of the SSC model). It can be seen in Table 12 that the mean birth size of daughter cells growing in the presence of 1.5 mg/ml HU is larger than the mean daughter cell at bud emergence in the absence of HU. It is also evident that in the presence of HU the mean increase in cell volume of daughter cells from birth to bud emergence is less than in the absence of HU. The distributions of daughter cell size at birth and at bud emergence in the absence and in the presence of HU are presented in Fig. 23. The majority of daughter cells in the presence of HU are born at a size greater than the mean daughter cell size at bud emergence in the absence of HU. The difference in the timing of start between parent and daughter cells which is due to a size control should therefore be negligible in the concentrations of HU used.

In this study it is particularly important to compare the α plots of the durations of the unbudded period since the budded period is more directly affected by HU. It is clear from Table 11 that HU increases the length and the variability of the budded period and consequently with increasing concentrations of HU the distributions of the lengths of the budded period will have an increasing effect on the shape of the α plots of cycle times. The distributions of the lengths of the unbudded periods of parent and daughter cells in the absence and in the presence of HU are presented as α plots in Fig. 24. The α plot of parent unbudded periods is little affected by the presence of HU. HU has a considerable effect on the shape of the α plot of daughter unbudded periods.

TABLE 12. The mean size of daughter cells, at three stages in the cell cycle, in the absence and in the presence of hydroxyurea.

	Mean size (μm^3)		
	Birth	Bud emergence	Cell separation
Without HU	26.8	37.6	38.2
	(7.0)*	(8.3)	(7.7)
With 1.5 mg/ml HU	46.1	54.2	55.8
	(11.3)	(10.2)	(9.5)

* values in brackets are standard deviations.

Figure 23

The distribution of the sizes of daughter cells at two stages of the cell cycle.

Histograms of the sizes of daughter cells at birth (solid line) and at bud emergence (broken line). A - cells growing in the absence of HU; B - cells growing in the presence of 1.5 mg/ml HU.

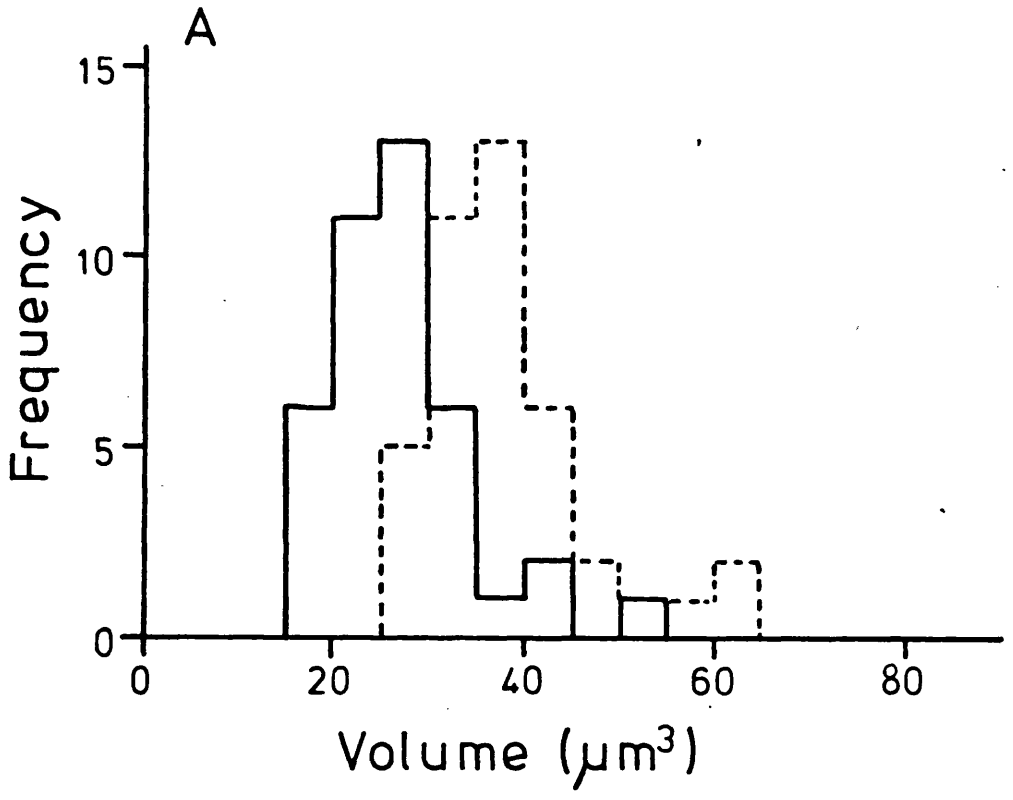
A
15
10
5
0
Frequency
0
20
40
60
80
Volume (μm³)

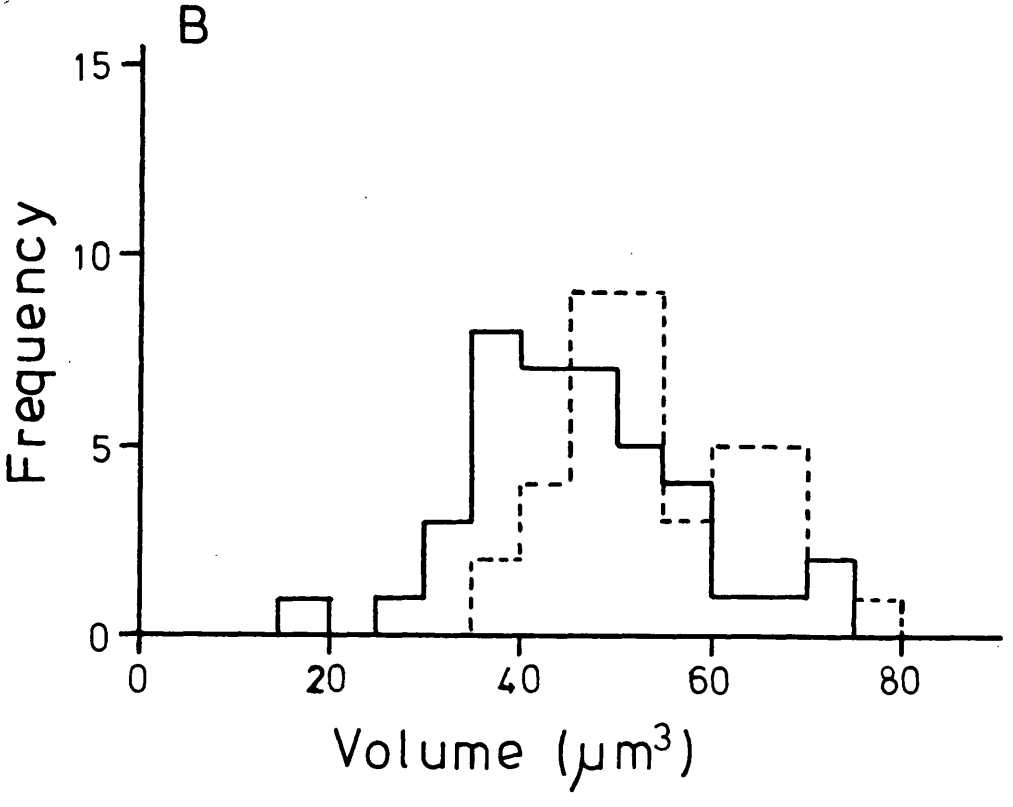
B
15
10
5
0
Frequency
0
20
40
60
80
Volume (μm³)

Figure 24

∝ plots of the unbudded periods of parent and daughter cells growing in the absence and in the presence of HU.

The percentage of cells with unbudded periods of duration, t_{ub}, greater than or equal to t (on a logarithmic scale) versus t. Data are of cells growing: in the absence of HU (o,●); in the presence of 1.5 mg/ml HU (△,▲); in the presence of 2.5 mg/ml HU (□,■). Open symbols, parent cells; closed symbols, daughter cells.

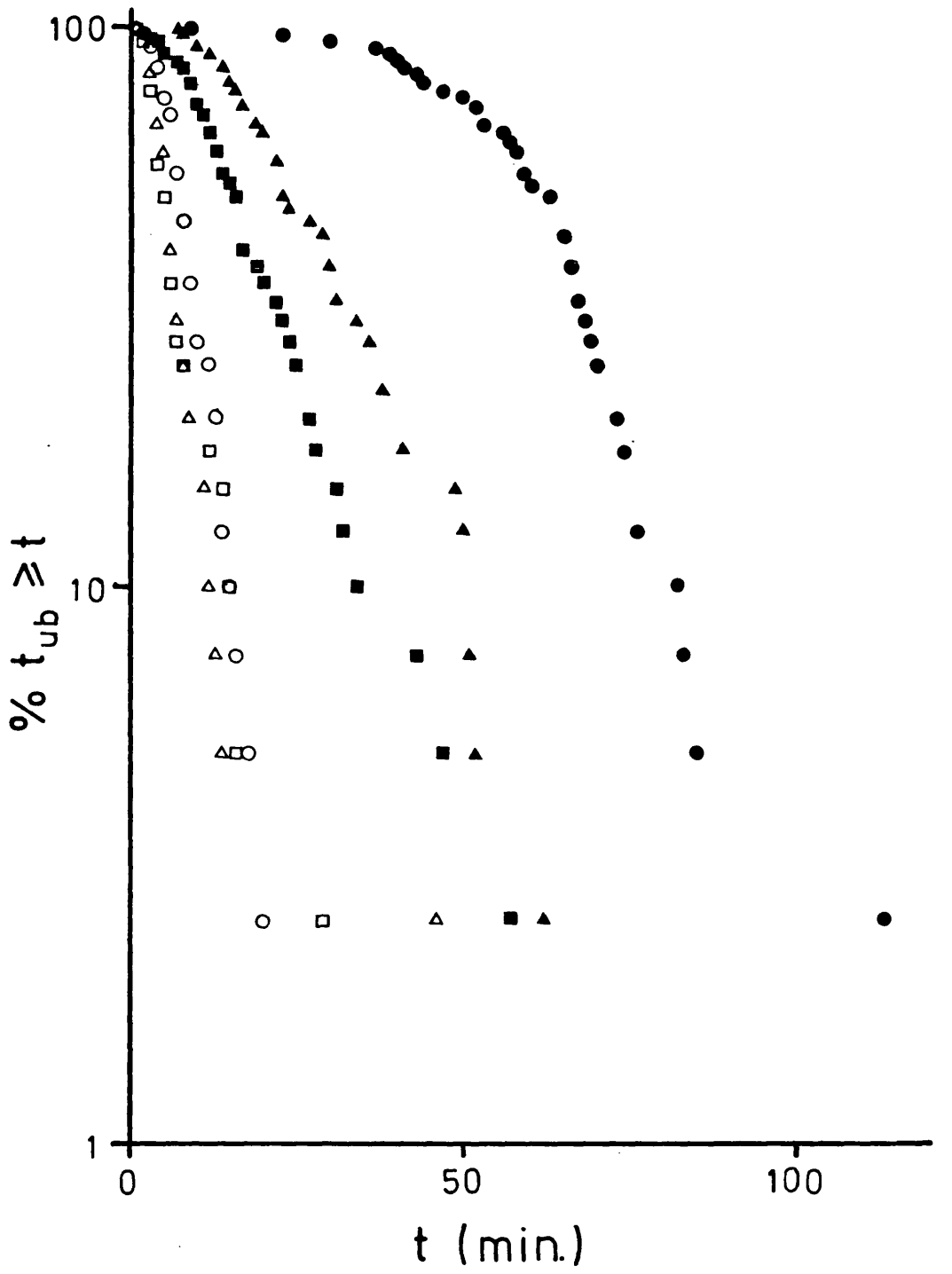
100
10
1
0
50
100
% $t_{ub} \geq t$
t (min.)

In the absence of HU this α plot has a pronounced initial downward curvature, which includes about 50% of the data, before becoming approximately linear. This initial curvature is greatly reduced in the presence of HU. All the daughter unbudded periods are shorter in the presence than in the absence of HU, the α curves are shifted more to the y axis as the concentration of HU is increased. There is little difference in the slopes of the (approximately) linear portions of the three curves of the daughter unbudded periods but in each case the slope is less steep than the slope of the corresponding parent α curve.

The relationship between cell size at cell separation and the length of the subsequent unbudded period is shown in Fig. 25 for cells grown in the absence and in the presence of 1.5 mg/ml HU. In both cases there is no correlation between the size at cell separation of parent cells and their subsequent unbudded period. There is a correlation between the birth size of daughter cells and the length of their unbudded period ($r=0.66$, which is significantly different from 0 at the 0.1% level) in the absence of HU. In the presence of 1.5 mg/ml HU there is less correlation between these parameters ($r=0.42$, which is not significantly different from 0). Therefore size does not play a role in determining the length of the unbudded period for cells grown with HU. The data points for HU grown daughter cells merge into the data points of HU grown parent cells because of the broader distribution of birth sizes and the shorter unbudded periods.

B. Release from α factor arrest

For this experiment cells of A364A were filmed growing on YEP Galactose-PVP medium at 30°C in the Powell chamber. At t=200 minutes α factor was added. This was achieved by replacing the medium in the reservoir with YEP Galactose-PVP medium containing α factor at a concentration of 5 μg/ml at t=198 minutes and adjusting the flow rate to maximum. After 5 minutes the flow rate was returned to the original

Figure 25

Cell size at cell separation versus the duration of the subsequent unbudded period in different concentrations of HU.

A - cells growing in the absence of HU; B - cells growing in the presence of 1.5 mg/ml HU. (△) parent cells; (▲) daughter cells. The correlation coefficients of daughter cell size at cell separation versus the duration of the unbudded period are: A,-0.66; B,-0.42.

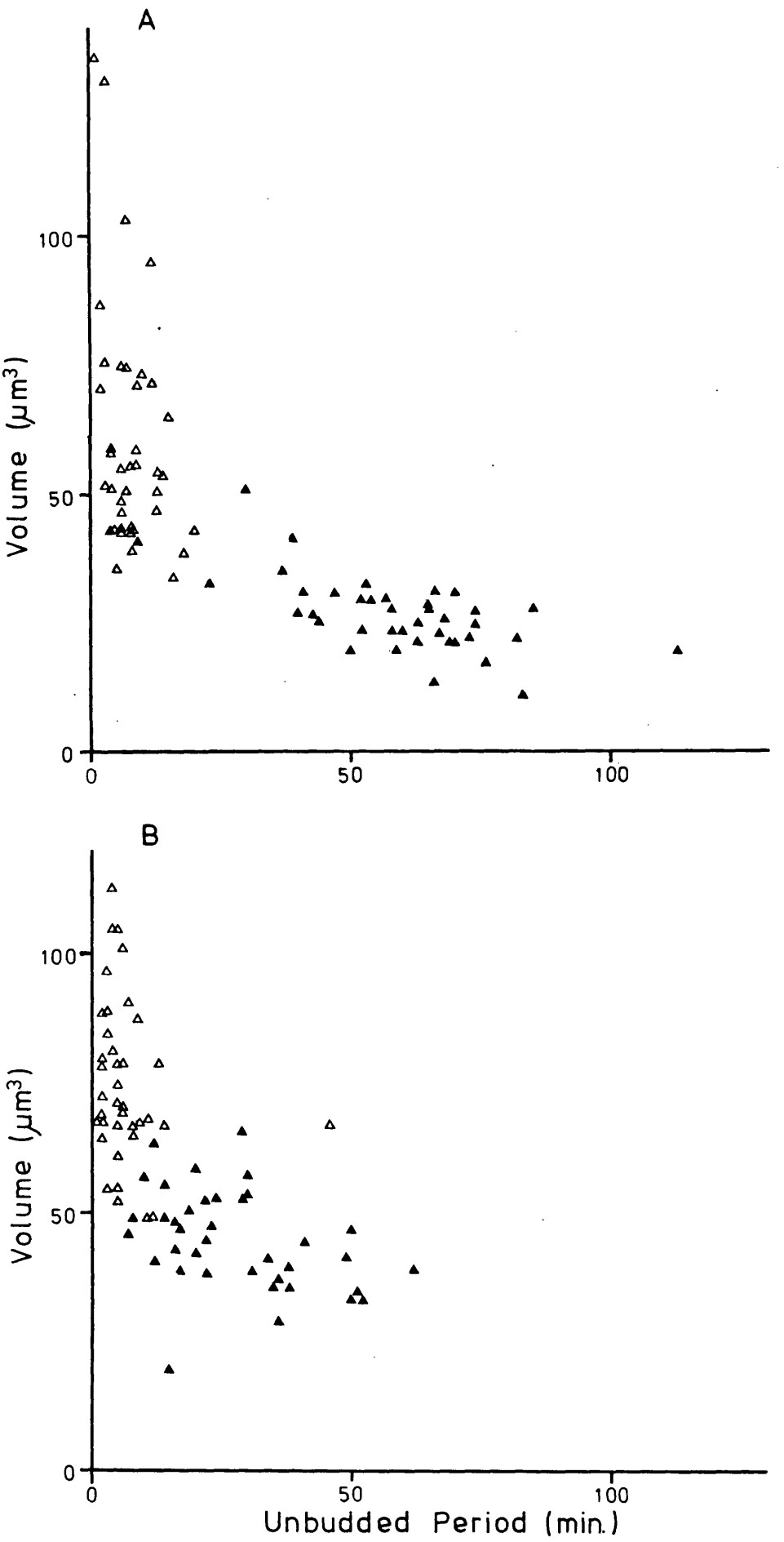
A
B
Volume (μm³)
100
50
0
0
50
100
Unbudded Period (min.)

setting. This procedure ensured that the α factor-containing medium came into contact with the cells at t=200 minutes and that all the medium without α factor was fully replaced in the chamber. α factor was removed at t=395 minutes by repeating the above procedure in reverse. The cells were exposed to α factor for a time at least as long as the longest daughter cycle time so that on release most or all daughter cells would be as large or larger than daughter cells at bud emergence in the medium without α factor. Filming was stopped when it was judged that all cells had produced a bud following α factor release.

In the analysis of the film all cells of each clone in focus were scored. The cells in even the largest clone were easily identified and followed since after release the cells produced buds orientated away from the centre of the clone in a radial array. The curve of increase in cell number with time is shown in Fig. 26. Complete cessation of division occurred 100 minutes after addition of α factor. The population doubling time was calculated, from the values at t=30 to 210 minutes inclusive, to be 113 minutes.

The mean durations of the measured periods in the cell cycle of cells prior to α factor arrest and of cells after α factor release are compared in Table 13. It should be noted that the unbudded period of cells following α factor release refers to the period of time from α factor release (i.e. t=395 min.) to bud emergence. The mean duration of the periods between nuclear migration and cell separation are equivalent for cells before α factor arrest and after α factor release. The budded period of cells after α factor release is, however, about 10 minutes shorter than that of cells before α factor arrest. Since the period between bud emergence and nuclear migration is shorter for cells after α factor release, either bud emergence may be delayed or those events which occur during this period may be completed quicker. The most interesting feature

Figure 26

Growth curve during the course of the ∝ factor arrest experiment.

∝ factor was added to the medium at t = 200 min. and was removed from the medium at t = 395 min.

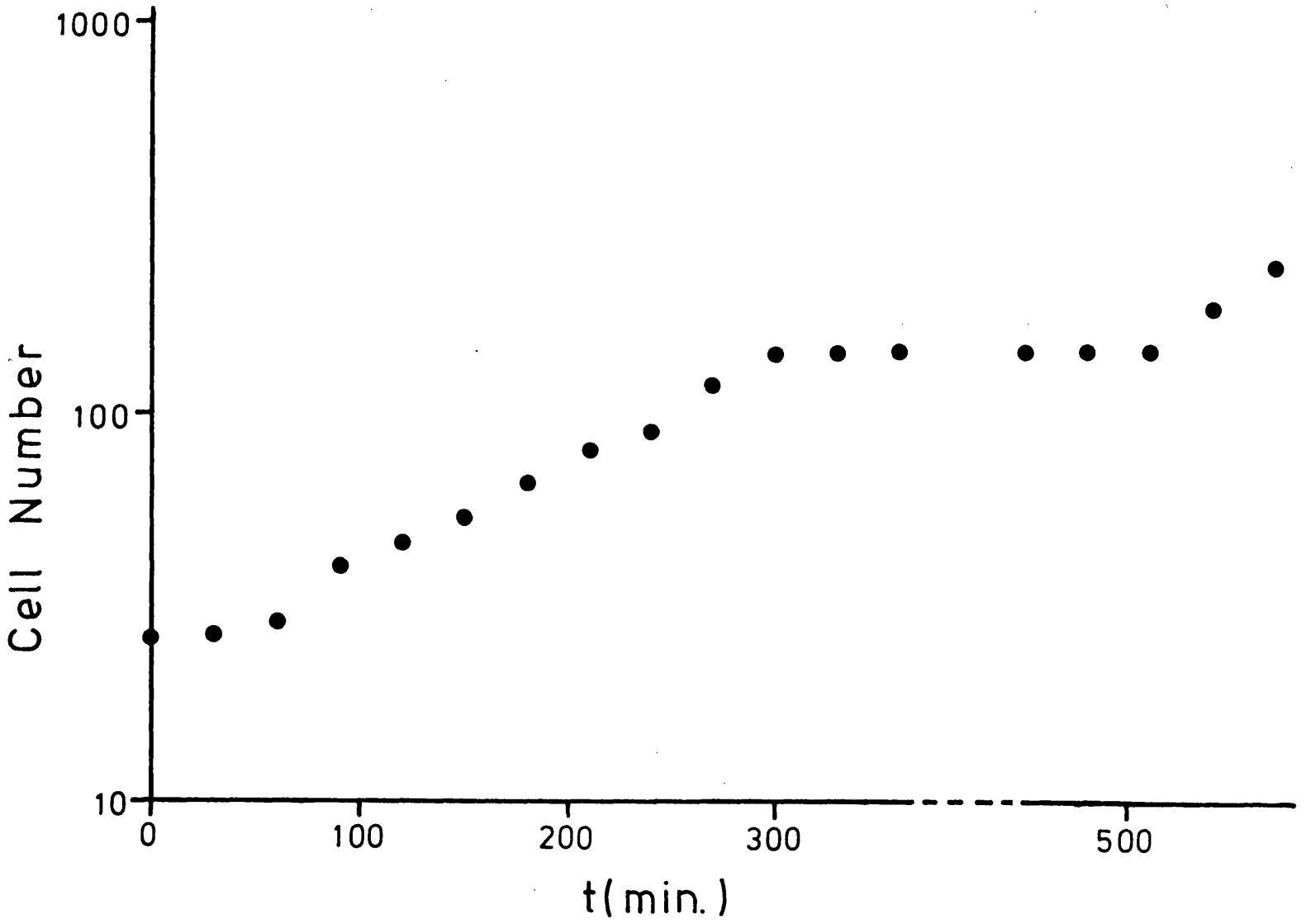
1000
100
10
Cell Number
0
100
200
300
500
t(min.)

TABLE 13. The mean durations of constituent periods of the cell cycle prior to and following release from ∝ factor arrest.

Period	Before ∝ factor arrest		After release from ∝ factor arrest	
	P[a]	D[a]	P	D
Cycle time	90.8 (9.9)[b]	129.6 (28.6)		
Unbudded period[c]	9.2 (6.4)	45.3 (25.9)	81.2 (24.7)	115.9 (34.3)
Budded period	81.6 (7.9)	84.1 (8.5)	73.2 (5.1)	71.8 (7.3)
Bud emergence to nuclear migration	51.6 (6.7)	55.6 (7.3)	44.1 (4.4)	43.8 (5.9)

TABLE 13. continued.

Nuclear migration to nuclear division	9.4 (2.0)	8.5 (1.9)	9.0 (2.3)	8.2 (1.7)
Nuclear division to cytokinesis	9.4 (3.0)	9.6 (2.5)	9.6 (2.8)	9.6 (2.4)
Cytokinesis to cell separation	11.3 (3.4)	10.9 (2.0)	10.6 (2.7)	9.9 (3.0)

All values are in minutes. 55 parent and 38 daughter cycles were monitored before ∝ factor arrest. After release from ∝ factor arrest, the unbudded periods of 64 parent and 78 daughter cells were measured and of these, 56 parent and 34 daughter cells were monitored through to cell separation. [a] P - parent cells, D - daughter cells; [b] standard deviations in brackets; [c] in the case of cells released from ∝ factor arrest the unbudded period refers to the time from removal of ∝ factor from the medium to bud emergence.

of these data is that parent cells have a shorter unbudded period than daughter cells both before α factor arrest and after α factor release, the mean differences being 36.1 and 34.7 minutes respectively.

The mean size of daughter cells at the time of α factor release was 58.3 μm^3 which is larger than the mean size of daughter cells at bud emergence (47.7 μm^3) before α factor arrest, although the distributions of the two sizes overlap completely (Fig. 27). Since there may be a substantial lag period after α factor release during which cells are unable to traverse start (Samokhin et al. 1981 and Fig. 28) it is likely that all daughter cells will be above a critical size (Tandem model) or will be in the high transition probability size range (SSC model). After α factor release, therefore, daughter cell size should not be a determining factor for traverse of start. Indeed there is no significant correlation between the size of daughter cells at α factor release and the time from α factor release to bud emergence (r=0.38).

Assuming that the lag period after α factor release is approximately the same for each cell (i.e. the lag period has little variability) the period of time from α factor release to bud emergence is comparable to the time from start to bud emergence since the duration of each is determined mainly by the rate of completion of start. Both the Tandem and the SSC model provide the same clear prediction about the shape of the α plots of the distributions of the length of time from α factor release to bud emergence for parent and daughter cells, namely that after a lag period, approximately constant for all cells, the α plots of this period should become linear and should be the same for parent and daughter cells and the linear portions of these α plots should be approximately parallel to the α plot of the lengths of the unbudded periods of parent cells prior to α factor arrest. These α plots are presented in Fig. 28.

The following features are evident from Fig. 28. 1) The α plot of

Figure 27

The distributions of daughter cell size at two stages of the cell cycle and at the time of ∝ factor release.

A - histograms of the sizes of daughter cells at birth (solid line) and at bud emergence (broken line) prior to ∝ factor arrest. B - histogram of the sizes of daughter cells at t = 395 min. (i.e. the time of removal of ∝ factor from the medium).

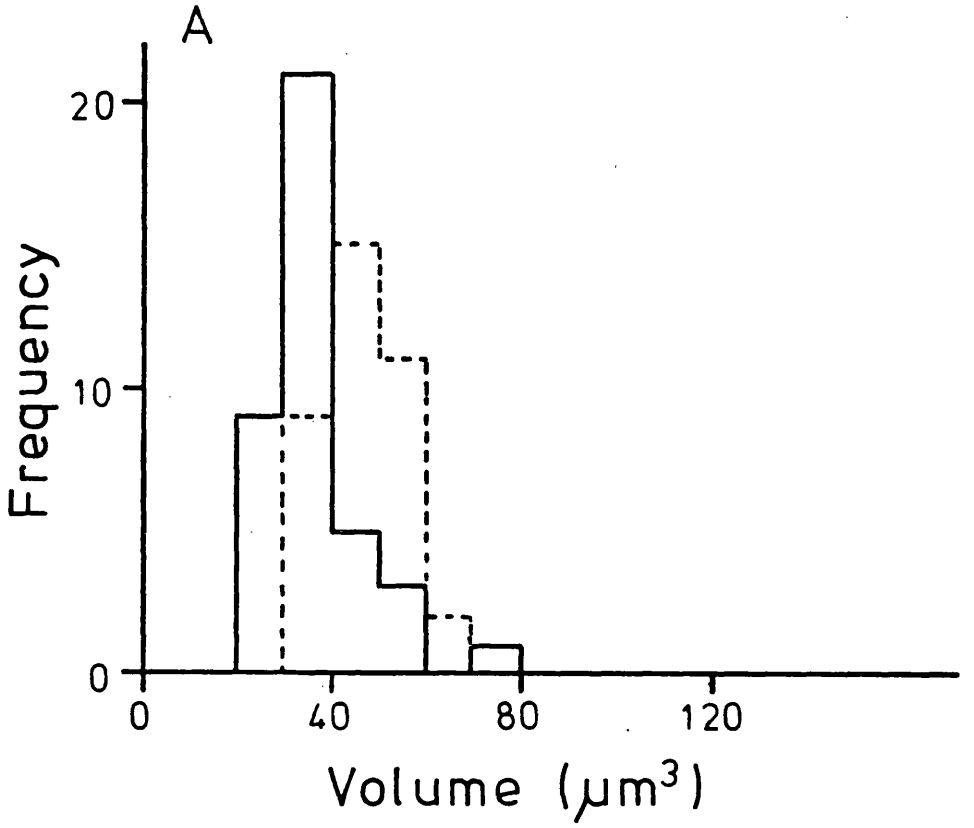
A
20
10
0
Frequency
0
40
80
120
Volume (μm³)

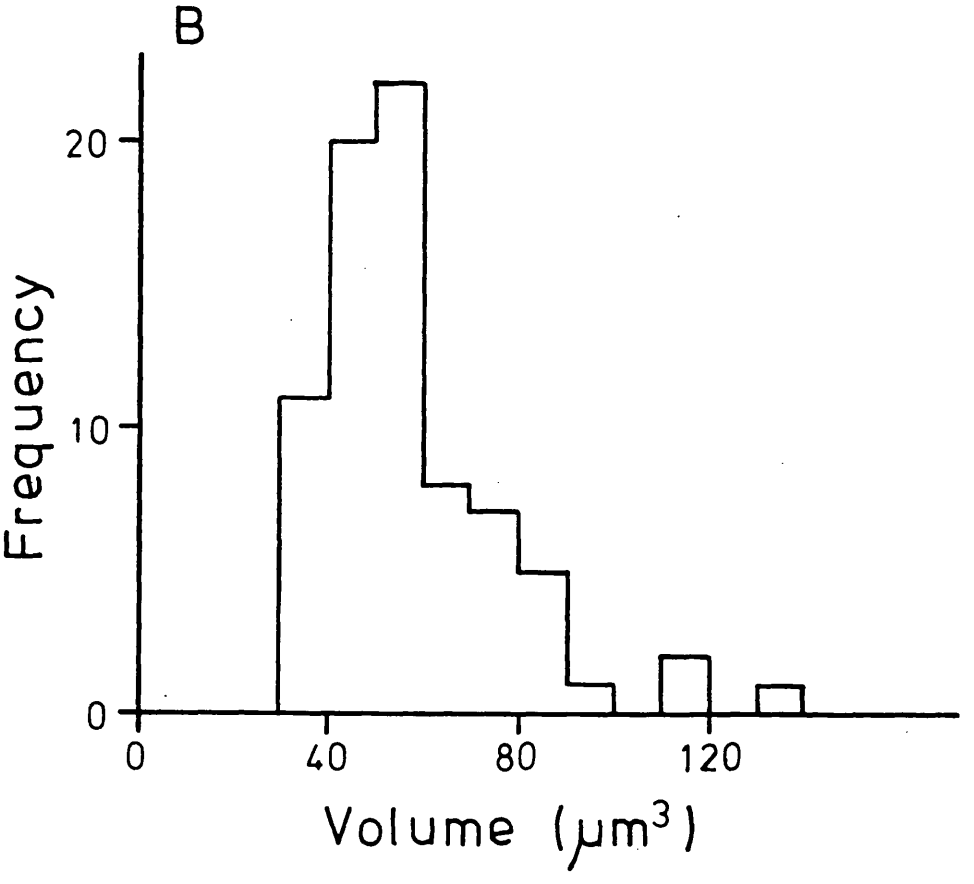
B
20
10
0
Frequency
0
40
80
120
Volume (μm³)

Figure 28

<u>∝ plots of the unbudded periods of parent and daughter cells prior to ∝ factor arrest and following release from ∝ factor arrest.</u>

The percentage of cells with unbudded periods of duration, t_{ub}, greater than or equal to t (on a logarithmic scale) versus t, prior to ∝ factor arrest (○,●). The percentage of cells with t_r (time from removal of factor to bud emergence) greater than or equal to t (on a logarithmic scale) versus t (△,▲). Open symbols, parent cells; closed symbols, daughter cells.

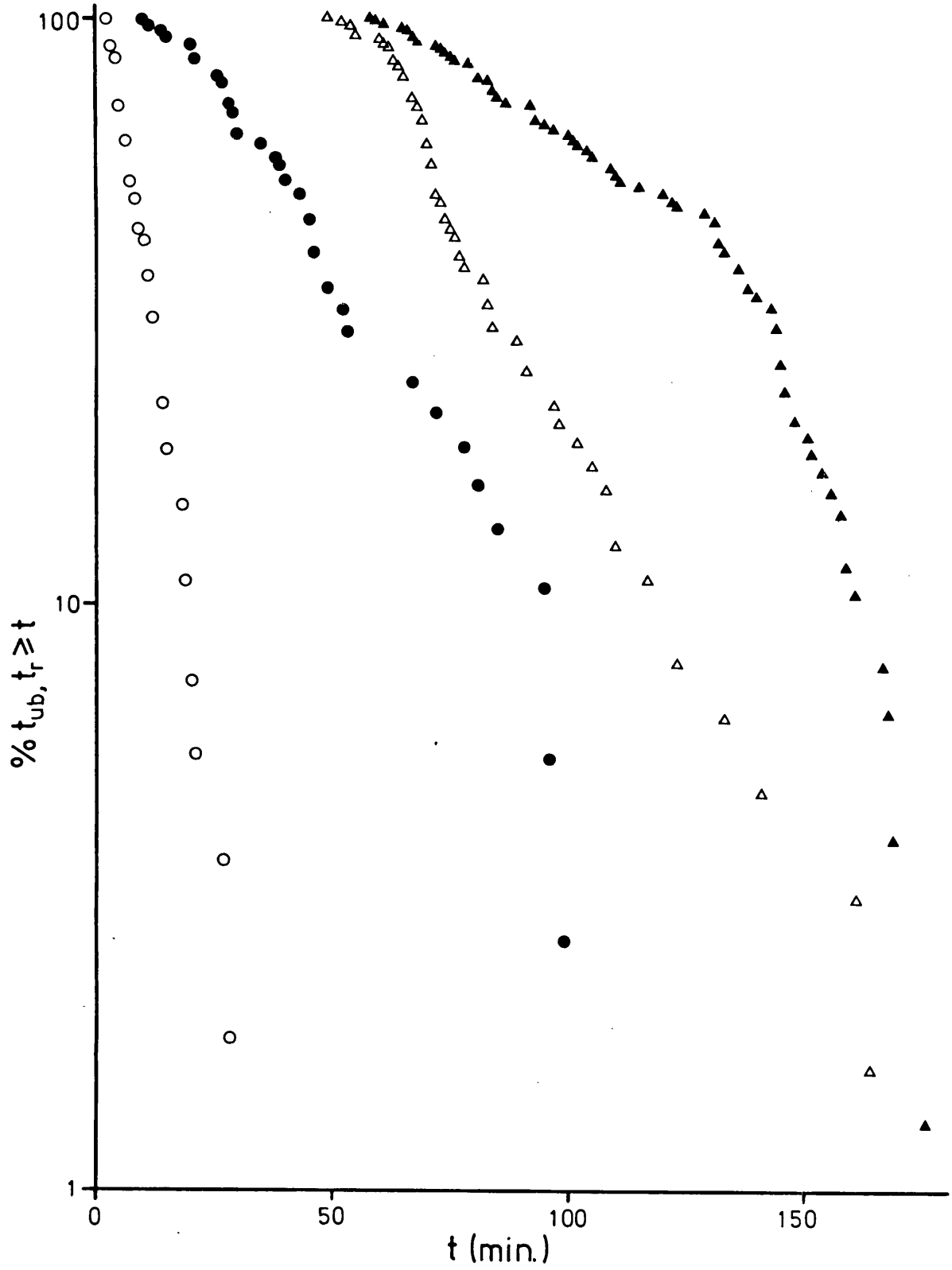
100
10
1
0
50
100
150
t (min.)
% $t_{ub}, t_r \geq t$

the parent unbudded periods is approximately linear. 2) The α plot of daughter unbudded periods is not linear. 3) There is a lag period of about 50 min. for parent cells and of about 60 min. for daughter cells, after α factor release before bud emergence occurs. 4) After the initial lag and an initial downward curvature the α plot for parent cells, after α factor release, becomes approximately linear but the slope is much less steep than the slope of the α plot of parent unbudded periods. 5)The α plot of the time from α factor release to bud emergence of daughter cells is not linear.

The distributions of the periods of time from α factor release to bud emergence, for parent and daughter cells, are presented more conventionally as histograms in Fig. 29. The distribution for parent cells is skewed as was expected as the α plot was mainly linear. In contrast the distribution for daughter cells is bimodal, suggesting that the daughter cells are not a homogeneous population but are constituted of at least two subsets. The origin of the bimodality is not apparent from any of these data. Neither cell size at the time of α factor release nor the length of time that daughter cells, after birth, were exposed to α factor determined the length of time from α factor release to bud emergence (data not shown). There is slight evidence (data not shown) that after α factor release, daughter cells from the same clone produce buds after a time which falls in the same half of the distribution in Fig. 29B. However, any explanation of clonal variation cannot satisfactorally explain why the data for parent cells appear homogeneous (Fig. 29A).

These results are seemingly inconsistent with the results of Shilo et al. (1977). They showed that the kinetics of bud emergence in an exponentially growing culture and in a cell population following α factor release were similar. They did'not, however, distinguish between parent and daughter cells. Fig. 30 is equivalent to Fig. 1 in Shilo et al. (1977).

Figure 29

The distributions of the times between release from ∝ factor arrest and bud emergence of parent and daughter cells.

A - histogram of the duration of the period between removal of ∝ factor and bud emergence of parent cells.

B - histogram of the duration of the period between removal of ∝ factor and bud emergence of daughter cells.

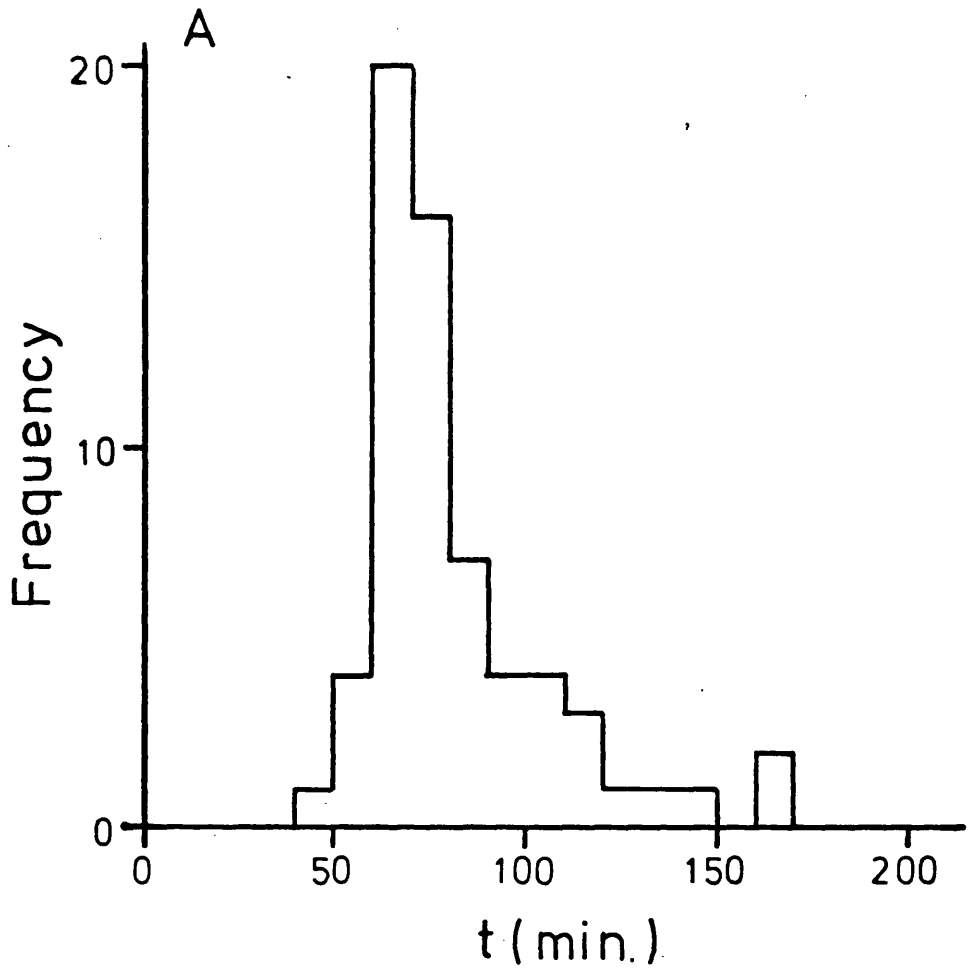
A
20
10
0
Frequency
0
50
100
150
200
t (min.)

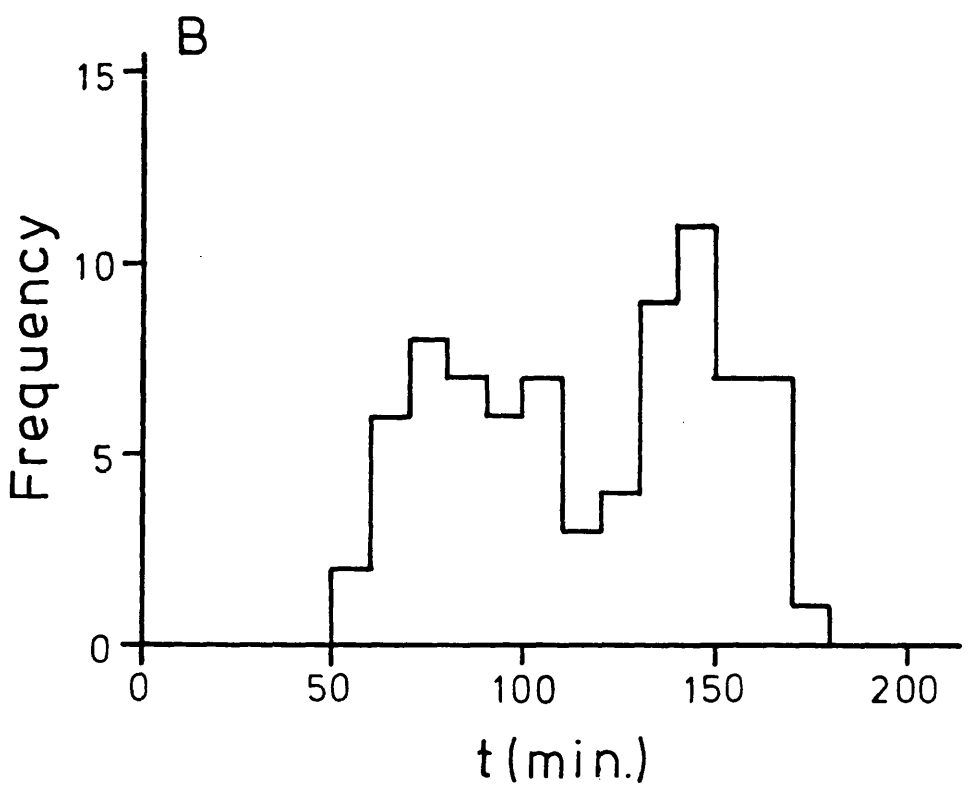
B
15
10
5
0
Frequency
0
50
100
150
200
t (min.)

The α plot of the lengths of the unbudded periods of cells (both parent and daughter cells) prior to α factor arrest is equivalent to the α plot of the % unbudded cells against the time after plating exponentially growing cells. The α plot of the lengths of the period from α factor release to bud emergence is equivalent to the α plot of the % unbudded cells against time after α factor release. As shown in Fig. 30, by pooling the data for parent and daughter cells as was, in effect, done by Shilo et al. (1977), the kinetics of bud emergence of exponentially growing cells do appear to be similar to the kinetics of bud emergence following α factor release.

Discussion

As expected, low concentrations of HU in the growth medium increased the length of the budded period and increased the size of daughter cells at birth. Whereas in the similar experiments of Singer & Johnston (1981) the population doubling time (γ) was unaltered by the presence of HU, in these experiments γ increased as the concentration of HU in the medium increased. The population volume doubling time (γ_v) in the presence of 1.5 mg/ml HU was approximately the same as in the absence of HU which suggests that this concentration of HU does not alter the (volume) growth rate. There are two possible reasons for the increase in γ. 1) If the sole effect of HU is to expand S phase and if the sum of the lengths of G1, G2 and M phases cannot be decreased below a minimum value, then beyond a threshold concentration of HU when the sum of G1, G2 and M phases becomes minimal, γ would increase due to the expansion of S phase with increasing concentrations of HU. 2) HU also slows down RNA and protein synthesis but to a much smaller extent than it slows DNA synthesis. The latter explanation is unlikely since the concentrations of HU used were low (0.02 M and 0.03 M) and Slater (1973) found that these concentrations of HU had little effect on RNA and protein synthesis.

Figure 30

∝ plots of the unbudded periods of cells prior to ∝ factor arrest and following removal of ∝ factor.

The data of parent and daughter cells were pooled for these ∝ plots. (□), the percentage of cells with unbudded periods of duration, t_{ub}, greater than or equal to t (on a logarithmic scale) versus t, prior to ∝ factor arrest. (■), the percentage of cells with t_r (time from removal of ∝ factor to bud emergence) greater than or equal to t (on a logarithmic scale) versus t.

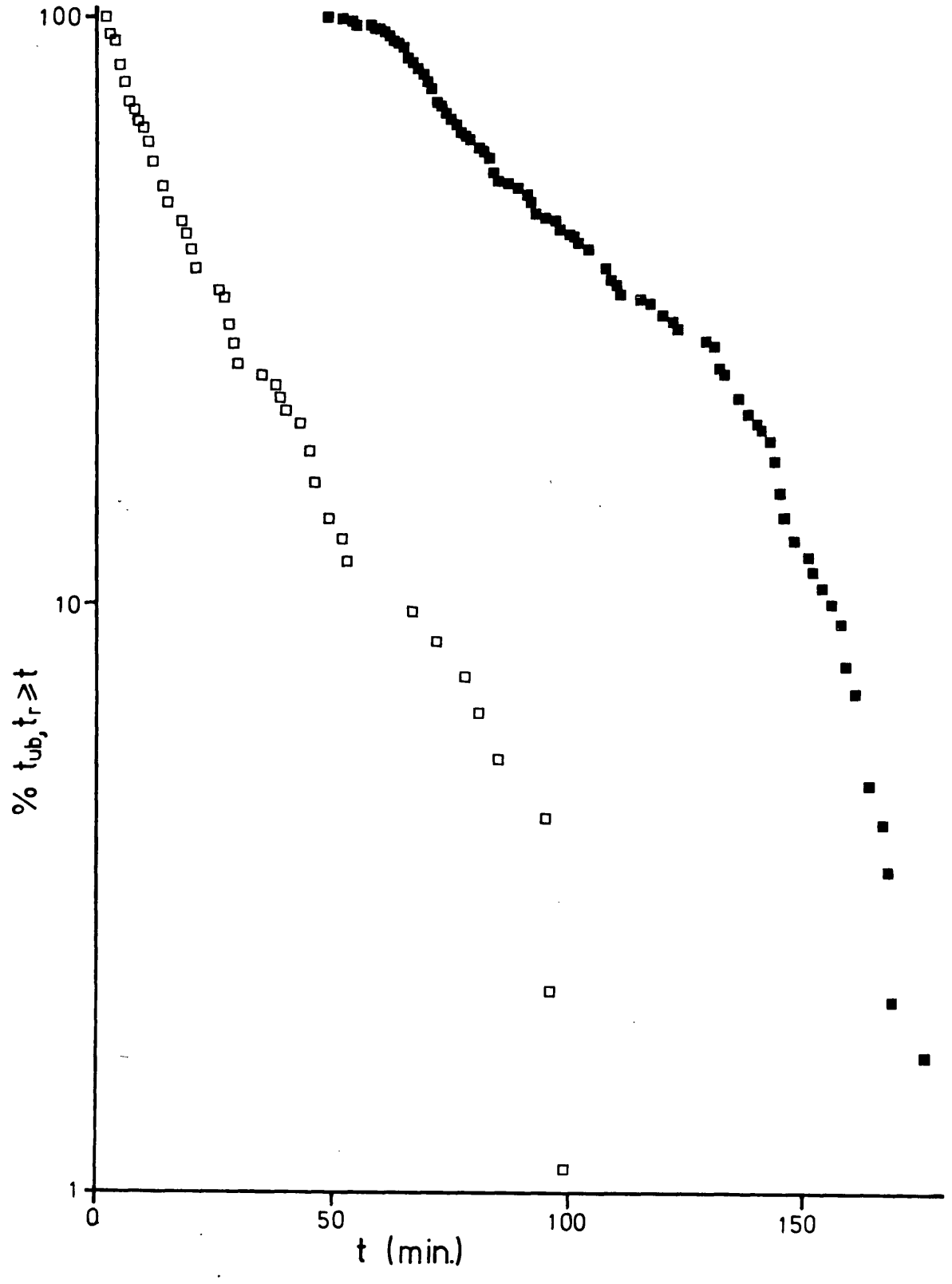
100
10
1
0
50
100
150
t (min.)
% $t_{ub}, t_r \geq t$

Apart from increasing the length of the budded period (between bud emergence and nuclear migration) the presence of HU has little effect on the duration of the other periods in the parent cycle (Table 11). The delayed occurrence of nuclear division, cytokinesis and cell separation in the presence of HU (Table 11) was expected since these events are dependent on completion of DNA synthesis (Hartwell 1974). Although it has been proposed that nuclear migration is independent of DNA synthetic events (Hartwell et al. 1974) the delay in the occurence of nuclear migration in the presence of HU (Table 11) suggests that this event is dependent on completion of DNA synthesis. The proposal of Hartwell et al. (1974) was based on the observations of Hartwell (1973) and Slater (1973) that nuclear migration takes place when completion of DNA synthesis is prevented. However, their observations were on fixed, Giemsa stained cells and it is possible that the fixation procedure affected the position of the nucleus. This possibility could be tested by repeating their experiments on unfixed cells using time lapse cinephotomicrography and immersion refractometry.

The rate of bud emergence (rate of exit from the unbudded period, Fig. 24) of parent cells is also little affected by HU. This and Table 11 suggest that, even in the absence of HU, the length of G1 is minimal and the rate of traverse of start is maximal in parent cells. It is clear that the unbudded period is shorter for daughter cells in the presence of HU.(Table 11). It is not clear whether the rate of traverse of start of daughter cells (rate of exit from the unbudded period Fig. 24) is altered by the presence of HU, since the shape of the α plot of the lengths of the unbudded period of daughter cells in the absence of HU is determined to some extent by the variation in the birth size of daughter cells.

The results are consistent with there being a size control since the difference between the cycle times (and in particular, between the

lengths of the unbudded periods) of parent and daughter cells is reduced when the birth size of daughter cells is increased. However, there is still a difference between parent and daughter cells in the durations of their unbudded periods in the presence of HU. The cause of this is evident from Fig. 24 and is that the rate of exit from the unbudded period, and by inference, the rate of traverse of start, is different for parent and daughter cells. The latter two observations are inconsistent with both the Tandem and the SSC models. These models predict that the length of the unbudded period and the rate of traverse of start should be the same for parent and daughter cells in the presence of HU (provided that the daughter cells are born large enough, which they are - see Table 12 and Fig. 23).

Either model can be modified to account for the results. The inclusion of the assumption that there is an additional period in the daughter cycle prior to bud emergence is one adequate way of modifying both models. This period would have to be of variable duration to account for the α plots in Fig. 24. This may signify a second transition point in the daughter cycle if the distribution of the length of this period is exponential but the shape of the distribution cannot be deduced from the data. The location of this period within the unbudded period cannot be deduced from the data either.

As shown by Fig. 30 the results of the α factor release experiment are not too dissimilar from the results of Shilo et al. (1977). However, I have looked at the kinetics of α factor release in much more detail having distinguished between parent and daughter cells. The conclusions from these results are quite different from the conclusions of Shilo et al. (1976, 1977). The rate of bud emergence of parent cells follows approximately first order kinetics both before α factor arrest and following release from the arrest, although the rate of bud emergence is

not the same. Samokhin et al. (1981) have shown that the rate of bud emergence following complete arrest is decreased when cells are transferred to medium containing low concentrations of α factor. This suggests the possibility that α factor was not completely washed out of the Powell chamber. Since a cells actively degrade α factor (Ciejek & Thorner 1979) and since any residual α factor within the chamber will have been continuously diluted by α factor-free medium the concentration of residual α factor in the chamber should have decreased with time. Even if the decrease in the concentration of α factor was slow the α plot of the time from release to bud emergence of parent cells (Fig. 28) would not be expected to be as linear (after the initial plateau) as it is. Instead, it would be a curve with increasing (negative) slope. It is perhaps more likely that the traverse of start following release from α factor arrest does not occur at the same rate as in steady state conditions due to some property intrinsic to the mode of action of α factor. The question then arises as to what the cells are doing during the lag period following removal of α factor from the medium, a lag period very similar in length to that observed by Shilo et al. (1977) and Samokhin et al. (1981).

To complicate the issue further, the kinetics of bud emergence of daughter cells following α factor release are strikingly different from the kinetics of bud emergence of i) daughter cells prior to α factor arrest, ii) parent cells prior to arrest, and iii) parent cells after release, (Fig. 28). The distribution of the times from α factor release to bud emergence of daughter cells is bimodal (Fig. 29B) which suggests that there is a difference in the kinetics of release from α factor arrest not only between parent and daughter cells but there is also a difference between at least two sub sets within the daughter cell population. The basis of the heterogeneity of the daughter cell population

following α factor release remains a mystery.

The duration of the budded period following α factor release is equivalent for parent and daughter cells but is some 10 minutes shorter than for cells in a steady state. This does not necessarily mean that the time between completion of start and cell separation is shorter in cells following α factor release although it is a possible reason for the shorter budded period. Another possibility is that events specific to the emergence of the bud (e.g. microfilament-ring formation) are executed at a slower rate because of the changes in the cell wall produced by the action of α factor (Lipke et al. 1976). This is plausible since the bud is formed, in most cases, at the 'shmooing tip' and the calcofluor-stainable ring at the base of the bud has a larger diameter on shmoos than on steady state cells (unpublished observation).

These experiments were designed to reveal how much influence 'pre-start' cell size has on the timing of start. Under the conditions of the experiments the pre start cell size of all cells was large enough in theory to essentially remove the effect of cell size in determining the timing of start. In the case of the timing of start in parent cells in balanced growth, size has little or no effect. Cell size is an important determining factor for the timing of start in daughter cells in balanced growth. The HU experiments confirm this and reveal that an additional factor (which I will refer to as Factor D) influences the timing of start in daughter cells but not in parent cells. The HU experiments also support the interpretation of the results (Fig. 15) presented in Chapter 4 that the daughter cell cycle contains an additional period whose duration is not influenced by cell size. Factor D is unique to daughter cells and may be an event (or events) distinct from,but a prerequisite for start events. 'If this were true then during α factor arrest, not only will the effect of cell size be reduced (by continued

growth) but the effect due to this pre start event will also be reduced. This is assuming that α factor blocks start events and not the hypothetical pre start event. In view of the difference in the kinetics of α factor release between parent and daughter cells, a pre start event unique to daughter cells is unlikely.

This leaves two further possibilities for Factor D. It may be an event which lies between start and bud emergence. Alternatively, it may lie within the complex of start events (complex since there are several start genes, Hartwell & Pringle 1981). In the former case the rate of traverse of the start complex would be the same for parent and daughter cells but the rate of bud emergence following start would be different for parent and daughter cells. In the latter case the rate of traverse of start would be different but the rate of bud emergence after start would be the same for parent and daughter cells. The rate of traverse of start was not directly monitored in the α factor arrest experiment and apart from this, there is a pronounced qualitative difference in the kinetics of bud emergence after α factor release between parent and daughter cells which is difficult to interpret. The α factor release experiment therefore, does not provide evidence to discriminate between these two possibilities.

It is widely held that the difference between the (mean) cycle times of parent and daughter cells of S.cerevisiae is due to the asymmetrical mode of division and the presence of a 'size control' (Hartwell & Unger 1977, Carter & Jagadish 1978). Furthermore, it is held that the difference is due to the difference in the (mean) pre start period of parent and daughter cells (Hartwell & Unger 1977, Singer & Johnston 1981). The results presented in this chapter imply that whilst the difference in cell size at division is the major cause of the difference in the (mean) pre start cycle time of parent and daughter cells, it is not the sole

cause. The difference in the (mean) pre start period of parent and daughter cells does appear, in the light of this evidence, to be caused solely by the difference in cell size at division. However, an additional source of the mean cycle time difference is apparent in daughter cells which if not within the start complex lies immediately after start.

These results further emphasize the need to treat populations of S.cerevisiae cells as comprising two distinct sub-populations. Treating them as homogeneous populations in cell cycle experiments can lead to misleading,if not erroneous conclusions.

CHAPTER SEVEN

Chapter 7

Clonal growth rates

Introduction

In this thesis, two possible sources of the variation in the duration of the unbudded period of yeast cells have been discussed. One source is the stochastic traverse of start which accounts for most or all of the variability in the length of the unbudded period of daughter cells. Another source in the case of daughter cells is the variation in cell size at birth combined with the existence of a size control.

A combination of any of several factors could produce variation in the birth size of daughter cells. For example; 1) the variability in the duration of the budded period; 2) the size of parent cells at bud emergence, assuming exponential growth in mass/volume; 3) differences in the amount of mass/volume accumulated during the budded period which is retained by parent cells; and 4) differences in the growth rate (rate of increase in cell size) between individual cells. Evidence for 1) and 2) is presented in Chapter 4. Table 9 (Chapter 5) shows that cells are larger at division than at the preceding bud emergence, so 3) is possible. In this chapter evidence for differences in the growth rate of individual cells, taken from the data of the time-lapse cinephotomicrographic studies of the preceding chapters, will be presented and discussed. This factor would influence the variability of the unbudded period of daughter cells both indirectly, gererating variability in birth size, and directly, as a source of the variation in the time taken to attain a 'critical' size.

Results

In the time-lapse studies of the preceding chapters, the volumes of

all cells were measured at intervals to determine the growth rate (rate of increase in total cellular volume) for the population as a whole. To investigate the possibility that the growth rate varies from cell to cell, the growth rate of each clone was calculated for each data set. Each clone was scored for total cellular volume at intervals from the single cell stage to up to the 10 cell stage. There should be differences in the clonal growth rates if individual growth rates are different. In addition, if growth rate is inheritable and differs between individual cells initiating a clone then an analysis of the growth rates of individual clones should reveal these differences.

The distributions of the clonal growth rates from each experiment are shown in Fig. 31. To establish whether or not the clonal growth rates were significantly different from the Null hypothesis that the growth rate of each clone was the same (but apparently different because of sampling and measurement error), the data were tested following the procedure outlined by Seber (1977). Briefly, the procedure involves preparing two analyses of variance tables. One is prepared by fitting the data points of each clone to individual regression equations (Model 1). The second table is prepared by fitting the data points to regression equations in which the rate constant is the same for each clone (Model 2). The residual sums of squares from the tables are then compared using the F statistic. The F ratio has the general form:

$$F_{(K-1,\ n_k-2K)} = \frac{(RSS_2 - RSS_1)}{K-1} \times \frac{n_k - 2K}{RSS_1}$$

where K=number of regressions (clones), n_k = number of data points, RSS_1 and RSS_2 are the residual sums of squares using Model 1 and Model 2 respectively. The F ratios obtained for each experiment are given in Table 14. All 8 sets of data indicate different clonal growth rates

Figure 31

The distributions of clonal growth rates in steady state populations.

Histograms of clonal growth rates. A - glucose agar-grown A364A cells; B - raffinose agar-grown A364A cells; C - sorbitol agar-grown A364A cells; D - galactose agar-grown A364A cells; E - galactose-grown A364A cells in the Powell chamber; F - galactose + 1.5 mg/ml HU-grown A364A cells in the Powell chamber; G - glucose agar-grown SA cells; H - glucose agar-grown S67.3a cells.

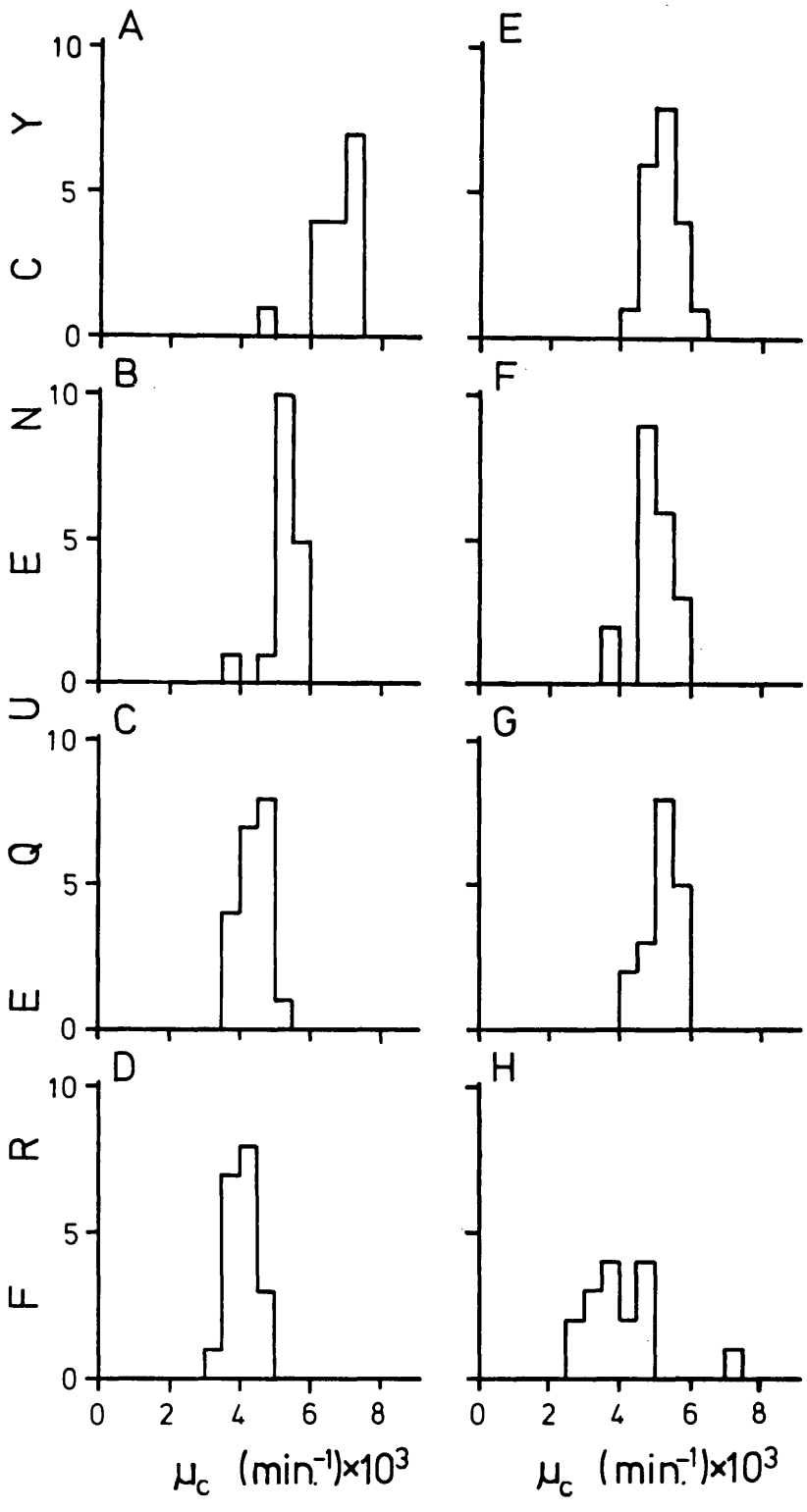
A
B
C
D
E
F
G
H
FREQUENCY
0
5
10
0
2
4
6
8
μ_c (min^{-1})×10^3

TABLE 14. The results of the F test of clonal growth rates of 8 populations of *S.cerevisiae* cells.

Experiment	strain	Medium	F ratio	No. of clones	No. of data points
A	A364A	YEP Glucose-PVP agar	5.12^{+++}	16	80
B	"	YEP Raffinose-PVP agar	4.21^{+++}	17	85
C	"	YEP Sorbitol-PVP agar	2.37^{++}	20	100
D	"	YEP Galactose-PVP agar	5.40^{+++}	19	114
E	"	YEP Galactose-PVP	2.67^{++}	20	100
F	"	YEP Galactose-PVP + HU	2.73^{++}	20	100
G	SA	YEP Glucose-PVP agar	4.93^{+++}	18	90
H	S67.3a	YEP Glucose-PVP agar	9.44^{+++}	16	80

$^{++}$ significantly different at the 1% level, $^{+++}$ significantly different at the 0.1% level.

significant at least at the 1% level.

Discussion

The results of the F tests (Table 14) suggest that there are significant differences between the growth rates of individual clones in exponentially growing cultures. What, then, are the possible causes of the differences in clonal growth rates?

In six of the experiments the cells were grown on agar medium. It is possible that in such a medium there are different local concentrations of nutrients so that some clones are growing in relatively high concentrations, whereas other clones are growing in relatively low concentrations of nutrients. Nevertheless, in the case of cells grown in the Powell chamber (Experiments E and F, Table 14) in which the substrate is homogeneous, there was still a significant difference (although the Null hypothesis was rejected at a lower level of significance).

Some populations contained one or two clones whose growth rate was somewhat lower than the majority of the clones (notably in experiments A, B and F, Fig. 31). The F test was repeated for experiments A and B omitting the data for the slowest growing clone in each case. F ratios of 2.3 (experiment A) and 1.49 (experiment B) were obtained which are significantly different at the 2.5% level and not significantly different respectively. The presence of one slow-growing clone, atypical of the population, therefore has a considerable effect on the outcome of the F test. In chapter 4 it was suggested that the likely reason for τ_v being longer than τ is that the measured size of cells which are out of the focal plane and/or which change their orientation during the course of the experiment will be less than their actual size. The accuracy of the size measurements on the atypically slow-growing clones may have been lower than on the majority of the clones for such a reason. However, since the presence of an atypical clone is apparent in only a few of the

experiments (see Fig. 1), it can be concluded that there is heterogeneity in clonal growth rates of S.cerevisiae cells.

The clonal growth rates of S67.3a cells are more evenly distributed than those of the other strains (Fig. 31). whi 1 cells, therefore, may exhibit considerable differences in individual growth rates.

Several authors (Kubitschek 1971, Castor 1980, Pardee et al. 1979) purport that the variation of individual growth rates is the primary cause of the variability in cycle times rather than solely the manifestation of a stochastic mechanism. According to the hypotheses of Castor (1980) and Pardee et al. (1979) variability in the rate of progression towards a start-like event leads to the variability in cycle time. Whilst the above results give good grounds to suspect the existence of constitutive differences in cellular growth rate within yeast cell populations, the results of α factor release experiments (Shilo et al. 1977, Samokhin et al. 1980, and Chapter 6) strongly suggest that cycle time heterogeneity is to a significant extent generated at, as well as prior to, start. If all the variability in cycle time is generated prior to start, then cells should release synchronously from start arrest. Therefore, variation in cellular growth rate presents an additional rather than alternative source of cycle time variability.

CHAPTER EIGHT

Chapter 8

General Discussion

Control of cell proliferation in S.cerevisiae is mediated by the start event, the rate of completion of which is thought to largely determine the rate of cell proliferation (Hartwell & Pringle 1981). The main aim of the work in this thesis was to obtain information about the nature of the cellular trigger of start. The conclusions from the observations of steady state populations (Chapter 4) were that any model of proliferation control in this organism must include a growth related element, more specifically an element whose function is to monitor cell size, and an element which generates variability in the timing of start. Two such models were considered. The Tandem model (Shilo et al. 1977) has as the growth related element the requirement of growth to a critical cell size and once this is attained, cells emerge from start with first order kinetics due to a probabilistic process, the latter being the variable element. Most of the data in Chapter 4 were consistent with this model only if further assumptions were introduced, the most likely assumption being that there is substantial variation in the critical size. Wheals (1982) also included a probabilistic process as the variable element in his Sloppy Size Control (SSC) model, but in this model the probabilistic element is an integral feature of the size related mechanism rather than a discrete process. The majority of the data in Chapter 4 were consistent with this model without further modification.

Evidence for a probabilistic proliferation control mechanism as the underlying cause of cycle time variability has, however, been disputed. Castor (1980) and Koch (1980) showed that the exponential component of the distribution of cycle times and of the distribution of differences in sibling cycle times (both taken as supportive evidence for the existence of a probabilistic control event [Smith & Martin 1973, Minor & Smith 1974])

can be generated in ways other than by a probabilistic event. Furthermore Koch (1980) showed that similar kinetics of cell proliferation to those produced by the Transition Probability model (Smith & Martin 1973) are produced by a growth control model if a small proportion of the cells had slower growth rates than the majority of cells in the population. Evidence for such growth rate heterogeneity was presented in Chapter 7. As was discussed in that chapter, whilst the inclusion of differences in growth rate in a growth control model can explain variability in daughter cycle times, it cannot explain the variability in and the approximately exponential component of the distribution of parent cycle times. Nor can it explain the asynchronous budding of yeast cells following release from start arrest (Shilo et al. 1976, 1977, Samokhin et al. 1981, Chapter 6). The failure of alternatives to a probabilistic model in explaining the asynchronous emergence from start makes a probabilistic mechanism the more likely variability-generating element in the Tandem and SSC models. Variability in growth rates simply adds variability to the cycle time via its effect on the size control element.

Common to both the Tandem and SSC models is that variability in cycle time is mainly generated during the pre start period, i.e. between division and completion of start. This is illustrated in Fig. 32. After completing start, cells enter the cell-division sequence in which DNA synthesis, bud emergence, nuclear migration, nuclear division, cytokinesis and, ultimately, cell separation occur. This sequence is shown as a think solid line to indicate its relatively constant duration. After division parent and daughter cells enter a variable pre-start period. The difference between parent and daughter cells is in the extent of the variability of the start period. For parent cells this is set by the rate constant of the probabilistic process. For daughter cells this is largely dictated by the smallest daughter cells due to the size control. The difference in the extent of the variability of the pre-start period between parent

Figure 32

Diagram of the yeast cell cycle.

Illustrated are the variable period (---); and the relatively constant period (▬▬) in relation to G1, S, G2 G2, M, and G1* (that part of G1 prior to cell division).

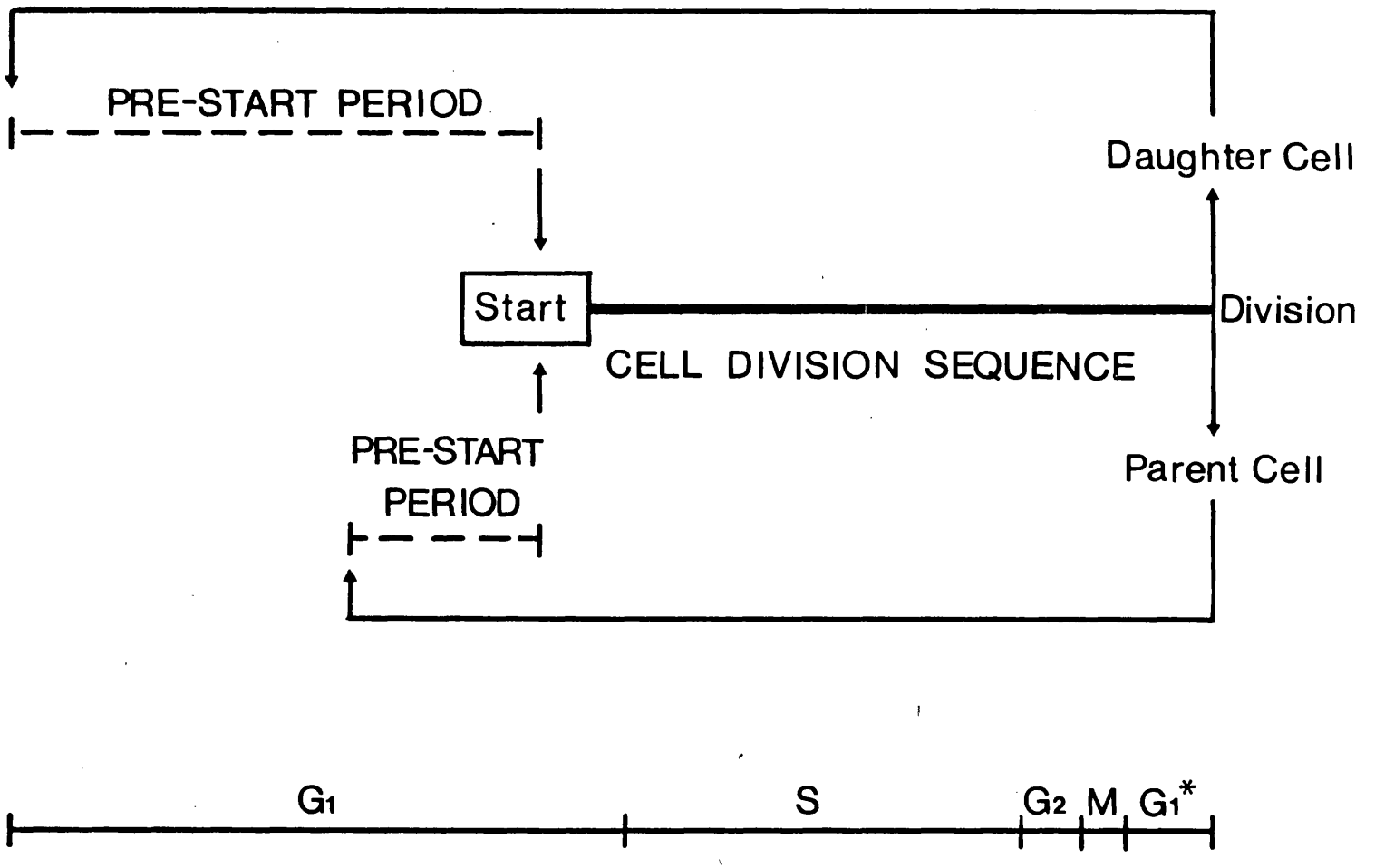
PRE-START PERIOD
Daughter Cell
Start
Division
CELL DIVISION SEQUENCE
PRE-START
PERIOD
Parent Cell
G1
S
G2
M
G1*

and daughter cells is due to the difference in size (through the operation of the size control element) and to 'Factor D' (see Chapter 6).

Either the size control element or the probabilistic element or both may be responsible for changes in the duration of cycle times in response to changes in nutritional conditions. The change in the growth rate brought about by a change in nutritional conditions would influence the rate of progression towards a critical size step (Tandem model) or the rate of increase in transition probability (SSC model) and this would lead to a change in the duration of daughter cycle times. The rate constant (Tandem model) or the maximal rate constant (SSC model) of the probabilistic process may change in direct response to changes in nutritional conditions (Shields & Smith 1977). This would lead to changes in the mean duration of the pre-start period and consequently to changes in the mean duration of both parent and daughter cycle times.

The experiments of Chapters 3 and 4 provide data with which to examine the factors involved in alterations of the duration of cycle times. Tables 4 and 5 show that the budded period increases in length as the doubling time increases. It can be inferred from this that the post-start period is not of fixed duration and that changes in the duration of this period contribute to the changes in cycle times in response to nutritional changes. Over a two-fold range of growth rates the parent unbudded period shows a modest increase in length with decreasing growth rate (Table 5). This could be due to an increase in the mean length of the pre-start period (as a result of a decrease in the rate constant of a probabilistic process) but could equally well be due to an increase in the period between start and bud emergence. However, a substantial increase in the length of the start to bud emergence period would be necessary to explain the increase in the parent unbudded period (over a four-fold range of growth rates) of the cells in the experiments of Chapter 3 (Table 4) if the rate constant of

the probabilistic process does not change with the growth rate. The increase in the daughter cycle time with increasing doubling time is mainly achieved by an increase in the duration of the unbudded period (Tables 4 and 5) and this is more likely to be a result of an increase in the length of the pre-start period. However, the increase in the duration of the daughter pre-start period is more probably due to an increase in the time necessary to fulfill a growth requirement than due to a change in the rate constant of a probabilistic process.

The experiments in Chapter 6 showed that the difference between the parent and daughter cycle times is not entirely due to the differences in cell size. For ease of discussion the (as yet unknown) factor reponsible for the difference is referred to as Factor D. The period of time in the daughter cycle resulting from the effect of Factor D may also change with the growth rate since Fig. 15 gave grounds to suspect that this period shows a modest increase with growth rate. Further evidence though, is needed and this could be obtained from kinetic studies of populations growing in the presence of low concentrations of HU (as in the experiments of Chapter 6) in different media, supporting different growth rates.

The results, therefore, imply that at least four factors are involved in alterations of cycle times. Only two of these play a significant role in changing the parent cycle time. All four may effect changes in the daughter cycle time.

Having established which factors are involved in altering the duration of cell cycles it is necessary to consider their relative contributions. Shilo et al. (1976) compared the rate of budding of cells in two different media (each supporting a different growth rate) following release from start arrest and found that the rate of budding was less in the slower growing population. They proposed, on the basis of these results, that alteration of the rate constant of the probabilistic process

is the major cause of the alteration of the rate of proliferation. In their experiment they blocked cdc 25 cells at start by shifting them to the restrictive temperature. At this temperature these mutants cease cellular growth (Hartwell et al.1973). The slower growing population may have had a lower rate of budding following release because the daughter cells in this population required a longer period of time to fulfil the growth requirement than those in the faster growing population. Even if, as Shilo et al. (1977) suggested, these cells cease growth only after fulfilling the growth requirement then since both populations were arrested for the same length of time it is conceivable that this time was insufficient for a large proportion of daughter cells in the slower growing population to attain a size at which the size control element was no longer a rate-limiting factor. The lower rate of budding after release, of the slower growing population may thus have been due to these daughter cells being subject to the size control element. The effect of Factor D may have been additionally responsible for the different rates of budding. However, Shilo et al. (1976) neither measured cell size nor distinguished between parent and daughter cells so these points remain unresolved.

The results of Rivin and Fangman (1980) suggested that the post-start period increases in length to at least the same extent as the pre-start period does, as the cycle time increases. This appears to be a feature only of nitrogen-limited populations since alterations of the growth rate by other means produce substantially more change in the duration of the pre-start period than in the duration of the post-start period (Carter & Jagadish 1978, Hartwell and Unger 1977).

In keeping with the view that the changes in cycle time are mainly effected by changes in the duration of the pre-start period (Carter & Jagadish. 1978, Hartwell & Unger 1977, Shilo et al. 1976, Wheals 1982).

the following scheme for the relative contribution of the factors mentioned above in the control of the rate of cell proliferation is proposed. 1) The post-start period increases modestly with decreasing growth rate and assumes increasingly less importance as the growth rate decreases. 2) The period due to Factor D also increases modestly with decreasing growth rate and since this period only occurs in daughter cells this ranks as less important than 1) for the population as a whole. 3) The increase in the pre-start period brought about through the operation of the size control element is evident over narrow ranges of growth rates. Although this factor is effective only in daughter cells it has a major impact on the rate of proliferation of the population as a whole. However, since the 'critical size' appears to decrease with decreasing growth rates and at slower growth rates becomes constant (Johnston et al. 1979 and Chapter 3, Fig. 10), the size element may become increasingly important as the growth rate decreases. 4) If changes in the rate constant of the probabilistic process do occur then these may be most evident over a wide range of growth rates and this factor may become increasingly important as the growth rate decreases. This scheme, it must be stressed, remains tentative until experiments such as those in this thesis are done for cell populations over a much broader range of growth rates.

Some evidence for the existence of both deterministic and probabilistic elements in the regulation of cell proliferation has been found for several cell types, such as bacteria (Schaechter et al. 1962, Shields 1978), yeast (Fantes 1977, this thesis), and mouse fibroblasts (Shields et al. 1978). This suggests the possibility that the basic mechanism of cell proliferation control is common to a wide variety of cell types. Apparent differences between the mode of cell proliferation control of different cell types probably reflect the relative expression of different aspects

of this same mechanism in different cell types.

Fantes and Nurse (1981) have discussed how some mechanisms of size control of cell proliferation can show probabilistic features. One mechanism, which would be applicable to the Tandem model, is that of a structure built up at a rate proportional to the size of a cell such that the structure would tend to be completed at a certain cell size. Once completed, the structure interacts with some intracellular site, the interaction being the signal for initiation, of the cell division sequence, or of mitosis (depending on the cell type). The assembly of the structure is the size related element and, since the structure is present as a single copy, its interaction with the site will be a random process which forms the probabilistic element. The difference in the relative contribution of the two elements in different cell types could be related to growth rate with such a mechanism. The mean time taken to complete the structure and the mean time taken for the structure to interact with the site may increase with the mean cycle time such that: the shorter the cycle time (i.e. at fast growth rates) the longer is the 'assembly time' than the 'mean interaction time'; and the longer the cycle time (i.e. at slow growth rates) the longer the 'mean interaction time' than the 'assembly time'. At the faster end of the growth rate spectrum, represented by most bacteria, the size control feature will be most evident and at the slower end of the spectrum, represented by mammalian cells, the probabilistic feature will be most evident.

Wheals (1982) suggested one possible mechanism for the SSC model as being that of an effector molecule which behaves like a heterotrophic allosteric enzyme showing positive cooperativity. He further suggested that differences in the relative expression of the deterministic and probabilistic features of the mechanism between different cell types may

be due to differences in their size. That is, small cells e.g., bacteria, mainly show the size-related feature as a consequence of their being born at sizes mainly in the 'slope' region of the curve of transition probability versus cell size (see Fig. 16), and large cells, e.g. mammalian cells, mainly exhibit the probabilistic feature as a consequence of their being born at sizes in the plateau region of the curve. Alternatively, the properties of the effector molecule of each cell type may differ such that the shape of the curve of transition probability versus cell size differ from one cell type to another. The shape of the curve may tend towards a step shape for those cells mainly exhibiting a size related element and may tend towards a horizontal line for those cells mainly exhibiting a probabilistic feature.

The Tandem model (Shilo et al. 1976, 1977) and the SSC model (Wheals 1982) are both partly based on the Transition Probability hypothesis (Smith & Martin 1973). Recently, this latter hypothesis has been revised by the addition of a second random process, to account for the observed lag period prior to initiation of DNA synthesis when quiescent mammalian cells are stimulated by growth factors, and to account for the assumed equivalence of the duration of the B phase of sister cells (Brooks et al. 1980). In the revised hypothesis, following stimulation cells exit the quiescent state (Q state) at random and commence a process (L) which takes a constant time to be completed. After this, cells enter an indeterminate state (A state) which they exit at random. Initiation of the cell division sequence and entry into the Q state occur immediately and simultaneously after exit from the A state. The sequence $Q \rightarrow L \rightarrow A$ is maintained in steady state proliferation and overlaps with the conventional cell cycle (i.e. G1 – S – G2 – M – G1). The exponential distribution of the differences in sister cell cycle times is explained as being solely due to the random transit from the A state since much of the $Q \rightarrow L$ sequence occurs in the

mother cell and thus is common to both sister cells. The hypothesis also explains the similarity between the duration of the lag period of quiescent cells following stimulation and the minimum intermitotic time (Brooks et al. 1980). The authors also suggested that the L process could be the assembly of a structure, the initial step of which occurs at random (the Q-transition) and that the A transition step is dependent on, and occurs at random after, the completion of the structure. As they pointed out, the behaviour of the mitotic centres in sea urchin eggs (Mazia et al. 1960) is strikingly analogous to the Q→L→A scheme. The initiation of duplication of these structures could correspond to Q state transition, their maturation to the L process, and separation of mother and daughter centres to the A state transition. Brooks et al. (1980) also drew attention to the evidence from S.cerevisiae of the link between cell cycle control and duplication of the spindle pole bodies, the mitotic centres of this yeast (Byers & Goetsch 1974, 1975). However, the behaviour of the spindle pole bodies during the cell cycle is not analogous to the physical interpretation of the two-transition model, proposed by Brooks et al. (1980). This follows because 1) duplication of the spindle pole body is not a 'lengthy' process, it occurs during a short period of time subsequent to start (Byers & Goetsch 1974, Hereford & Hartwell 1974), and 2) initiation of DNA synthesis is not dependent on the duplication of the spindle pole body, since at the restrictive temperature, cdc 31 mutants do not duplicate the spindle pole body but do initiate DNA synthesis (B. Byers, cited in Hartwell & Pringle 1981).

In its present form, the two-transition hypothesis cannot account for the difference in cycle times of parent and daughter S.cerevisiae cells nor can it account for the evidence for a size control over cell proliferation in S.cerevisiae. As discussed by Nurse (1980) the L process may be subject to a size control, in which case the mechanism may be

analogous to that described by Fantes & Nurse (1981) of a deterministic mechanism with probabilistic properties. Nevertheless, there are difficulties in applying these structural models to S.cerevisiae particularly in accounting for the difference in cycle times of parent and daughter cells.

There are two possible schemes for the behaviour during the cell cycle of the structure in the model of Fantes & Nurse (1981). Either 1) the assembly of the structure is initiated at or near to the end of the cell division sequence, or 2) assembly of the structure is initiated upon exit from an A state (i.e. assembly of the structures required for initiation of the sibling parent and daughter cell cycles is begun during the previous cell cycle. For scheme 1) it would be necessary to assume that parent cells complete the structure very quickly to account for the short unbudded (and presumably pre-start) period of parent cells. Alternatively the structure may be retained by the parent cell and consequently, after division, parent cells must complete only a random transition, whereas daughter cells must assemble the structure in addition to completing a random transition, in order to initiate the cell division sequence. For scheme 2) it would be necessary to assume that one structure (that distributed to the parent cell) is built at a faster rate than the other structure (that distributed to the daughter cell). Scheme 2) is analogous to the model of Brooks et al. (1980) with the incorporation of a size control over the L process and the last assumption would also have to be made for this model.

Other models can be formulated to account for random transitions apart from the above structural models. One example, suggested by Brooks et al. (1980), is a model in which the concentration of some critical substance fluctuates at random about a mean, and transitions occur only when the concentration exceeds a threshold. A deterministic

feature of this model may be that there is a size control over the mean value. Such a mechanism would account for the difference in parent and daughter cycle times and interestingly would provide control of cell proliferation as described by the SSC model (Wheals 1982).

The above are rather vague descriptions of possible mechanisms and have been proposed mainly on the basis of kinetic studies. Recently, the usefulness of kinetic data in deducing mechanisms of cell proliferation has been questioned. In a paper on the limitations of kinetic data, Smith et al. (1981) pointed out in their opening remarks that kinetic observations are at best suggestive of mechanisms. However, they concluded that attempts to deduce mechanisms from kinetic data are pointless on the grounds that several models may equally well fit the data. The very fact that kinetic data do suggest mechanisms hardly makes kinetic experiments pointless. Apart from that one rather sceptical remark, these authors do make several valid points about the limitations of kinetic observations, and in this thesis some of the limitations have been overcome. 1) Models cannot be practicably distinguished from the distributions of cycle times in steady state populations because the amount of dataneeded cannot be achieved experimentally. Some, however, can be distinguished from kinetic data from perturbed cell populations. The experiments of Chapter 6 illustrate the latter point, in distinguishing between probabilistic mechanisms and 'rate' mechanisms. In any case the former mechanism is more plausible than the latter when the kinetics of parent cells in steady state populations are considered. 2) A probabilistic model may be rejected from an analysis of the distribution of cycle times in steady state populations if the variation in the 'determined' part of the cycle is substantial. Through the use of an improved microscopical technique in this work, the budded period was measured directly. Since this period

constitutes most of the determined (in this case the post-start) period, this problem is overcome by analysing the distribution of the durations of the unbudded period. Because of the problem it was particularly important to compare the distribution of the durations of the unbudded period between steady state populations growing in the absence of, and those growing in the presence of HU (Chapter 6). 3) Models cannot be proved by kinetic observations although some may be ruled out by them. Time lapse cinephotomicrographic experiments provide not only kinetic data but also size data (although it is difficult to measure the size of irregular-shaped cells with a reasonable degree of accuracy). Since many models of cell proliferation contain size control elements it is crucial to monitor both size and time parameters in such experiments in order to examine and to distinguish between the models. These parameters have been measured in these experiments.

The kinetic analyses in this thesis have shown that simple models such as the Critical Size Hypothesis (Fantes et al. 1975) and the Transition Probability Hypothesis (Smith & Martin 1973) do not satisfactorally explain the control of cell proliferation in S.cerevisiae. However, models which combine these two hypotheses (i.e. the Modified Tandem model and the SSC model) are good approximations of the control. It is unlikely that further kinetic experiments will prove the validity of either the Modified Tandem model or the SSC model. Clearly more direct, molecular evidence is needed. Successes in the development of genetic manipulation techniques (Glover 1980) mean that it is now possible to probe the molecular basis of control of cell proliferation. Indeed, Nasmyth & Reed (1980) have recently developed a procedure for isolating cell cycle genes from S.cerevisiae so it should be possible to isolate genes involved in control of cell proliferation and to isolate and characterize the transcriptional and translational products of these

genes.

As discussed earlier, a possible mechanism underlying the Tandem model involves the assembly of a structure. Characterization of the translational products of cell cycle control genes could establish whether or not a structure is involved. The products may, for example, form all or part of the spindle pole body. A possible underlying mechanism of the SSC model is of an effector molecule whose concentration changes proportionately with cell size. This hypothesis could be tested by monitoring the level of 'control' gene products relative to cell size. It may also be possible to identify the site, or sites, of interaction of the effector molecules and to examine if the interaction is probabilistic in nature. These are only a few examples but illustrate how the models are suggestive of further experiments.

In conclusion, although the molecular basis of control of cell proliferation cannot be directly deduced from kinetic studies, models based on such studies do provide working hypotheses for more specific analyses.

APPENDIX

Appendix

Age distribution for S.cerevisiae.

The age distribution derived by Hartwell and Unger (1977) is

$$\left.\begin{array}{ll} \phi(t) = \alpha e^{\alpha t}(1 - e^{-\alpha P}) & D \geq t > P \\ \phi(t) = \alpha e^{\alpha t} & P \geq t > 0 \\ \phi(t) = 0 & \text{other values} \end{array}\right\} \quad [A1]$$

where $\phi(t)$ is the probability density function, t is the age of a cell at a particular point in the cycle in terms of the time between that point and division (the age at division is 0), D is the daughter cycle time, P is the parent cycle time , and $\alpha = \frac{\ln 2}{\tau}$. D, P and τ , the population doubling time are related by the expression.

$$e^{\alpha D}(1 - e^{-\alpha P}) = 1$$

or, rearranging, $e^{-\alpha D} + e^{-\alpha P} = 1$ [A2]

It follows from A1 that the frequency of daughter cells at $t(D \geq t > 0)$ is

$$\frac{d}{dt} = \alpha e^{\alpha t}(1 - e^{-\alpha P}) \quad [A3]$$

and the frequency of parent cells at $t\ (P \geq t > 0)$ is

$$\frac{d}{dt} = \alpha e^{\alpha t} \cdot e^{-\alpha P} \quad [A4]$$

Duration of the budded period, B.

The fraction of budded cells is

$$F_B = \int_0^B \alpha e^{\alpha t}\, dt$$

$$= e^{\alpha B} - 1$$

$$B = \frac{\ln (F_B + 1)}{\ln 2} \cdot \tau \quad [A5]$$

Duration of D and P

The duration of the daughter cycle time, D, can be calculated from the fraction of daughter cells which are budded, F_{DB} (the frequency of budded daughter cells divided by the frequency of daughter cells).

$$F_{DB} = \frac{\int_0^B \alpha e^{\alpha t}\,(1 - e^{-\alpha P})\,dt}{\int_0^D \alpha e^{\alpha t}\,(1 - e^{-\alpha P})\,dt}$$

$$= \frac{e^{\alpha B} - 1}{e^{\alpha D} - 1}$$

$$= \frac{F_B}{e^{\alpha D} - 1}$$

$$D = \frac{\ln[(F_B/F_{DB}) + 1]}{\ln 2} \cdot \tau \qquad [A6]$$

Using similar reasoning the duration of the parent cycle time, P, can be calculated from the fraction of parent cells which are budded, F_{PB}.

$$P = \frac{\ln[F_B/F_{PB} + 1)]}{\ln 2} \cdot \tau \qquad [A7]$$

Maximum likelihood estimation of D, P and B

Estimates of $D' (= \frac{D}{\tau})$, $P' (= \frac{P}{\tau})$ and $B' (= \frac{B}{\tau})$ are obtained from the maximisation function (derived by Peter Green, University of Durham).

$$N_{UD} \ln (1 - \tilde{s}\,\tilde{t}) + (N_{UP} + N_B) \ln \tilde{s}$$

$$+ (N_B + S) \ln \tilde{t} + N_{UP} \ln (1 - \tilde{t})$$

$$+ S \ln \tilde{u} + N_B \ln (1 - \tilde{u}) \qquad [A8]$$

subject to

$$\tilde{s} \quad 1; \quad \tilde{t} \quad 1; \quad \tilde{u} \quad 1;$$

$$(1 + \tilde{s})\,\tilde{t}\,\tilde{u} = 1,$$

where

$\tilde{s} = (\frac{1}{2})^{D'-P'}$; $\tilde{t} = (\frac{1}{2})^{P'-B'}$; $\tilde{u} = (\frac{1}{2})^{B'}$;

N_{UD} = number of unbudded daughter cells;

N_{UP} = number of unbudded parent cells;

N_B = number of budded cells;

S = total number of scars

Genealogical age distribution.

The fraction of daughter cells is, from A3,

$$F_D = \int_0^D \alpha e^{\alpha t} (1 - e^{-\alpha P})\, dt$$

$$= e^{\alpha D} (1 - e^{-\alpha P}) - (1 - e^{-\alpha P})$$

$$F_D = e^{-\alpha P} \qquad [A9]$$

At division the frequency of cells dividing for the first time (i.e. the frequency of daughter cells at t = 0) is, from equation A3, $\alpha(1 - e^{-\alpha P})$. Immediately after division these cells give rise to unbudded daughter cells which enter the cycle at t = D and unbudded parent cells with one bud scar which enter the cycle at t = P. Therefore at t = P in the cycle the frequency of parent cells with one bud scar is $\alpha(1 - e^{-\alpha P})$. From equation A4 the frequency of parent cells at t = P is α. Therefore at t = P the fraction of the parent cells which have one bud scar is $(1 - e^{-\alpha P})$. This fraction is maintained as the cells pass from t = P to t = 0 in the cycle. So that the frequency of P_1 cells (parents cells with one bud scar) at t $(P \geq t \geq 0)$ is

$$= \alpha e^{\alpha t} . e^{-\alpha P} (1 - e^{-\alpha P}) \qquad [A10]$$

The frequency of P_2 cells at t = P is the same as that of P_1 cells at t = 0 which is $\alpha e^{-\alpha P} (1 - e^{-\alpha P})$. The fraction of parent cells which have two bud scars, therefore is $e^{-\alpha P} (1 - e^{-\alpha P})$. So the frequency of P_2 cells at t $(P \geq t \geq 0)$ is

$$= \alpha e^{\alpha t} (e^{-\alpha P})^2 (1 - e^{-\alpha P}) \qquad [A11]$$

The frequency of P_3 cells at t $(P \geq t \geq 0)$ is found by similar reasoning and is

$$= \alpha e^{\alpha t} (e^{-\alpha P})^3 (1 - e^{-\alpha P}) \qquad [A12]$$

The general formula for the frequency of Pn cells, where n = 1,2,3 etc. at t $(P \geq t \geq 0)$ follows from equations A10, A11 and A12 and is

$$= \alpha e^{\alpha t} (e^{-\alpha P})^n (1 - e^{-\alpha P}) \qquad [A13]$$

The general formula for the fraction of Pn cells, from A13 is

$$F_{Pn} = (e^{-\alpha P})^{n-1} (1 - e^{-\alpha P})^2 \qquad [A14]$$

At the maximum balanced growth rate (μ_{bmax}), when D = P = τ, equation A14 becomes $F_{Pn} = (\frac{1}{2})^{n+1}$. Therefore at μ_{bmax} cells of different genealogical ages (n = 0,1,2, etc) are distributed such that their frequencies form a geometric series in which the frequency of cells of genealogical age n is $(\frac{1}{2})^{n+1}$.

Median cell volume

Assuming that the volume of a cell increases exponentially from birth to division such that the time in which a cell doubles its volume is the same as the population doubling time, then the median cell volume is the volume of a cell at the median cell age. From equation A1 where t_m is the median cell age (in units of τ)

$$\int_0^{t_m} \alpha e^{\alpha t} = 0.5$$

$$e^{\alpha t_m} - 1 = 0.5$$

$$t_m = \frac{\ln 1.5}{\ln 2}$$

$$= 0.5850$$

The volume of a cell at t in the cycle is given by (Tyson et al. 1979) as

$$V_t = V_P e^{\alpha(P-t)} \qquad [A15]$$

where V_P is the volume at P, and P is in units of τ.

Therefore the median cell volume is

$$V_m = V_P e^{\alpha(P-0.5850)} \qquad [A16]$$

LITERATURE CITED

Literature cited

Absher, P.M., R.G. Absher & W.D. Barnes. 1974. Genealogies of clones of diploid fibroblasts. Exp. Cell Res. 88 : 95-104.

Adams, J. 1977. The interrelationship of cell growth and division in haploid and diploid cells of S.cerevisiae. Exp. Cell Res. 106 : 267-275.

Barford, J.P. & R.J. Hall. 1976. Estimation of the length of cell cycle phases from asynchronous cultures of S.cerevisiae. Exp. Cell Res. 102 : 276-284.

Beran, K. 1968. Budding of yeast cells, their scars and ageing. Adv. Microb. Physiol. 2 : 143-171.

Beran, K., I. Malek, E. Streiblova & J. Leiblova. 1967. The distribution of the relative age of cells in yeast populations, p.57-67. In E.O. Powell, C.G.T. Evans, R.E. Strange & D.W. Tempest (ed.), Microbial physiology and continuous culture. H.M.S.O., London.

Beran, K., E. Streiblova & J. Leiblova. 1966. On the concept of the population of the yeast S.cerevisiae, p.353-363. In Second International Symposium on Yeasts (Bratislava, 1966). Slovak Academy of Sciences, Bratislava.

Brooks, R.F., D.C. Bennett & J.A. Smith. 1980. Mammalian cell cycles need two random transitions. Cell 19 : 493-504.

Burns, V.W. 1956. Temporal studies ofcell division. I. The influence of ploidy and temperature on cell division in S.cerevisiae. J. Cell. Comp. Physiol. 47 : 357-375.

Byers, B. & L. Goetsch. 1974. Duplication of spindle plaques and integration of the yeast cell cycle. Cold Spring Harbor Symp. Quant. Biol. 38 : 123-131.

Byers, B. & L. Goetsch. 1975. Behaviour of spindles and spindle plaques in the cell cycle and conjugation of S.cerevisiae. J. Bacteriol. 124 : 511-523.

Cabib, E. 1975. Molecular aspects of yeast morphogenesis. A. Rev. Microbiol. 29 : 191-214.

Carter, B.L.A. & M.N. Jagadish. 1978. The relationship between cell size and cell division in the yeast S.cerevisiae. Exp. Cell Res. 112 : 15-24.

Carter, B.L.A. & P.E. Sudbery. 1980. Small-sized mutants of S.cerevisiae. Genetics 96 : 561-566.

Castor, L.N. 1980. A G1 rate model accounts for cell cycle kinetics attributed to 'transition probability'. Nature (London) 287 : 857-859.

Ciejek, E. & J. Thorner. 1979. Recovery of S.cerevisiae a cells from G1 arrest by α factor pheromone requires endopeptidase action. Cell 18 : 623-635.

Cook, J.R. & T.W. James. 1964. Age distribution of cells in logarithmically growing cell populations, p.485-495. In E. Zeuthen (ed.), Synchrony in cell division and growth. Wiley Interscience, New York.

Cooper, S. & C.E. Helmstetter. 1968. Chromosome replication and the division cycle of E.coli B/r. J. molec. Biol. 31 : 519-540.

Donachie, W.D. 1968. Relationship between cell size and time of initiation of DNA replication. Nature (London) 219 : 1077-1079.

Edmunds,L.N. & K.J. Adams. 1981. Clocked cell cycle clocks. Science (New York) 211 : 1002-1013.

Elliot, S.G. & C.S. Mclaughlin. 1978. Rate of macromolecular synthesis through the cell cycle of the yeast S.cerevisiae. Proc. natn. Acad. Sci. USA. 75 : 4384-4388.

Fantes, P.A. 1977. Control of cell size and cycle time in Schizosaccharomyces pombe. J. Cell Sci. 24 : 51-67.

Fantes, P.A., W.D. Grant, R.H. Pritchard, P.E. Sudbery & A.E. Wheals. 1975. Regulation of cell size and the control of mitosis. J. theor. Biol. 50 : 213-244.

Fantes, P.A. & P. Nurse. 1977. Control of cell size at division in fission yeast by a growth-modulated size control over nuclear division. Exp. Cell Res. 107 : 377-386.

Fantes, P.A. & P. Nurse. 1981. Division timing: controls, models and mechanisms, p. 11-33. In P.C.L. John (ed.), The cell cycle. S.E.B. Seminar Series 10. C.U.P., Cambridge.

Freifelder, D. 1960. Bud position in S.cerevisiae. J. Bacteriol. 80 : 567-568.

Glover, D.M. 1980. Genetic engineering - cloning DNA. Chapman & Hall, London.

Hartwell, L.H. 1973. Three additional genes required for DNA synthesis in S.cerevisiae. J. Bacteriol. 115 : 966-974.

Hartwell, L.H. 1974. S.cerevisiae cell cycle. Bacteriol. Rev. 38 : 164-198.

Hartwell, L.H. 1978. Review: cell division from a genetic perspective. J. Cell. Biol. 77 : 627-637.

Hartwell, L.H., J. Culotti, J.R. Pringle & B.J. Reid.1974. Genetic control of the cell division cycle in yeast. Science (New York) 183 : 46-51.

Hartwell, L.H., R.K. Mortimer, J. Culotti & M. Culotti. 1973. Genetic control of the cell division cycle in yeast: V. Genetic analysis of cdc mutants. Genetics 74 : 267-286.

Hartwell, L.H. & J.R. Pringle.1981. The S.cerevisiae cell cycle. In J.N. Strathern, E.W. Jones & J.R. Broach (ed.) The molecular biology of the yeast Saccharomyces. Cold Spring Harbor Laboratory, New York.

Hartwell, L.H. & M.W. Unger. 1977. Unequal division in S.cerevisiae and its implications for the control of cell division. J. Cell. Biol. 75 : 422-435.

Hayashibe, M. & S. Katohda. 1973. Initiation of budding and chitin-ring. J. Gen. Appl. Microbiol. 19 : 23-39.

Hayashibe, M. & N. Sando. 1970. Characterisation of different sized cells of baker's yeast. J. Gen. Appl. Microbiol. 16 : 15-27.

Hereford, L.M., & L.H. Hartwell. 1974. Sequential gene function in the initiation of S.cerevisiae DNA synthesis. J. molec. Biol. 84 : 445-461.

Hirschberg, J. & G. Simchen. 1977. Commitment to the mitotic cell cycle in yeast in relation to meiosis. Exp. Cell Res. 105 : 245-252.

Howard, A. & S.R. Pelc. 1953. Synthesis of DNA in normal and irradiated cells and its relation to chromosome breakage. Heredity (Suppl.) 6 : 261-274.

Jaenicke, L., K. Scholz & M. Donike. 1970. Synthese der dihydrofolat-reduktase in synchronisierter hefe. Eur. j. biochem. 13 : 137-141.

Jagadish, M.N. & B.L.A. Carter. 1977. Genetic control of cell division in yeast cultured at different growth rates. Nature (London) 269 : 145-147.

Johnson, B.F. 1965. Morphometric analysis of yeast cells. Adult cell volume of S.cerevisiae. Exp. Cell Res. 39 : 577-583.

Johnson, B.F. & E.J. Gibson. 1966. Autoradiographic analysis of regional cell wall growth of yeasts. III S.cerevisiae. Exp. Cell Res. 41 : 580-591.

Johnston, G.C., C.W. Ehrhardt, A. Lorincz & B.L.A. Carter. 1979. Regulation of cell size in the yeast S.cerevisiae. J. Bacteriol. 137 : 1-5.

Johnston, G.C., J.R. Pringle & L.H. Hartwell. 1977. Coordination of growth with cell division in the yeast S.cerevisiae. Exp. Cell Res. 105 : 79-98.

Kauffman, S. & J.J. Wille. 1975. The mitotic oscillator in Physarum polycephalum. J. theor. Biol. 55 : 47-93.

Klevecz, R.R. 1976. Quantized generation time in mammalian cells as an expression of the cellular clock. Proc. natn. Acad. Sci. USA. 73 : 4012-4016.

Koch, A.L. 1977. Does the initiation of chromosome replication regulate cell division? Advances in Microbial Physiology 16 : 49-98.

Koch, A.L. 1980. Does the variability of the cell cycle result from one or many chance events? Nature (London) 286 : 80-82.

Kubitschek, H.E. 1971. The distribution of cell generation times. Cell Tiss. Kinet. 4 : 113-122.

Kubitschek, H.E. & M. Cassle. 1966. Alternative states in control of the constancy and rate of cell division in S.cerevisiae. Exp. Cell Res. 42 : 281-290.

Leiblova, J., K. Beran & E. Streiblova. 1964. Fractionation of a population of S.cerevisiae yeasts by centrifugation in a dextran gradient. Folia Microbiol. 9 : 205-213.

Lillie, S.H. & J.R. Pringle. 1980. Reserve carbohydrate metabolism in S.cerevisiae: responses to nutrient limitation. J. Bacteriol. 143 : 1384-1394.

Lipke, P.N., A. Taylor & C.E. Ballou. 1976. Morphogenic effects of α factor on S.cerevisiae a cells. J. Bacteriol. 127 : 610-618.

Manney, T.R. & J.H. Meade. 1977. Cell-cell interactions during mating in S.cerevisiae, p.283-321. In J.L. Reissig (ed.) Receptors and Recognition Series B, Volume 3. Chapman and Hall, London.

Matile, P., H. Moor & C.F. Robinow. 1969. Yeast cytology, p.219-302. In A.H. Rose and J.S. Harrison (ed.), The Yeasts, vol. 1. Acad. Press, London.

Mazia, D. 1978. Origin of twoness in cell reproduction, p. 1-14. In E.R. Dirkson, D.M. Prescott & C.F. Fox (ed.), Cell Reproduction: In Honor of Daniel Mazia. Acad. Press, New York.

Mazia, D., P.J. Harris & T. Bibring. 1960. The multiplicity of the mitotic centres and the time course of their duplication and separation. J. Biophys. Biochem. Cytol. 7 : 1-20.

Minor, P.D. & J.A. Smith. 1974. Explanation of degree of correlation of sibling generation times in animal cells. Nature (London) 248 : 241-243.

Mortimer, R.K. & J.R. Johnston. 1959. Life span of individual yeast cells. Nature (London) 183 : 1751-1752.

Muller, I. 1971. Experiments on ageing in single cells of S.cerevisiae. Arch. Mikrobiol. 77 : 20-25.

Nasmyth, K.A. 1979. A control acting over the initiation of DNA replication in the yeast Schizosaccharomyces pombe. J. Cell Sci. 36 : 155-168.

Nasmyth, K.A., P. Nurse & R. Fraser. 1979. The effect of cell mass on the cell cycle timing and duration of S phase in fission yeast. J. Cell Sci. 39 : 215-233.

Nasmyth, K.A. & S.I. Reed. 1980. Isolation of genes by complementation in yeast - molecular cloning of a cell cycle gene. Proc. natn. Acad. Sci. USA 77 : 2119-2123.

Nurse, P. 1977. Cell cycle controls in yeast. Biochem. Soc. Trans. 5 : 1191-1193.

Nurse, P. 1980. Cell cycle control - both deterministic and probabilistic? Nature (London) 286 : 9-10.

Nurse, P. & P. Thuriaux. 1977. Controls over the timing of DNA replication during the cell cycle of fission yeast. Exp. Cell Res. 107 : 365-375.

Nurse, P. & P. Thuriaux. 1980. Regulatory genes controlling mitosis in the fission yeast Schizosaccharomyces pombe. Genetics 96 : 627-637.

Pardee, A.B., B.Z. Shilo & A.L. Koch. 1979. Variability of the cell cycle, p.373-392. In G.H. Sato & R. Ross (ed.) Hormones and Cell Culture. Cold Spring Harbor Conference on Cell Proliferation, vol. 6. Cold Spring Harbor Laboratory. New York.

Powell, E.O. 1955. Some features of the generation times of individual bacteria. Biometrika 42 : 16-44.

Powell, E.O. 1956. An improved culture chamber for the study of living bacteria. J. R. microsc. Soc. 75 : 235-243.

Pritchard, R.H., P.T. Barth & J. Collins. 1969. Control of DNA synthesis in bacteria. Symp. Soc. gen. Microbiol. 19 : 263-297.

Reed, S.I. 1980. The selection of S.cerevisiae mutants defective in the start event of cell division. Genetics 95 : 561-577.

Reid, B.J. & L.H. Hartwell. 1977. Regulation of mating in the cell cycle of S.cerevisiae. J. Cell Biol. 75 : 355-365.

Rivin, C.J. & W.L. Fangman. 1980. Cell cycle phase expansion in nitrogen limited cultures of S.cerevisiae. J. Cell Biol. 85 : 96-107.

Robinow, C.F. 1975. The preparation of yeasts for light microscopy. Methods in Cell Biology 11 : 1-22.

Sachsenmaier, W., U. Remy & R. Plattner-Schobel. 1972. Initiation of synchronous mitosis in Physarum polycephalum. Exp. Cell Res. 73 : 41-48.

Samokhin, G.P., L.V. Lizlova, J.D. Bespalova, M.I. Titov & V.N. Smirnov. 1981. The effect of ∝ factor on the rate of cell cycle initiation in S.cerevisiae. Exp. Cell Res. 131 : 267-275.

Schaechter, M., J.P. Williamson, J.R. Hood & A.L. Koch. 1962. Growth, cell and nuclear divisions in some bacteria. J. Gen. Microbiol. 29 : 421-434.

Seber, G.A.F. 1977. Linear Regression Analysis. John Wiley & Sons, New York.

Shields, R., R.F. Brooks, P.N. Riddle, D.F. Capellaro & D. Delia. 1978. Cell size, cell cycle and transition probability in mouse fibroblasts. Cell 15 : 469-474.

Shields, R. & J.A. Smith.1977. Cells regulate their proliferation through alterations in transition probability. J. cell. Physiol. 91 : 345-356.

Shilo, B., V. Shilo & G.Simchen.1976. Cell cycle initiation in yeast follows first order kinetics. Nature (London) 264 : 767-769.

Shilo, B., V. Shilo & G. Simchen. 1977. Transition probability and cell cycle initiation in yeast. Nature (London) 267 : 648-649.

Simchen, G. 1974. Are mitotic functions required in meiosis? Genetics 76 : 745-753.

Simchen, G. 1978. Cell cycle mutants. A. Rev. Genet. 12 : 161-191.

Singer, R.A. & G.C. Johnston. 1981. Nature of the G1 phase of the yeast S.cerevisiae. Proc. natn. Acad. Sci. USA 78 : 3030-3033.

Slater, M.L. 1973. Effect of reversible inhibition of DNA on the yeast cell cycle. J. Bacteriol. 113 : 263-270.

Smith, J.A., D.J.R. Laurence & P.S. Rudland. 1981. Limitations of cell kinetics in distinguishing between cell cycle models. Nature (London) 293 : 648-651.

Smith, J.A. & L. Martin. 1973. Do cells cycle? Proc. natn. Acad. Sci. USA 70 : 1263-1267.

Streiblova, E. 1970. Study of scar formation in the life cycle of heterothallic S.cerevisiae. Can. J. Microbiol. 16 : 827-831.

Streiblova, E. & K. Beran. 1963. Demonstration of yeast scars by fluorescent microscopy. Exp. Cell Res. 30 : 603-605.

Sudbery, P.E., A.R. Goodey & B.L.A. Carter. 1980. Genes which control cell proliferation in the yeast S.cerevisiae. Nature (London) 288 : 401-404.

Sudbery, P.E. & W.D. Grant. 1975. The control of mitosis in Physarum polycephalum. The effect of lowering the DNA : mass ratio by UV irradiation. Exp. Cell Res. 95 : 405-415.

Sumrada, R. & T.G. Cooper. 1978. Basis amino acid inhibition of cell division and macromolecular synthesis in S.cerevisiae. J. Gen. Microbiol. 108 : 45-56.

Throm, E. & W. Duntze. 1970. Mating type dependent inhibition of DNA synthesis in S.cerevisiae. J. Bacteriol. 104 : 1388-1390.

Thompson, P.W. & A.E. Wheals. 1980. Asymmetrical division of S.cerevisiae in glucose-limited chemostat culture. J. Gen. Microbiol. 121 : 401-409.

Tukey, J.W. 1977. Exploratory Data Analysis. Addison-Wesley, Reading, Mass.

Tyson, C.B., P.G. Lord & A.E. Wheals. 1979. Dependency of size of S.cerevisiae cells on growth rate. J. Bacteriol. 138 : 92-98.

Tyson, J.J. & W. Sachsenmaier. 1978. Is nuclear division in Physarum controlled by a continuous limit cycle oscillator? J. theor. Biol. 73 : 723-737.

Wheals, A.E. 1982. Sloppy size control of the S.cerevisiae cell cycle. Molec. cell. Biol. (in press).

Wiemken, A., P. Matile & H. Moor. 1970. Vacuolar dynamics in synchronously budding yeast. Arch. Mikrobiol. 70 : 89-103.

Wilkinson,L.E. & J.R. Pringle. 1974. Transient G1 arrest of S.cerevisiae cells of mating type _ factor produced by cells of mating type a. Exp. Cell Res. 89 : 175-187.

Yanagita, T. 1977. Cellular age in microorganisms, p.1-36. In T. Ishikawa, Y. Maruyama (ed.), Growth and differentiation in microorganisms. University of Tokyo Press, Tokyo.

JOURNAL OF BACTERIOLOGY, June 1980, p. 808-818
0021-9193/80/06-0808/11$02.00/0

Vol. 142, No. 3

Asymmetrical Division of *Saccharomyces cerevisiae*

PETER G. LORD AND ALAN E. WHEALS*

Microbiology Group, School of Biological Sciences, University of Bath, Bath, United Kingdom

The unequal division model proposed for budding yeast (L. H. Hartwell and M. W. Unger, J. Cell Biol. 75:422-435, 1977) was tested by bud scar analyses of steady-state exponential batch cultures of *Saccharomyces cerevisiae* growing at 30°C at 19 different rates, which were obtained by altering the carbon source. The analyses involved counting the number of bud scars, determining the presence or absence of buds on at least 1,000 cells, and independently measuring the doubling times (τ) by cell number increase. A number of assumptions in the model were tested and found to be in good agreement with the model. Maximum likelihood estimates of daughter cycle time (D), parent cycle time (P), and the budded phase (B) were obtained, and we concluded that asymmetrical division occurred at all growth rates tested (τ, 75 to 250 min). D, P, and B are all linearly related to τ, and D, P, and τ converge to equality (symmetrical division) at $\tau = 65$ min. Expressions for the genealogical age distribution for asymmetrically dividing yeast cells were derived. The fraction of daughter cells in steady-state populations is $e^{-\alpha P}$, and the fraction of parent cells of age n (where n is the number of buds that a cell has produced) is $(e^{-\alpha P})^{n-1}(1 - e^{-\alpha P})^2$, where $\alpha = \ln 2/\tau$; thus, the distribution changes with growth rate. The frequency of cells with different numbers of bud scars (i.e., different genealogical ages) was determined for all growth rates, and the observed distribution changed with the growth rate in the manner predicted. In this haploid strain new buds formed adjacent to the previous buds in a regular pattern, but at slower growth rates the pattern was more irregular. The median volume of the cells and the volume at start in the cell cycle both increased at faster growth rates. The implications of these findings for the control of the cell cycle are discussed.

Most cells reproduce by symmetrical binary fission, each cell producing two daughter cells of equal size whose cycle times are (on average) the same as each other and their parent cell. The division of a budding yeast is asymmetrical, giving two cells, one of which is the old (parent) cell and one of which is the new (daughter) cell. At all growth rates the daughter cell immediately after division is always smaller than the parent cell. As the growth rate decreases, this difference in size becomes more accentuated (2, 7, 12, 15, 17, 32, 33). Under steady-state conditions the cycle time of daughter cells is always longer than that of parent cells at all except maximum growth rates (5, 7, 8, 12, 15, 17, 32). The difference in cycle times also becomes more accentuated as the growth rate decreases. These facts concerning budding yeasts have been known for several years, but it was not until it was shown that cells need to attain a critical size in order to initiate the DNA division cycle that a formal model to explain the observations could be presented (19). With more evidence from time-lapse photomicroscopy, Hartwell and Unger (12) developed the model further (referred to below as the Hartwell-Unger model). The model states that as the growth rate decreases, daughters are born at a smaller size and therefore require a longer period of growth before reaching the critical size necessary for initiation of the DNA division cycle (at start in the cycle). Hartwell and Unger also derived the age distribution for asymmetrically dividing cells in an asynchronous steady-state culture, which should be compared with the age distribution derived for symmetrically dividing cells (34). The latter would only apply for budding yeasts at their maximum balanced growth rate (μ_{bmax}), when daughters would be born at the critical size and thus commence the DNA division cycle immediately. In this case the daughter cycle time (D) would be the same as the parent cycle time (P), and each would be equal to the population doubling time (τ) (i.e., $D = P = \tau$). This is easily seen by substituting τ for D and P in the age distribution equation for unequally dividing cells (see Appendix, equation 3). Hartwell and Unger derived the relationship between D, P, and τ. The measurements of D, P, and τ which they obtained from time-lapse photomicroscopy clearly fitted the relationship. These equations allow quantitative estimates to be made about

the cell cycle from cell population data.

When yeast cells bud, a ring of chitin builds up at the bud isthmus (14). This chitin ring remains on the parent cell after the bud (newborn daughter cell) has separated from the parent, and it is then termed a bud scar. Bud scars on intact cells can be visualized by fluorescence microscopy, using fluorescent stains (14, 28). It is therefore possible to ascertain the age of a cell in terms of how many cycles it has passed through from the number of bud scars it possesses. We call this age the genealogical age because it indicates that yeast populations contain several morphologically distinct generations of cells. A cell with no bud scar (a daughter cell) has not completed a cycle, belongs to the youngest generation, and is of genealogical age 0. A cell with one bud scar has completed one cycle, belongs to the next youngest generation, and is of genealogical age 1, and so on.

To assess the general applicability of the Hartwell-Unger model to studies on the yeast cell cycle, we needed to determine how the quantitative predictions of the model compared with experimental observations. We chose two ways of testing the model. The first was to obtain estimates of D, P, and the budded phase (B) from the frequency of budded and unbudded parents and daughters and determine whether they fitted the constraints of the model. The second was to see how the genealogical age distribution varied with the growth rate. If budding yeast divided symmetrically, the fractions of cells of the different genealogical ages would form a geometric series. In this case there would be one-half as many cells of genealogical age $n + 1$ as there would be cells of age n (since the fraction of cells of age n is given by $[\frac{1}{2}]^{n+1}$, where $n = 0, 1, 2$, etc.), and this would be true at all growth rates (34). We derived the genealogical age distribution for asymmetrically dividing cells (see Appendix). For the fraction of daughters (age $n = 0$), this is $e^{-\alpha P}$, where α is the specific growth rate of the population, and for the fraction of cells of genealogical age n ($n = 1$, 2, 3, etc.), it is $(e^{-\alpha P})^{n-1}(1 - e^{-\alpha P})^2$. Only the fractions of cells of genealogical age 1 and above form a geometric series. The distribution varies with growth rate since $\alpha = \ln 2/\tau$. It can readily be shown (see Appendix) that at μ_{bmax}, the genealogical age distribution is the same as for symmetrically dividing cells.

(This work was reported at the Society for Applied Bacteriology summer meeting, Newcastle, United Kingdom, July 1979 [J. Appl. Bacteriol. 47:v-vi, 1979].)

MATERIALS AND METHODS

Organism. A wild-type haploid strain of *Saccharomyces cerevisiae* obtained from C. F. Roberts, Genetics Department, University of Leicester, was used throughout. Designated S288C/1, this strain is a clone isolated from the stock strain S288C, but differs from it in a number of respects (see below).

Media. The compositions of the two basal media used were as described previously (30). Yeast extract peptone and Edinburgh minimal medium both contained 20 g of a carbon source per liter. All media (see Table 1) were filtered through microfilters to give particle-free solutions and were sterilized by autoclaving, except for the vitamin constituent of Edinburgh minimal medium, which was filter sterilized.

Growth conditions. Cells were grown with shaking at 30°C in 100 ml of medium in 250-ml Erlenmeyer flasks. Samples were taken periodically. Each sample was fixed with a solution containing 0.9% NaCl and 4% formaldehyde and briefly sonicated to disperse clumped cells. Growth was determined by total cell count.

Cell counts and volume. Cell counts and volume were determined by using a model 111 LTS Electrozone/Celloscope (Particle Data Inc., Elmhurst, Ill.) fitted with a 60-μm orifice tube. Cell volume distributions were obtained by using a Nuclear Data model 1100 Analyser System (Nuclear Data Inc., Palatine, Ill.) coupled to a Hewlett-Packard X-Y plotter (Hewlett-Packard Inc., Pasadena, Calif.). Median cell volumes were obtained from the peaks of the normal distributions of volumes (on a log scale). The equipment was calibrated by using standard 5.7-μm-diameter latex spheres (Dow Chemical Co.).

Bud scar analysis. Bud scar analysis was carried out on samples of cells which were in the midexponential phase of growth. Cell suspensions were concentrated by either (i) centrifugation at 6,000 rpm for 15 min in a Measuring and Scientific Equipment bench centrifuge or (ii) collection on a microfilter; after the cells were concentrated, they were resuspended in 0.5 to 1 ml of medium. These suspensions were stained with a 2-mg/ml solution of calcofluor (a gift from J. Peberdy). The cells were observed at ×1,250 by using incident UV light with appropriate filters and a Leitz Orthoplan phase-contrast microscope. The number of cells in each of the following cell categories was determined: (i) unbudded daughters, (ii) budded daughters, (iii) unbudded parents with n scars, and (iv) budded parents with n scars, where n took a value between 1 and 17.

The numbers of budded cells and total scars also followed from these data. The fluorescence observed at the bud isthmus on a budded cell was not counted as a scar. At least 1,000 cells were scored in each experiment.

RESULTS

Asymmetrical age distribution. Relationships for the relative frequencies of cell types can be found directly from the expression describing the age distribution derived by Hartwell and Unger (12; see Appendix, equation 3). Estimates of D, P, and B can be found by using these relationships and experimentally determined values of fractions of cell types. D, P, and

α are related by

$$e^{-\alpha D} + e^{-\alpha P} = 1 \quad (1)$$

Substituting equations 7 and 8 (see Appendix) into equation 1 yields

$$F_{DB} \cdot F_{PB} = F_B^2 \quad (2)$$

where F_{DB}, F_{PB}, and F_B are the fraction of daughters that are budded, the fraction of parents that are budded, and the fraction of budded cells, respectively. This equation provided a test for a number of assumptions of the model (see below). We substituted experimental values of F_{DB}, F_{PB}, and F_B (Table 1) into equation 2 and found excellent agreement with the equation at all growth rates; the mean departure from the expected values was 0.003.

Maximum likelihood estimation. There are several different ways to calculate D and P from the raw data (see Appendix, equations 7 through 9). Each uses only a part of the data; hence, the values of D and P obtained may differ in each case. More importantly, there is no guarantee that the resulting estimates exactly satisfy the constraints of $D > P > B > 0$ and equation 1, which are specified by the model. A method which uses all of the data and gives estimates which satisfy the above constraints is the method of maximum likelihood. This optimizes the estimates in a fashion analogous to linear regression so that the deviation of observed values from expected values is minimized. To apply this method to the data, a computer program (obtainable from A.E.W.) was devised by Peter Green, Department of Mathematics, University of Durham, Durham, United Kingdom. This program uses the number of unbudded daughters, the number of unbudded parents, the number of budded cells, and the total number of scars, from which F_{DB} and F_{PB} are calculated (Table 1). To begin the program, rough estimates of P and B are entered, which are calculated as described in the Appendix (equations 8 and 4, respectively). The estimates obtained are dimensionless and are expressed in units of τ.

Cell cycle parameters. Maximum likelihood estimates of D, P, and B are shown in Fig. 1 as functions of τ. Each parameter increases linearly with τ. The empirical relationship between each parameter and τ was determined by linear regression (Table 2). The curves of D versus τ and P versus τ are very good fits to the data, as is obvious from the coefficients of determination.

As stated above, the age distribution for asymmetrically dividing cells should become the same as that for symmetrically dividing cells at the μ_{bmax}, when $D = P = \tau$. By extrapolation, the curves of D versus τ and P versus τ intercept when $D = P = 65.1$ min and $\tau = 65.9$ min. Therefore, the μ_{bmax} for this strain should be achieved when τ is about 65 min.

The interval from the birth of a parent to bud emergence (the P-B period) also has a linear relationship to τ.

Genealogical age distribution. The age dis-

TABLE 1. *Numbers of budded and unbudded parents and daughter cells at different τ*

Medium[a]	τ (min)	No. of:				
		Unbudded daughters	Budded daughters	Unbudded parents	Budded parents	Bud scars
YEP + glucose	76.3	247	408	160	407	1,264
YEP + glucose	79.6	224	306	140	377	1,095
YEP + glucose	84.1	279	302	118	348	1,006
YEP + fructose	86.6	304	327	132	264	908
YEP + mannose	91.2	266	268	192	324	1,015
YEP + mannose	92.9	354	296	119	308	942
YEP + raffinose	114.1	264	298	160	307	911
YEP + cellobiose	114.6	351	260	119	320	932
YEP + raffinose	122.5	410	196	167	259	953
YEP + galactose	127.3	537	201	201	207	897
YEP + glycerol	128.9	387	235	170	301	1,049
YEP + glycerol	153.6	478	181	164	225	896
YEP + glycerol	156.7	418	183	155	276	984
YEP + sorbitol	156.9	424	204	166	241	869
YEP + mannitol	162.7	439	172	206	218	979
YEP + mannitol	193.3	512	154	172	208	847
EMM + galactose	203.9	538	125	201	208	875
YEP + mannitol	222.6	507	155	211	177	934
EMM + galactose	242.3	590	86	244	167	925

[a] YEP, Yeast extract peptone; EMM, Edinburgh minimal medium.

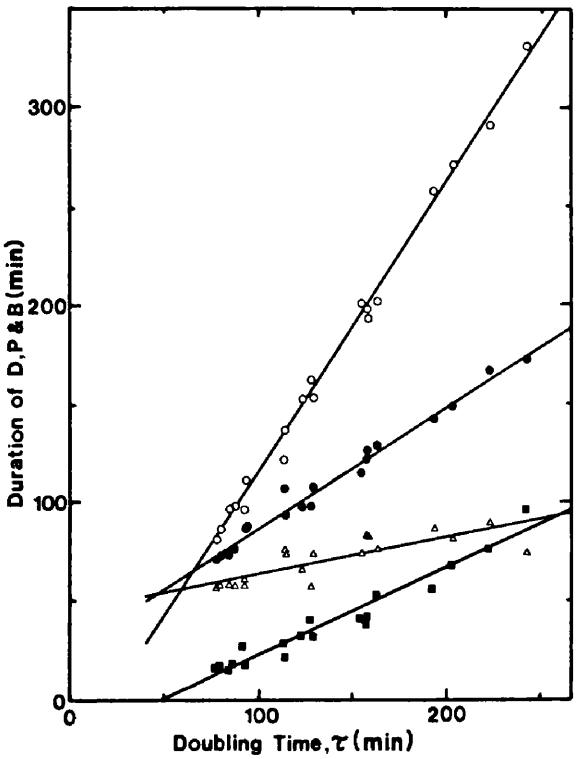

FIG. 1. *Duration of cell cycle parameters as function of τ. All values are maximum likelihood estimates, calculated from the data in Table 1. The straight lines were fitted by linear regression (see Table 2). Symbols: ○, D; ●, P; △, B; ■, duration of P-B period. The P-B period is the time from birth of the parent to bud emergence.*

TABLE 2. *Empirical relationships of cell cycle parameters in two strains of S. cerevisiae*

Period	Relationship in strain:[a]	
	S288C/1[b]	C276[c]
D	$1.48\tau - 32$ ($r^2 = 0.99$)[d]	$1.41\tau - 28$
P	$0.62\tau + 24$ ($r^2 = 0.98$)	$0.53\tau + 45$
B	$0.18\tau + 46$ ($r^2 = 0.66$)	$0.17\tau + 87$
P–B	$0.44\tau - 22$ ($r^2 = 0.94$)	$0.36\tau - 42$
D–B	$1.30\tau - 78$ ($r^2 = 0.97$)	$1.24\tau - 28$

[a] All values are in minutes.
[b] From bud scar analysis at 30°C in batch culture.
[c] From time-lapse photomicroscopy at 24°C in batch culture (12).
[d] r^2, Coefficient of determination.

tribution of budding yeasts can be divided into several component parts (Fig. 2 and Appendix). The area of an individual part represents the relative frequency of cells of a particular genealogical age. The fraction of cells of each age should vary with growth rate since the fraction is a function of P and τ. Figure 3 shows the predicted variation in the percentages of cells of different genealogical ages with τ, when equations 9 and 14 (see Appendix) and $P = 0.62\tau + 24$ (Table 2) were used.

Genealogical age distribution at different growth rates. Table 3 shows the values obtained in these experiments for the percentages of cells of the different ages. Figure 4 shows the

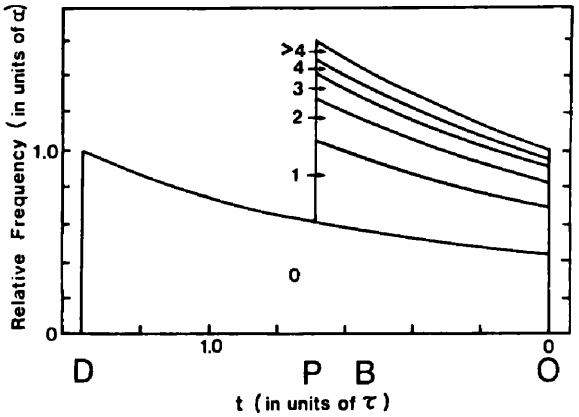

FIG. 2. *Cell age distribution for asymmetrically dividing yeast cells. Based upon reference 12, this diagram shows the frequency of cells of different genealogical ages as a function of cell age in exponentially grown steady-state populations. The numbers on the figure indicate the numbers of bud scars (genealogical age) of each class of cells. D, P, and B were all measured from division at zero time.*

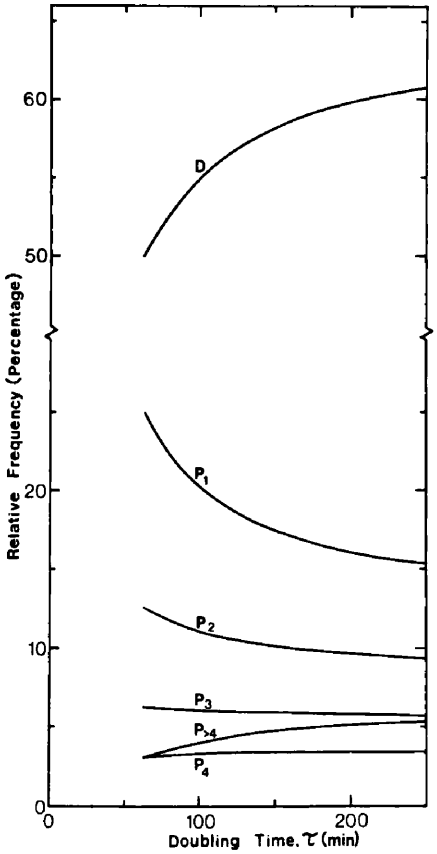

FIG. 3. *Theoretical relative frequency of cells of different genealogical ages as a function of growth rate. The curves are based on equations 9 and 14 and $P = 0.62\tau + 24$. P_1, frequency of parents of age 1, etc.*

TABLE 3. *Percentages of cells of different genealogical ages at each τ*

τ (min)	% of cells at genealogical age:[a]						Chi-square test[b]
	0	1	2	3	4	>4	
76.3	53.60	20.54	11.29	6.47	3.85	4.26	—
79.6	50.62	20.73	13.28	9.55	2.87	2.96	0.1
84.1	55.49	19.68	12.51	5.73	3.15	3.44	—
86.6	61.44	15.68	10.42	5.84	3.51	3.12	0.1
91.2	50.86	23.52	14.38	6.00	2.67	2.57	—
92.9	60.35	16.81	10.77	5.57	3.16	3.34	—
114.1	54.62	22.64	12.44	5.05	2.82	2.43	—
114.6	58.19	17.71	13.33	4.57	3.05	3.14	1
122.5	58.72	17.73	8.43	5.04	3.78	4.36	—
127.3	64.40	15.18	9.69	5.32	2.36	3.05	0.1
128.9	56.91	18.21	11.99	5.58	3.39	3.93	—
153.6	62.88	14.50	9.92	6.87	2.77	3.05	1
156.7	58.33	16.47	11.82	5.81	3.78	3.49	—
156.9	60.68	17.49	10.82	5.89	2.71	2.42	5
162.7	59.61	17.27	9.85	6.83	3.12	4.29	—
193.3	63.67	15.39	9.85	4.78	3.06	3.25	5
203.9	61.85	16.14	11.29	5.04	3.17	2.52	1
222.6	63.05	15.52	9.05	5.33	2.95	4.10	—
242.3	62.19	17.02	8.28	6.16	3.04	3.31	5

[a] Genealogical age (n) is equal to the number of bud scars. At least 1,000 cells were scored for each growth rate.

[b] Chi-square test of goodness of fit of the data. The null hypothesis was that there was no significant difference between the observed frequency of cells of each of the six genealogical age classes (as numbers) and the expected frequency (as numbers) based on $P = 0.62\tau + 24$ and equations 9 and 14. —, No significant difference; 5, significant difference at the 5% level; 1, significant difference at the 1% level; 0.1, significant difference at the 0.1% level.

variation in the percentage of cells of age 1 with τ. The data do not fit the predicted values for symmetrical division at any growth rate but are a good fit to the predicted course for asymmetrical division, decreasing as τ increases. Similar plots for cells of each age class show equally good fits to the expected values (data not shown). However, chi-square analysis was performed on the data at each growth rate, and a significant difference from the expected geometric series was found in one-half the experiments (Table 3). To determine whether this was a random effect or whether the frequencies of some age classes showed a systematic departure from expectation, a "box and whiskers" plot (29) for each age class was constructed (Fig. 5).

This method of analysis revealed information which would otherwise have been obscured by conventional statistical procedures. Two conclusions are apparent from the plot. First, although there is obvious scatter, the data do follow the general trend predicted from the model extremely well (the median values are close to zero). Second, there is an excess of daughters and fewer cells of genealogical age greater than 4.

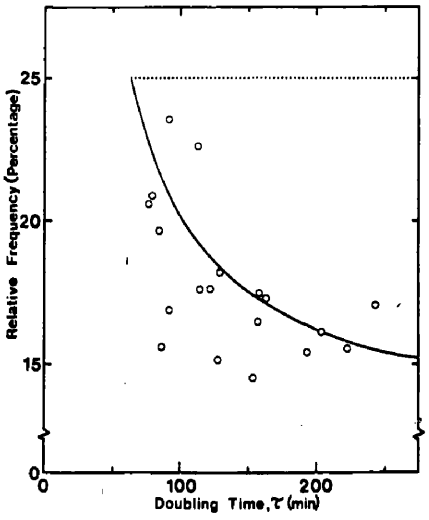

FIG. 4. *Relative frequency of cells of genealogical age 1 at different growth rates. Cells of genealogical age 1 are parents with one bud scar. The solid line is the expected frequency of cells of age 1 based on P = 0.62τ + 24 and equation 14. The dotted line is the predicted frequency for symmetrically dividing cells. The data are from Table 3.*

Pattern of budding. The formation of buds in a regular spiral sequence from one pole of the cell to the other has been described previously (27) for most haploid cells. We noted that at slower growth rates a small fraction of cells do not form buds in a spiral arrangement. There is a gap in the sequence of bud scars on some of these cells, and on others bud scars occur at opposite poles. The fraction of cells with these

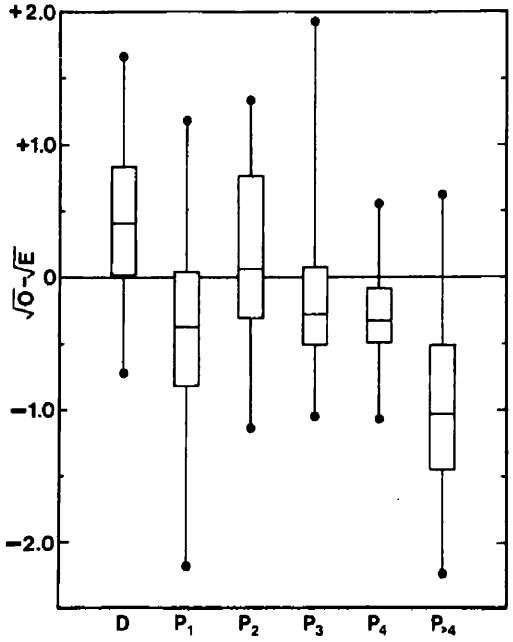

FIG. 5. *Relationship of observed to expected frequencies of cells of different genealogical ages over a range of growth rates. A value of $P = 0.62\tau + 24$ and equations 9 and 14 were used to calculate the expected frequencies of cells (as numbers) of different genealogical ages (P_1, parents of age 1, etc.) at each growth rate. The observed values (as numbers) were taken from Table 3. Since the relative frequency of cells declines with genealogical age, a normalizing procedure was performed; this was done by taking square roots of both observed (O) and expected (E) values in order to make the differences of comparable magnitude. The difference between the square roots of the observed and expected frequencies at each of 19 growth rates is presented in the form of a box enclosing the central 50% of the data points (the median is indicated by a cross bar), and whiskers extend to the extreme values. (A difference of ±0.5 on the ordinate indicates a departure from the expected value of ±16 when the number counted was 250.)*

bud scar patterns increased from 0.3% at τ = ca. 120 min to 1.5% at τ = 200 min. We observed that the majority of cells had this irregular pattern of budding in a population of cells growing at τ = ca. 400 min (data not shown).

Volume measurements. The median cell volume increased with the growth rate (Fig. 6), the largest increases occurring at the faster growth rates. A curve of increasing slope (from slow to fast growth rates) gave the best fit to the data.

DISCUSSION

Hartwell and Unger have provided a model of the yeast cell cycle based on the following two simple, but far-reaching ideas: (i) that budding yeast cells attain a critical cell size before initiating the DNA division cycle at start, and (ii) that budding yeasts divide asymmetrically, a consequence of which is that daughter cells have a cycle time different from that of parent cells.

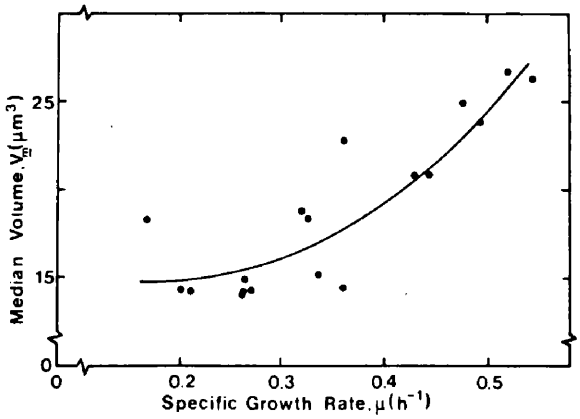

FIG. 6. *Median cell volume as a function of growth rate. The curve was fitted by eye.*

In formulating their model and deriving cell age distribution equations, Hartwell and Unger made the following assumptions: (i) the population was asynchronous and growing exponentially; (ii) all parents had the same cycle time (P); (iii) all daughters had the same cycle time (D); and (iv) $D > P$. Implicitly, it was also assumed that (v) all cells had the same budded period (B), (vi) that $P > B$, and (vii) that all cells were immortal.

Let us consider these points separately. Assumption i was satisfied in our experiments since cells were growing exponentially, as judged by increases in cell numbers, both before and after sampling for bud scar analysis.

Assumptions ii and iii are clearly false, since considerable cycle time variability has been shown for both parents and daughters (12, 25; L. Daniel and A. E. Wheals, unpublished data). Nevertheless, Hartwell and Unger have shown that the mean values of D and P can be used successfully as approximations. More importantly, we need to consider whether the mean P value is different for parents of different genealogical ages. Figure 5 reveals that this is not so. The observed frequency of cells of different genealogical ages (P_1 to P_4) was close to the predicted value, assuming a constant P. Since the rate of entry of parents into age category $n + 1$ is determined by the rate of exit of parents of age n, a departure from expected values could occur only if cells spent longer or shorter times in each parent cycle. There was little departure from expected values, so we can conclude that P is constant for at least cells of ages P_1 to P_4. Cells of age greater than 4 could have shorter (or longer) cycle times, but this is not the cause of the shortage of cells of age $P_{>4}$. Since this last term is the sum of all older age groups, the total frequency should be as expected, whatever the distribution of cycle times of cells of different

ages. The cause of the shortage is discussed below.

Similarly, it is important to know whether the cycle times of daughters born from parents of different genealogical ages vary. Since the D values measured by Hartwell and Unger (12) for parents of different ages formed a single continuous distribution, this assumption is reasonable.

Assumption iv is supported by a large body of evidence, both qualitative and quantitative, and is confirmed in this study since $F_D > 0.5$.

Since we have evidence that P is constant for cells of different ages, we can test assumption v by looking at the ratio of budded parents to total parents at each genealogical age. Since this value varies with growth rate, we calculated the fraction of budded parents at each age for each growth rate (F_{PBn}) and subtracted this value from the mean value ($\bar{F}_{PB}$) of the five age groups P_1 to P_4 and $P_{>4}$ at that growth rate. Table 4 shows the median difference for each age group for all 19 growth rates. There was no evidence that this fraction changed systematically with genealogical age. Hence, we can conclude that the budded period for parents in age groups P_1 to P_4 was also constant. Using the symbols B_d for budded daughter period, U_{p1} for unbudded period of parent age 1, etc., we can write $U_{p1} = U_{p2}$. By using time-lapse photomicrography, it has been shown (12; Lord and Wheals, unpublished data) that $B_d + U_{p1} = B_{p1} + U_{p2}$, so we conclude that $B_d = B_{p1}$ and that B is constant for all cells.

Assumption vi is satisfied by numerous observations of growing yeasts and an understanding of the cell cycle circuitry, in which cell separation normally occurs before a new bud is initiated, thus creating an unbudded period for a newborn parent cell.

Micro-manipulation of yeast cells has shown them to be capable of up to 46 cycles; a mean value of 30 was obtained in one set of experiments (22), a number equivalent to a death rate of approximately 10^{-10} per cell per generation (hence, immortality for all practical purposes [assumption vii]). However, the shortage of $P_{>4}$ cells can only be explained on the basis of cell loss from this class since entry into this class was at the appropriate rate. Indeed, we noticed several highly fluorescent moribund cells in all experiments, so we suggest an increasing probability of death with increasing genealogical age in batch cultures. Since immortality is assumed, death of older cells has the effect of decreasing F_P and hence increasing F_D above its expected value, as was observed (Fig. 5). In this sense, F_D is an unreliable value on which to base estimates of cell cycle parameters, and we used equation 8 rather than $P = -\ln F_D/\alpha$ (from equation 9) to calculate P.

Finally, we substituted experimental values of F_{DB}, F_{PB}, and F_B into equation 2 for all of the growth rates and found good agreement. Equation 2 is derived from equations 1, 7, and 8. Since equation 1 is based upon assumptions i through iv and vii, and equations 7 and 8 are in addition based upon assumptions v and vi, equation 2 thus simultaneously tests all seven assumptions, confirming that although the assumptions are often simplifications, they are not a gross distortion of reality. (The other important solution for this equation is when assumption v does not hold but instead $F_{DB} = F_{PB}$; this would occur only at symmetrical division.)

We are thus justified in using the maximum likelihood method to obtain the best estimates of D, P, and B subject to the constraints and assumptions i to vii described above. Figure 1 clearly shows the direct linear relationships of D, P, and B to τ. A similar conclusion was reached previously on the basis of a more limited sample analyzed by time-lapse photomicroscopy (12). There is good quantitative agreement between the two sets of data, even though different strains, temperatures, and methods to vary the growth rate were used (Table 2). Qualitatively similar results have also been obtained from bud scar analyses of chemostat-grown cells (7).

Our results confirm the view that division is asymmetric at all growth rates tested and that the ratio of D to P increases at slower growth rates, such that at τ = 250 min, parents are cycling twice as fast as daughters.

Start has been defined as the stage of commitment in the cell cycle and is detectable as the point of arrest after nutrient limitation or after mating pheromone treatment and the location of the temperature-sensitive *cdc28* step (11). Attainment of a critical cell size has also been postulated as a prerequisite for traverse of start (19). The precise temporal location of start is more uncertain. One study (16) has shown that the α-factor-sensitive and *cdc28* temperature-sensitive steps occur at about the same time and

TABLE 4. *Median value of ($\bar{F}_{PB} - F_{PBn}$) for each parental age group*[a]

Genealogical age	Median value of ($\bar{F}_{PB} - F_{PBn}$)
1	0.0058
2	0.0107
3	−0.0231
4	0.0012
>4	0.0109

[a] F_{PBn}, Number of budded cells/total number of cells for parental age group n; $\bar{F}_{PB}$, mean value of F_{PBn} when n = 1, 2, 3, 4, and >4.

at a constant period before division over a range of growth rates, suggesting an increasing interval between birth of a parent and start at slower growth rates. A similar study on the α-factor-sensitive step came to the same conclusion and seems to be correct, even though the data were incorrectly calculated and presented (12; L. H. Hartwell, personal communication). However, since the effect on the cell cycle of cycloheximide (used for altering the growth rate) has not been determined, some caution should be exercised in interpreting these results. Two other studies (1, 26) conclude that the initiation of DNA synthesis (I) and bud emergence occur at approximately the same time (one indicating I before bud emergence [26] and the other indicating bud emergence before I [1]). Although start is presumed to occur shortly before both of these events (11), the studies are of limited value since neither P nor start was directly monitored.

A contrary view, that there may be a substantial interval between start and bud emergence (but not necessarily between start and I), comes from a number of different experiments in which 8 measurements of I, 3 measurements of F (the α-factor-sensitive step), and 12 measurements of bud emergence were made over a range of growth rates (C. Rivin, Ph.D. thesis, University of Washington, Seattle, 1978). The I and F occurred at about the same time, but the period from I or F to bud emergence (the I,F-B period) varied from 30 min at $\tau = 100$ min to 150 min at $\tau = 400$ min (I/F-$B = 0.43\tau - 23$), a relationship very similar to our data on the P-B period. We also suggest that start occurs at, or shortly after, P in the cycle. To initiate the cell cycle, all daughters have to attain the critical size. After this and during B, a budded cell remains the same size or even increases in size. After division therefore, the parent cell is born at a size at or above the critical size and thus can reenter the cycle immediately at start. The P-B period is thus poststart, and preparation for bud emergence is one of the processes during this interval.

If, as we suggest, start and P are contemporaneous, then a size control is both a necessary and a sufficient cause for initiation of the cycle in parent cells growing under balanced growth conditions in the absence of mating pheromone. If, however, start occurs shortly before bud emergence, then the P-B period is essentially prestart, and it raises the question of what control, in addition to the necessary but insufficient size control, prevents parent cells from traversing start soon after their birth. (If a cell needs to have completed a cycle before a new one is initiated, one possibility is that the end of a cycle occurs not at division but during the following unbudded phase.)

Although I for parents occurs shortly after start, B may be delayed. It is possible that bud emergence is an event conditional upon start, but there may be a second, temporal control on its timing.

The P period corresponds to the time from the start of the cell cycle to division. It is thus analogous to the $C + D$ period of bacteria (24), but differs in that it increases in duration as the growth rate decreases. Similarly, the budded period, sometimes thought to be invariant (20), also shows a consistent increase in duration (0.18 min for each 1-min increase in τ). This increase is apparent in all the published data, the magnitude varying with strain and experiment. Previously, the cells from which our clone was isolated have shown an increase of 0.5 min/min of τ under apparently identical conditions (30). The time from birth to bud initiation also increases in duration to such an extent that 50% of the parent cycle is unbudded at $\tau = 250$ min, compared with 16% at $\tau = 75$ min.

Extrapolating beyond the limits of the data can be misleading but focuses our attention on some of the logic of the control of cell division. $D = P = \tau$ at 65 min; thus, μ_{bmax} is 0.64 h^{-1} for balanced growth. At mass doubling times faster than this, the equations imply that the time required for P is greater than that available. Growth would thus be unbalanced, population doubling time and D would equal P, and daughters would be born at a size greater than the initiation volume (V_P). Cells would be growing faster than they could divide, and the mean cell size of the population would increase. The equations also imply that when B and the population doubling time (now P) are equal (about 50 min), the whole of the parent and daughter cycle is budded. At growth rates faster than this, it is implied that there is insufficient time for a budded cycle. To overcome this, a cell may form a second bud before the first bud separates. Hypertrophism (or abnormally rapid growth rates) has been achieved in a two-stage fermentor with the yeast *Candida utilis* (31). Interestingly, at a τ of less than 1 h both unbalanced growth and secondary bud formation were observed, and similar results have been achieved with *S. cerevisiae* in chemostat cultures (P. Thompson and A. E. Wheals, unpublished data).

Several authors have noted that in populations of budding yeasts, as the growth rate decreased, the fraction of daughter cells increased (2–4, 7, 15, 32). Beran and co-workers (2–4) have also shown that the fractions of cells of different genealogical ages vary with the growth rate. An explanation of this was attempted by Gani and Saunders (10), who assumed that budding yeasts divided symmetrically. They tested the hypoth-

esis that the results were due to differences in birth rates of daughter and parent cells. They concluded that this was untenable and suggested that a difference between daughter and parent budding times would provide a better explanation. Our analysis, based on the Hartwell-Unger model, provides a satisfactory quantitative explanation at all growth rates. Only two discrepancies arose. First, there was a shortage of cells of age greater than 4 and a corresponding excess of daughters, the reason for which, we believe, was the increased mortality of older cells (see above). Second, at nearly one-half of the growth rates the observed frequencies were significantly different from the expected geometric series, as tested by a chi-square test (Table 3). Part of the reason was undoubtedly due to the first feature described above. In addition, it must be remembered that the Hartwell-Unger model is a simplified, deterministic one and that D and P should be regarded as mean values. The variability in cycle times of D and P increases the total variance beyond that simply due to sampling error, and hence a chi-square test gives a false indication that the results are significantly different from the expected values.

Buds on haploid cells of most *S. cerevisiae* strains are formed in a highly ordered sequence. The first bud is formed at the same pole as the birth scar (9, 27), and successive buds are formed adjacently in rows, rings, or spirals (27). The cells used in these experiments formed buds predominantly in a precise spiral sequence (evident on cells with many bud scars). It would be of interest to know how a cell, in order to achieve such ordered sequences, determines the sites of budding. A clue is provided by the behavior during the cell cycle of the spindle pole body (SPB), which is embedded in the nuclear membrane (6). Duplication of the SPB appears to be a prerequisite for bud emergence. The duplicated SPB is orientated toward the emerging bud, and cytoplasmic microtubules extend from the duplicated SPB to the base of the emerging bud. Immediately after division the SPB is orientated toward the pole opposite the bud scar in the mother cell and opposite the birth scar in the daughter cell (21). If the site of budding is determined by the position of the SPB, then buds should be born alternately at opposite poles of the cell. Because buds are formed adjacently, the SPB must reorient after each division in a precisely controlled manner to become aligned with the previous site of budding. At slow growth rates (τ = 400 min) buds are formed in a less ordered sequence, which is similar to the sequence on diploid cells (13, 23, 27), so the precision of the control may be lost under these circumstances.

The median size of the cells varied with the growth rate (Fig. 6), as was observed previously (30), although in this study the variation in size was not as dramatic, the largest cells being 1.9 times the size of the smallest cells. It was possible to calculate the size of a cell at time P (V_P) (i.e., close to start) in the cycle from the data by using equation 15. The volume increased with the growth rate, the greatest increase occurring at fast growth rates, as was found previously (30). (We incorrectly stated [30] that the mean cell volume had been measured, whereas the median cell volume had been measured. We recalculated V_P from the data of reference 30 by using equation 15 and found that the recalculated values of V_P were only slightly different [less than 4%]; thus, none of the previous conclusions was invalidated.) Direct measurements of cells of a different strain which had just initiated budding have shown that the volume of a cell at bud emergence increases with increasing growth rate (18). The magnitude of the increase is such that this would occur primarily as a consequence of the increase in V_P. A comparison of strain S288C/1 with the parent strain studied previously (30) shows that (i) the duration of B has a different relationship to τ, and (ii) V_P is smaller at all growth rates. Clearly, the strain has changed in some respects; nevertheless, all of the changes are quantitative rather than qualitative.

These results emphasize the necessity for analyzing yeast populations in terms of the unequal division model. The conceptual, experimental, and mathematical bases of this asymmetry have now been presented (12, 19, 30) and should allow a more precise interpretation of population experiments.

ACKNOWLEDGMENTS

We thank Peter Green for the application of the method of maximum likelihood, Bernard Silverman for introducing us to the box and whiskers plot, Lee Hartwell for advice, and John Pringle for extremely valuable criticism and equation 2.

We thank the Science Research Council for financial support.

APPENDIX

The following equations depend upon assumptions i to vii described in the text and follow from the arguments of Hartwell and Unger (12).

Cell age distribution. The expression describing the age distribution derived by Hartwell and Unger (12) is

$$\int_P^D \alpha e^{\alpha t}(1 - e^{-\alpha P})dt + \int_0^P \alpha e^{\alpha t}dt = 1 \quad (3)$$

where t is the age of a cell at a particular point in the cycle in terms of the time taken to reach division, and $\alpha = \ln 2/\tau$.

Duration of *B*. The fraction of budded cells is

$$F_B = \int_0^B \alpha e^{\alpha t} dt$$

$$= e^{\alpha B} - 1$$

$$B = \frac{\ln(F_B + 1)}{\ln 2} \cdot \tau \quad (4)$$

***D* and *P*.** The distribution of daughters is given by

$$\int_0^D \alpha e^{\alpha t}(1 - e^{-\alpha P})dt = F_D \quad (5)$$

The distribution of parents is found by subtracting equation 5 from equation 3 and is

$$\int_0^P \alpha e^{\alpha t} \cdot e^{-\alpha P} dt = F_P \quad (6)$$

The fraction of daughter cells which are budding (F_{DB}; frequency of budded daughters/frequency of daughters) is given by

$$F_{DB} = \frac{\int_0^B \alpha e^{\alpha t}(1 - e^{-\alpha P})dt}{\int_0^D \alpha e^{\alpha t}(1 - e^{-\alpha P})dt}$$

$$= \frac{e^{\alpha B} - 1}{e^{\alpha D} - 1}$$

$$= \frac{F_B}{e^{\alpha D} - 1}$$

$$D = \frac{\ln[(F_B/F_{DB}) + 1]}{\ln 2} \cdot \tau \quad (7)$$

By similar reasoning it can be shown that

$$P = \frac{\ln[(F_B/F_{PB}) + 1]}{\ln 2} \cdot \tau \quad (8)$$

where F_{PB} is the fraction of parent cells which are budding.

Genealogical age distribution. The fraction of daughter cells is (by solving equation 5)

$$F_D = e^{\alpha D}(1 - e^{-\alpha P}) - (1 - e^{-\alpha P})$$

Since from equation 1, $e^{\alpha D}(1 - e^{-\alpha P}) = 1$

$$F_D = 1 - 1 + e^{-\alpha P}$$

$$= e^{-\alpha P} \quad (9)$$

The frequency of cells which are budding for the first time at division (i.e., frequency of budded daughters at $t = 0$) is (from equation 5) $\alpha(1 - e^{-\alpha P})$. Immediately after division these cells give rise to unbudded daughters which enter the cycle at D and unbudded parents with one bud scar which enter the cycle at P. Therefore, at P in the cycle the frequency of parent cells with one bud scar is $\alpha(1 - e^{-\alpha P})$. From equation 6 the frequency of parent cells at P is α. Therefore, at this point in the cycle the fraction of the parent cells which have one bud scar is $(1 - e^{-\alpha P})$. This fraction is maintained as the cells pass from $t = P$ to $t = 0$ in the cycle. It follows that the distribution of P_1 cells (parent cells with one bud scar) is

$$\int_0^P \alpha e^{\alpha t} \cdot e^{-\alpha P}(1 - e^{-\alpha P})dt = F_{P1} \quad (10)$$

The frequency of P_2 cells at $t = P$ is the same as that of P_1 cells at $t = 0$ and from equation 10 is $\alpha e^{-\alpha P}(1 - e^{-\alpha P})$. The fraction of the parent cells which have two bud scars, therefore, is $e^{-\alpha P}(1 - e^{-\alpha P})$. Thus, the distribution of P_2 cells is

$$\int_0^P \alpha e^{\alpha t}(e^{-\alpha P})^2(1 - e^{-\alpha P})dt = F_{P2} \quad (11)$$

The distribution of $P_{(3)}$ cells is found by similar reasoning and is

$$\int_0^P \alpha e^{\alpha t}(e^{-\alpha P})^3(1 - e^{-\alpha P})dt = F_{P3} \quad (12)$$

It is obvious from equations 10 through 12 that the general formula for the distribution of P_n cells, where $n = 1, 2, 3$, etc., is

$$\int_0^P \alpha e^{\alpha t}(e^{-\alpha P})^n(1 - e^{-\alpha P})dt = F_{Pn} \quad (13)$$

The general formula for the fraction of P_n cells, from equation 13, is

$$F_{pn} = (e^{-\alpha P})^{n-1}(1 - e^{-\alpha P})^2 = F_{Pn} \quad (14)$$

At μ_{bmax}, when $P = \tau$, equation 14 becomes $F_{Pn} = (\frac{1}{2})^{n+1}$ and equation 9 becomes $\frac{1}{2}$. Therefore at μ_{bmax} cells of different genealogical ages ($n = 0$, 1, 2, etc.) are distributed such that their frequencies form a geometric series in which the frequency of cells of age n is $(\frac{1}{2})^{n+1}$.

Median cell volume. Assuming that the volume of a cell increases exponentially from birth to division such that the time in which the volume doubles is the same as the population doubling time, then the median cell volume is the volume of a cell at the median cell age.

The median cell age (in units of τ) from equation 3 is

$$\int_0^t \alpha e^{\alpha t} dt = 0.5$$

$$e^{\alpha t} - 1 = 0.5$$

$$t = \frac{\ln 1.5}{\ln 2}$$

$$= 0.5850$$

The volume of a cell at age t in the cycle is given by Tyson et al. (30) as

$$V_t = V_P e^{\alpha(P-t)}$$

Therefore, the median cell volume (V_m) is (where P and t are in units of τ)

$$V_m = V_P e^{\alpha(P-0.5850)} \qquad (15).$$

LITERATURE CITED

1. **Barford, J. P., and R. J. Hall.** 1976. Estimation of the length of cell cycle phases from asynchronous cultures of *Saccharomyces cerevisiae*. Exp. Cell Res. **102**:276–284.
2. **Beran, K.** 1968. Budding of yeast cells, their scars and ageing. Adv. Microb. Physiol. **2**:143–171.
3. **Beran, K., I. Malek, E. Streiblova, and J. Leiblova.** 1967. The distribution of the relative age of cells in yeast populations, p. 57–67. *In* E. O. Powell, C. G. T. Evans, R. E. Strange, and D. W. Tempest (ed.), Microbial physiology and continuous culture. Her Majesty's Stationery Office, London.
4. **Beran, K., E. Streiblova, and J. Leiblova.** 1969. On the concept of the population of the yeast *Saccharomyces cerevisiae*, p. 353–363. *In* Second International Symposium on Yeasts (Bratislava, 1966). Slovak Academy of Sciences, Britislava.
5. **Burns, V. W.** 1956. Temporal studies of cell division. I. The influence of ploidy and temperature on cell division in *Saccharomyces cerevisiae*. J. Cell. Comp. Physiol. **47**:357–375.
6. **Byers, B., and L. Goetsch.** 1975. Behavior of spindles and spindle plaques in the cell cycle and conjugation of *Saccharomyces cerevisiae*. J. Bacteriol. **124**:511–523.
7. **Carter, B. L. A., and M. N. Jagadish.** 1978. The relationship between cell size and cell division in the yeast *Saccharomyces cerevisiae*. Exp. Cell Res. **112**:15–24.
8. **Flegel, T. W.** 1978. Difference in generation times for mother and daughter cells in yeasts. Can. J. Microbiol. **24**:827–833.
9. **Freifelder, D.** 1960. Bud position in *Saccharomyces cerevisiae*. J. Bacteriol. **80**:567–568.
10. **Gani, J., and I. W. Saunders.** 1977. Fitting a model to the growth of yeast colonies. Biometrics **33**:113–120.
11. **Hartwell, L. H.** 1974. *Saccharomyces cerevisiae* cell cycle. Bacteriol. Rev. **38**:164–198.
12. **Hartwell, L. H., and M. W. Unger.** 1977. Unequal division in *Saccharomyces cerevisiae* and its implications for the control of cell division. J. Cell Biol. **75**: 422–435.
13. **Hayashibe, M.** 1977. Cytodifferentiation in the cell cycle of yeasts, p. 165–191. *In* T. Ishikawa, Y. Maruyama, and H. Matsumiya (ed.), Growth and differentiation in micro-organisms. University of Tokyo Press, Tokyo.
14. **Hayashibe, M., and S. Katohda.** 1973. Initiation of budding and chitin-ring. J. Gen. Appl. Microbiol. **19**: 23–39.
15. **Hayashibe, M., and N. Sando.** 1970. Characterization of different sized cells of baker's yeast. J. Gen. Appl. Microbiol. **16**:15–27.
16. **Jagadish, M. N., and B. L. A. Carter.** 1977. Genetic control of cell division in yeast cultured at different growth rates. Nature (London) **269**:145–147.
17. **Johnson, B. F., and E. J. Gibson.** 1966. Autoradiographic analysis of regional cell wall growth of yeasts. III. *Saccharomyces cerevisiae*. Exp. Cell Res. **41**:580–591.
18. **Johnston, G. C., C. W. Ehrhardt, A. Lorincz, and B. L. A. Carter.** 1979. Regulation of cell size in the yeast *Saccharomyces cerevisiae*. J. Bacteriol. **137**:1–5.
19. **Johnston, G. C., J. R. Pringle, and L. H. Hartwell.** 1977. Coordination of growth with cell division in the yeast *Saccharomyces cerevisiae*. Exp. Cell Res. **105**: 79–98.
20. **Lorincz, A., and B. L. A. Carter.** 1979. Control of cell size at bud initiation in *Saccharomyces cerevisiae*. J. Gen. Microbiol. **113**:287–295.
21. **Matile, P., H. Moor, and C. F. Robinow.** 1969. Yeast cytology, p. 219–302. *In* A. H. Rose and J. S. Harrison (ed.), The yeasts, vol. 1. Academic Press Inc., London.
22. **Müller, I.** 1971. Experiments on ageing in single cells of *Saccharomyces cerevisiae*. Arch. Mikrobiol. **77**:20–25.
23. **Nickerson, W. J.** 1963. Symposium on biochemical bases of morphogenesis in fungi. IV. Molecular bases of form in yeasts. Bacteriol. Rev. **27**:305–324.
24. **Pritchard, R. H.** 1974. On the growth and form of a bacterial cell. Phil. Trans. R. Soc. London Ser. B **267**: 303–336.
25. **Shilo, B., V. Shilo, and G. Simchen.** 1977. Transition probability and cell cycle initiation in yeasts. Nature (London) **267**:648–649.
26. **Slater, M. L., S. O. Sharrow, and J. J. Gart.** 1977. Cell cycle of *Saccharomyces cerevisiae* in populations growing at different rates. Proc. Natl. Acad. Sci. U.S.A. **74**: 3850–3854.
27. **Streiblova, E.** 1970. Study of scar formation in the life cycle of heterothallic *Saccharomyces cerevisiae*. Can. J. Microbiol. **16**:827–831.
28. **Streiblova, E., and K. Beran.** 1963. Demonstration of yeast scars by fluorescence microscopy. Exp. Cell Res. **30**:603–605.
29. **Tukey, J. W.** 1977. Exploratory data analysis. Addison-Wesley, Reading, Mass.
30. **Tyson, C. B., P. G. Lord, and A. E. Wheals.** 1979. Dependency of size of *Saccharomyces cerevisiae* cells on growth rate. J. Bacteriol. **138**:92–98.
31. **Vrana, D.** 1973. Some morphological and physiological properties of *Candida utilis* growing "hypertrophically" in excess of substrate in a two stage continuous cultivation. Biotechnol. Bioeng. Symp. **4**:161–173
32. **Vrana, D.** 1976. Daughter cells as an important factor in determining the physiological state of yeast populations. Biotechnol. Bioeng. **18**:297–309.
33. **Vrana, D., and K. Beran.** 1977. Cytomorphological characterization of *Saccharomyces cerevisiae* and *Candida utilis* and an index of the physiological state of the culture. Mikrobiologiya **46**:161–164.
34. **Yanagita, T.** 1977. Cellular age in microorganisms, p. 1–36. *In* T. Ishikawa, Y, Maruyama, and H. Matsumiya (ed.), Growth and differentiation in microorganisms. University of Tokyo Press, Tokyo.

J. Cell Sci. **50**, 361–376 (1981)
Printed in Great Britain © Company of Biologists Limited 1981

VARIABILITY IN INDIVIDUAL CELL CYCLES OF *SACCHAROMYCES CEREVISIAE*

P. G. LORD AND A. E. WHEALS*
Microbiology Group, School of Biological Sciences, University of Bath, Bath, U.K.

SUMMARY

The kinetics of cell proliferation of *Saccharomyces cerevisiae* were studied at 4 growth rates using time-lapse cinephotomicrography. Cells were grown on media with a high refractive index to reveal greater intracellular detail under the phase-contrast microscope. The morphological cell-cycle events scored were: bud emergence, nuclear migration, nuclear division, onset of cytokinesis and cell separation. Cell size was measured at cell separation and at bud emergence. The daughter-cycle time was always longer than the parent-cycle time mainly due to the large difference in the lengths of the unbudded phases. Parent cells had a shorter budded period than daughter cells. The large variance in daughter-cycle times was accounted for by the large variance in the lengths of the unbudded phase of daughter cells. The duration and variability of the periods in the cycle from nuclear migration onwards were equivalent for parent and daughter cells. Daughter cells were always smaller than parent cells at division. There was wide variation in cell size at both division and bud emergence. The results indicated that a modified deterministic model could best explain cell proliferation kinetics in yeast. The data were used to evaluate 2 different models. The 'sloppy size control' model of Wheals (1981*a*) was more consistent with the data than the 'tandem' model of Shilo, Shilo & Simchen (1976). The distribution of unbudded periods of daughter cells suggested that there was an additional incompressible period not present in parent cells.

INTRODUCTION

Several models have been postulated to explain control of cell proliferation in a variety of cell types (Donachie, 1968; Kauffman & Wille, 1975; Kubitschek, 1971; Pritchard, Barth & Collins, 1969; Smith & Martin, 1973). Two models in particular have received much attention recently. Briefly, the models are as follows. (1) The critical-size hypothesis (Fantes *et al.* 1975) is a deterministic model, which suggests that cells have a mechanism for monitoring their instantaneous size and that when a critical size has been reached a series of events is initiated leading to division. (2) The transition probability hypothesis (Smith & Martin, 1973) is a probabilistic model, which suggests that cells in G_1 phase exist in a state (the A state) from which they enter a sequence leading to division (the B phase), with first-order kinetics. The principal difference between the 2 models is thus the set of rules governing entry into the division sequence. Both models have been applied with some success to explain control of cell proliferation in the budding yeast, *Saccharomyces cerevisiae* (Shilo *et al.* 1976; Hartwell & Unger, 1977). The point of commitment to the division sequence has been identified, from mutational and physiological studies, as an event

* All correspondence to Dr Wheals at the above address.

in G_1 termed start (Hartwell, Culotti, Pringle & Reid, 1974). In balanced growth conditions a requirement for traverse of start has been found to be attainment of a critical cell size (Johnston, Pringle & Hartwell, 1977). The size requirement explains why the daughter-cycle time is longer than the parent-cycle time. Since budding yeast cells divide asymmetrically, at division the parent cell is at or above critical size and the daughter cell is less than critical size and requires a period of growth before traversing start (Hartwell & Unger, 1977).

In contrast, it has been shown that cells released from a block at start enter the division sequence with first-order kinetics, as predicted by the transition probability hypothesis (Shilo *et al.* 1976; Shilo, Shilo & Simchen, 1977). The variability in cycle times observed in steady-state conditions could be produced by such a control.

Neither model can fully account for both sets of data. The critical-size hypothesis could account for variation in daughter-cycle times by postulating that there is variation in birth size. However, parent cells (born above critical size) should show negligible variability in their cycle time, and cells released from start should show quasi-synchronous entry into the division sequence; these are both contrary to observation. Conversely, the transition probability hypothesis cannot explain the difference in parent- and daughter-cycle times or the observation that there is a size requirement for traverse of start. Consequently, it has been suggested that the deterministic and probabilistic controls act in tandem, that is, when cells reach critical size they enter an A state from which their exit is probabilistic (Shilo *et al.* 1977).

An alternative model has been proposed, which fuses the elements together in a novel way (Wheals, 1981*a*). In this 'sloppy' size control (SSC) model the probability of entering the division sequence (B phase) increases with size such that small cells have a low probability and large cells a high probability. The probabilistic element is in this case an integral part of the sizing mechanism. Simultaneous measurements of size and cycle time are necessary in order to discriminate between the 2 models. Data of this sort obtained from time-lapse cine films provided evidence against the tandem model and consistent with the SSC model (Wheals, 1981*a*). However, the analysis was limited by the microscopical technique used because the only morphological event whose timing could be measured unambiguously was bud emergence. Therefore, cell size was measured at bud emergence and cycle time was taken to be the interval between successive events of bud emergence. It is crucial for a satisfactory test of the SSC model that, in addition, both size at birth and true inter-division time are known.

We have used the technique of raising the refractive index of the growth medium to improve the phase-contrast image of *S. cerevisiae* cells (Robinow, 1975). When the refractive index of the surrounding medium is close to that of the cell contents much more intracellular detail is revealed (see Fig. 1). Using time-lapse cinephotomicrography we have measured the size of cells at division (as well as at bud emergence) and true cycle time. In addition, the timing of bud emergence, nuclear migration, nuclear division and septum formation during the cycle were measured. We have filmed cell populations growing on 4 different carbon sources (supporting

4 different growth rates) to see how the timing of events varies with growth rate. The data we have collected have allowed us to compare further the validity of the tandem and SSC models.

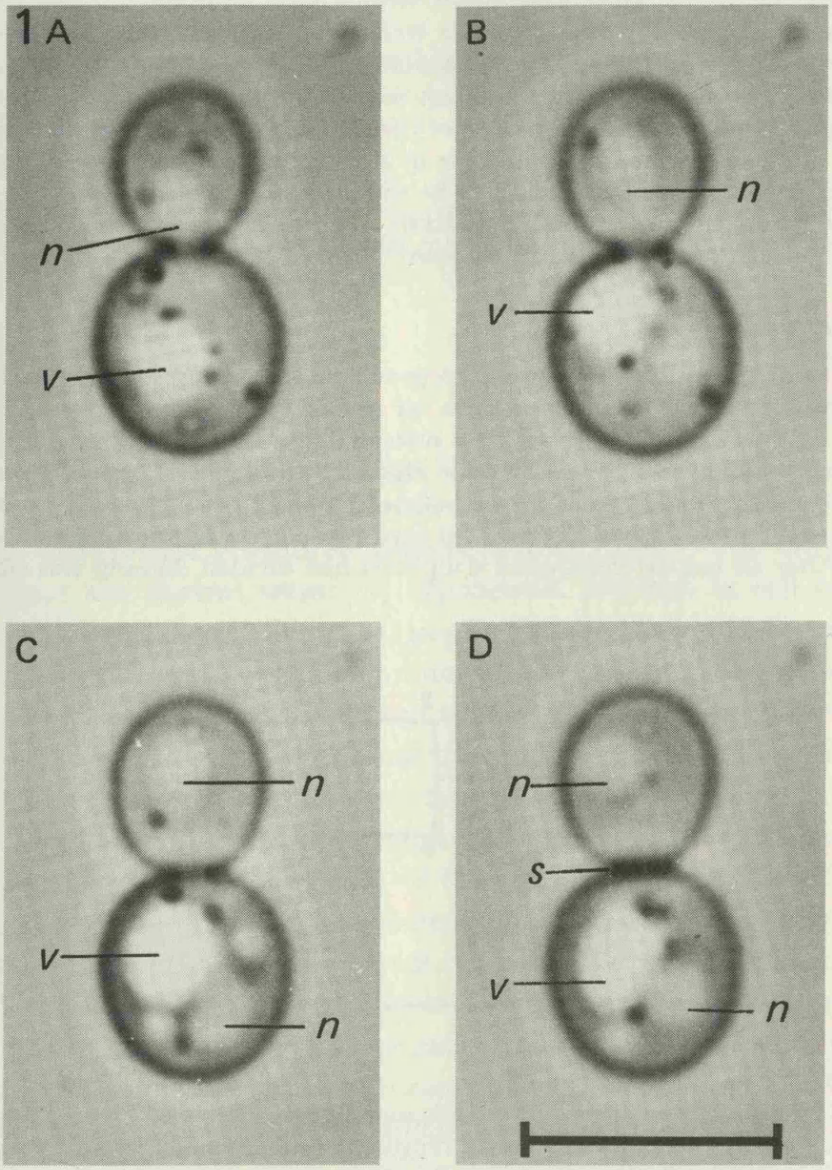

Fig. 1. Photographs of a cell (*S. cerevisiae* A364A) growing on YEP/PVP/glucose/agar taken at intervals to show the different stages in the cell cycle. A, medial nuclear division; B, late nuclear division; C, onset of cytokinesis; and D, late septum formation. Bar 5 μm. Vacuole (*v*), nucleus (*n*), septum (*s*).

MATERIALS AND METHODS

Organism

A haploid strain of *S. cerevisiae*, A364A (Hartwell, 1967), obtained from L. H. Hartwell was used throughout.

Media

Cells were grown on YEP/PVP agar. The composition of the agar was: 28–30 g polyvinylpyrrolidone (PVP-40, Sigma), 7 g purified agar, 3 g bacteriological peptone, 1·5 g yeast

extract, 3 g carbon source (glucose, raffinose, sorbitol or galactose), 5 μg adenine in 100 ml distilled water.

Filming equipment

The microscope was a Wild M20 fitted with a long working distance phase condenser. A 10× eyepiece and 20× phase objective were used throughout. The camera was a Bolex H16 5BM controlled by a Bolex/Wild Variotimer timing system. An electromagnetic shutter, operated by the timer unit, was fitted beneath the condenser so that cells were not continously exposed to light. Films were taken at a rate of 1 frame/min on Eastman Ektachrome Commercial 7252 16 mm film. Cells were grown on agar in a heated slide made of aluminium with a glass-bottomed well in the centre for the agar. The slide was heated electrically and the temperature maintained at 30 °C by a thermistor regulator. All operations including filming were carried out at 29 °C in a temperature-controlled room.

Culture conditions

Cells had to be growing exponentially to provide data appropriate for the analysis (Powell, 1955). This was achieved by growing cells for several generations, prior to filming, at 30 °C on a slab of agar (under a coverslip) on a microscope slide. Cells were transferred from this slide to the heated slide with a bent Pasteur pipette. A coverslip was then placed over the cells and secured onto the heated slide with wax (along 2 sides only, allowing aeration). A suitable field of cells near to the edge of the agar (to ensure adequate aeration) was chosen, and filming was begun. After all second-generation daughters had divided, filming was stopped.

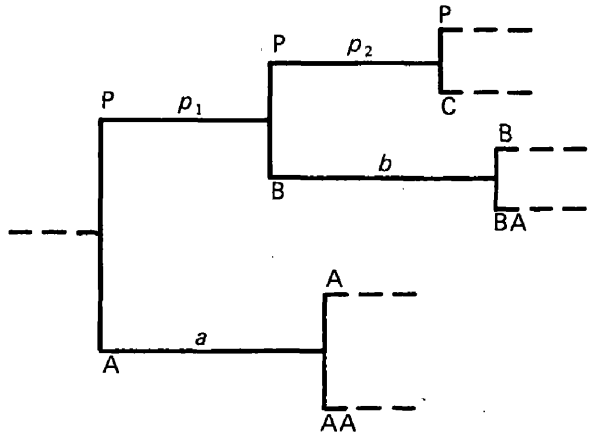

Fig. 2. Genealogical relationship of cells used in analysis. The vertical lines represent cell separation. The horizontal lines represent inter-division cycles. P is the parent (original) cell. p_1 and p_2 are first 2 cycles of the parent cells after time zero. A, B and C are first 3 daughter cells of the parent cells produced after time zero. *a* and *b* are the cycles of daughter cells A and B, respectively. AA and BA are the daughter cells produced by cells A and B, respectively. The sizes of all these cells were measured at cell separation as was the size at bud emergence of cells P (during p_1 and p_2), A and B.

Analysis of films

Films were projected onto a screen from a Specto MK III analysis projector. All clones in focus were followed and the timing of events was scored from the first division of the original cell. This cell (the parent) was followed for 2 cycles and its first 2 daughter cells, were each followed for 1 cycle, yielding 2 parent and 2 daughter cycles for each clone (see Fig. 2). The events scored were: (1) bud emergence; (2) nuclear migration, the time when the nucleus first appeared at the bud isthmus; (3) nuclear division, when the nucleus clearly

separated into two; (4) onset of cytokinesis, the time of the appearance of a dark band between the parent cell and its bud; and (5) cell separation, seen as a slight movement of the bud and/or a diminution of the dark band. The volumes of cells at bud emergence and at cell separation were calculated from the lengths of the major (a) and minor (b) axes using the formula: volume = $(\pi/6)ab^2$, assuming that yeast cells have the regular shape of a prolate spheroid. The population doubling time (τ) was calculated from the semi-logarithmic plot of cell number *versus* the time from the start of the film. The volume of all the cells was measured at intervals to construct a semi-logarithmic plot of total cell volume *versus* time, to obtain the population volume doubling time (τ_v).

Accuracy of measurements

The cycle time of a cell chosen at random was measured on 10 separate occasions and the standard error of measurement found to be 0·66 min. The standard error of measurement for volume was 0·72 μm^3 and was calculated from 10 separate measurements of a randomly chosen cell.

RESULTS

In order to test the predictions of either deterministic or transition probability models, it is necessary that the data be collected from exponentially growing cells under balanced, steady-state growth conditions (Powell, 1955). The criteria used to establish this (data not shown) were: (1) exponential increase in cell number; (2) exponential increase in total cell volume; (3) population doubling time from (1) equal to volume doubling time from (2); (4) mean duration of first and second parent cycles equal; and (5) mean cycle times of first and second generation daughters equal. All criteria except (3) were achieved. We found that the volume doubling time was 6–15% longer than the population doubling time. This was not found in a previous study (Wheals, 1981*a*). Since the only difference here was the presence of PVP-40, we speculate that this was the cause of the discrepancy. All the other criteria were achieved, so the conditions approximated to steady state with the proviso that average cell size was slightly decreasing over the course of the experiments.

The mean duration and variability of various periods in the cell cycle are shown in Table 1 for parent and daughter cells at each growth rate. The major conclusions from these data are as follows. (1) The mean daughter-cycle time is always longer than the mean parent-cycle time, this difference being mostly due to the longer unbudded period of daughter cells. (2) The variability of daughter-cycle times is much greater than that of parent-cycle times, the difference being attributable to the more variable unbudded period of daughter cells. (3) The budded period is 5–8 min longer for daughter cells compared to parent cells, this increase being accounted for by the time from bud emergence to nuclear migration. (4) There is a tendency for all periods to increase in length with increasing population doubling time. This feature is most evident for the unbudded period (especially for daughter cells), the budded period and the period from bud emergence to nuclear migration.

The distributions of cycle times of parent and daughter cells are shown in Fig. 3. The data are presented as α plots, i.e. the percentage of undivided cells on a logarithmic scale against cycle time (Smith & Martin, 1973). A straight line would indicate a constant probability of division per unit time, as is suggested by the transition

Table 1. *The duration and variability of cell-cycle phases at different growth rates*

Period	Doubling time	Parent cells		Daughter cells	
		Mean	S.D.‖	Mean	S.D.
Cycle time	96·9*	72·6	6·4	117·7	27·8
	121·5†	87·2	10·3	140·9	29·3
	142·0‡	98·4	9·3	174·8	35·1
	160·0§	108·9	14·7	205·1	56·7
Unbudded period	96·9	8·6	3·7	47·5	25·3
	121·5	13·2	4·5	62·6	27·1
	142·0	11·5	3·5	80·5	31·0
	160·0	15·1	8·3	103·9	53·1
Budded period	96·9	64·0	6·0	69·9	7·6
	121·5	73·9	9·4	78·6	8·2
	142·0	86·9	8·4	94·6	12·3
	160·0	93·8	12·1	101·2	15·3
Bud emergence to nuclear migration	96·9	36·1	5·8	41·5	6·4
	121·5	44·9	5·8	48·8	7·2
	142·0	53·3	7·7	58·9	10·7
	160·0	58·7	9·2	66·0	13·6
Nuclear migration to nuclear division	96·9	8·8	2·2	8·1	1·7
	121·5	8·5	1·9	9·2	2·0
	142·0	8·9	1·8	9·0	1·9
	160·0	9·8	2·1	9·8	2·3
Nuclear division to onset of cytokinesis	96·9	9·7	4·1	11·1	3·8
	121·5	8·1	3·1	9·0	2·2
	142·0	12·4	3·2	16·0	4·7
	160·0	10·2	3·6	10·8	2·9
Onset of cytokinesis to cell separation	96·9	9·7	2·2	9·0	1·6
	121·5	12·6	5·1	11·5	3·9
	142·0	11·9	3·7	11·5	2·4
	160·0	15·0	4·1	14·6	4·5

All values are in minutes. The number of cycles measured were: *, 32 parent and 32 daughter cycles; †, 34 parent and 33 daughter cycles; ‡, 40 parent and 40 daughter cycles; and §, 38 parent and 37 daughter cycles. ‖, S.D. is the standard deviation. Data from first and second cycles of parent cells were pooled since Student's *t*-tests showed that there was no significant difference between the mean values of any parameter for first and second cycles of parent cells. Similarly, Student's *t*-test showed that it was permissible to pool the data from first- and second-generation daughter cells.

probability hypothesis. The data present a homogeneous series showing the following features. (1) The minimum cycle time for both parent and daughter cells increases with increasing population doubling time. (2) The shortest 30% of cycle times of parent and daughter cells show substantial downward curvature. (3) The longest 50% of parent- and daughter-cycle times show an approximately exponential distribution. (4) The slopes of the straight-line portions tend to decrease with increasing population doubling time (especially those of daughter-cycle time plots). (5) For each population doubling time the minimum cycle time is less, the initial curvature

less pronounced and the slope steeper for parent cells than for daughter cells. In addition, no daughter cell had a cycle time less than that of its sibling parent (i.e. $a > p_1$, $b > p_2$ in Fig. 2). An examination of the distributions of the budded and unbudded periods of parent and daughter cells indicates that both periods contribute to the slope and initial curvature of the α plots (data not shown). However, as was inferred in Table 1, it was the unbudded period that determined the overall shape of α plots of the daughter-cycle time.

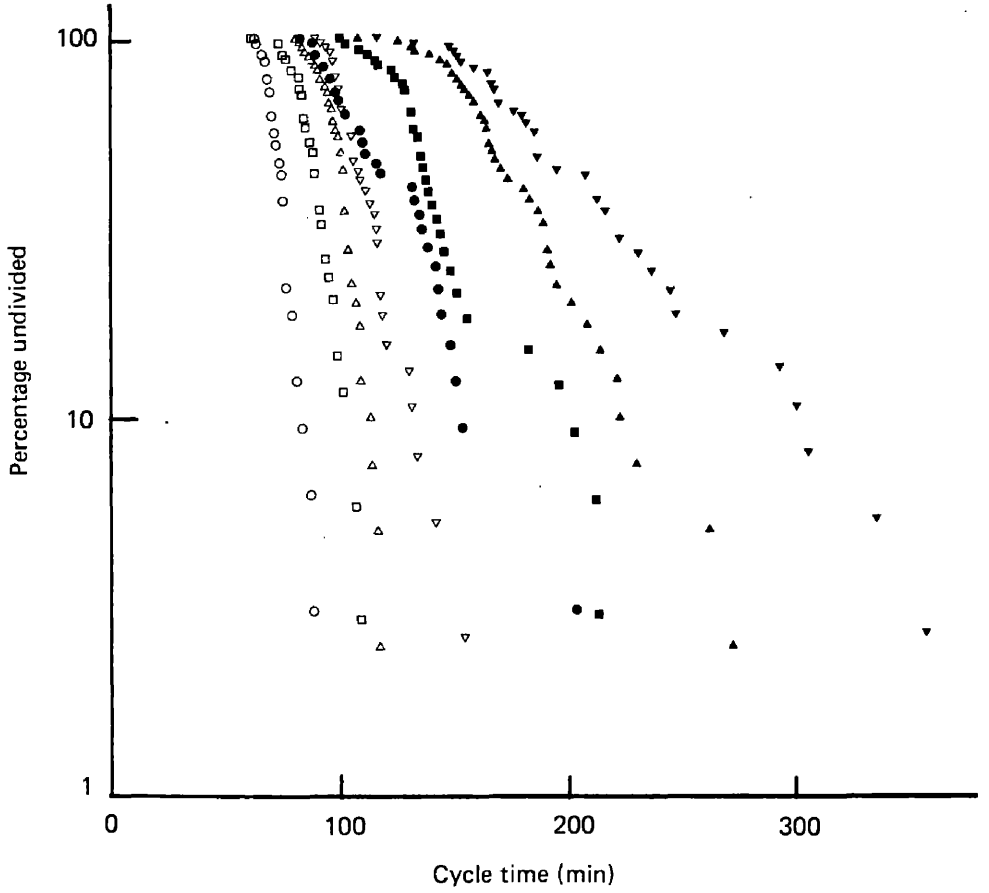

Fig. 3. α plots of parent- and daughter-cycle times of cells growing at 4 different growth rates. Glucose-grown cells (○, ●); raffinose-grown cells (□, ■); sorbitol-grown cells (△, ▲); galactose-grown cells (▽, ▼); open symbols, parent cells; closed symbols, daughter cells. An α plot is the percentage of cells remaining undivided (on a logarithmic scale) plotted against cycle time.

In order to see whether there was any evidence of homeostatic regulation during the budded period, or whether this was a constant sequential process with small standard deviation, the following test was done. If no regulation occurred, the sum of the variances of the individual intervals of the budded period should equal the variance of the budded period. If regulation did occur then the variance of the budded period should be less than the sum of the individual variances. Within the limits of experimental error the variances were equal, suggesting that there is no additional control at division as has been shown for *Schizosaccharomyces pombe* (Fantes, 1977).

The volumes of daughter cells at cell separation were always smaller than their sibling parent cells (data not shown). There was wide variation in the birth size of daughter cells and similar variation in their size at bud emergence, with some overlap between the distributions (Fig. 4). Since bud emergence occurs shortly after start (Hartwell & Unger, 1977; Hereford & Hartwell, 1974; Shilo *et al.* 1976), the size at bud emergence is taken as an approximate measure of the size at start. There

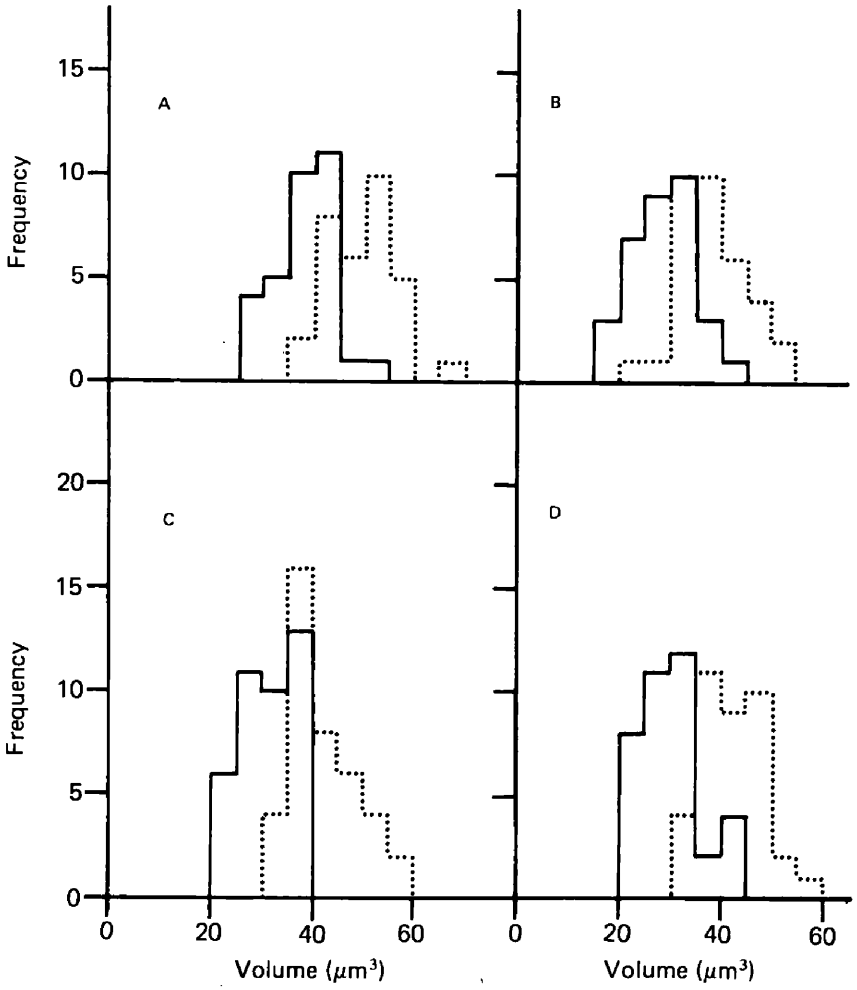

Fig. 4. Distributions of the sizes of daughter cells at 2 stages of the cell cycle. Histograms of the sizes of daughter cells (A and B in Fig. 2) at birth (——) and at bud emergence (.....) at each growth rate.

was no correlation between the size at birth and the size at bud emergence for individual cells. This suggests that cells do not grow a constant amount from birth to bud emergence (data not shown).

Table 2 shows that the mean size of daughter cells born from parent cells (i.e. P in Fig. 2) was approximately 3–4 μm^3 larger than those born from first-generation parent cells (i.e. A and B in Fig. 2). Daughter cells from older parent cells were born at the same size at each generation (i.e. A = B = C in Fig. 2) except for raffinose-grown cells where the third-generation daughter cells were smaller. Although the fastest growing cells were larger than the slowest growing cells, as expected,

Table 2. *Mean birth size of daughter cells*

Medium	Doubling time (min)	Mean birth size (μm^3)				
		A*	B	C	AA	BA
YEP/glucose	96·9	37·9	37·4	35·5	34·4	31·3
YEP/raffinose	121·5	28·1	28·3	23·3	25·4	26·0
YEP/sorbitol	142·0	30·9	31·7	29·6	27·0	25·8
YEP/galactose	160·0	30·5	29·2	29·7	27·3	25·4

* A, B, C, AA, BA refer to daughter cells in Fig. 2.

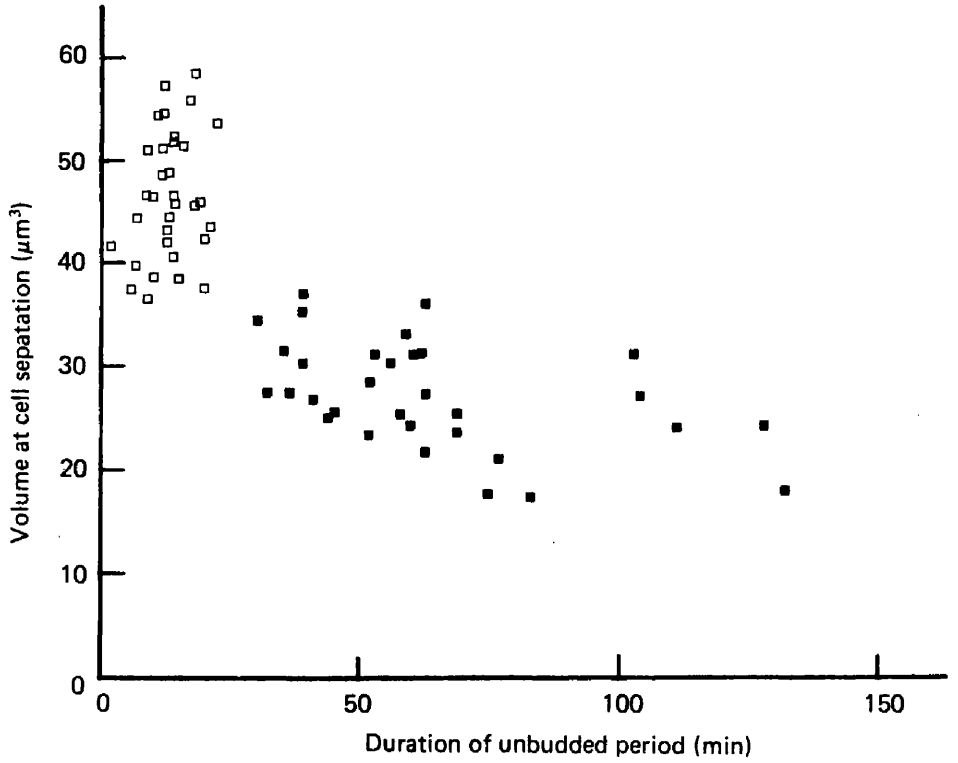

Fig. 5. Cell size at cell separation *versus* the length of the cells subsequent unbudded phase. Parent cells (□); daughter cells (■). The data are from raffinose-grown cells.

raffinose-grown cells were the smallest of all. A plot was made (for each growth rate) of the size of daughter cells at birth *versus* the size at bud emergence of the parent cell from which it was produced (data not shown). There was a trend for larger parent cells to produce larger daughter cells but the correlation was very weak ($t < 0{\cdot}5$ in all cases).

The duration of the unbudded period is approximately equal to the pre-start period. A plot of size at cell separation (birth) against the duration of the unbudded period will reveal whether the birth size is important in determining when start occurs. A representative graph (that of raffinose-grown cells, Fig. 5) shows that, for parent cells, birth size is not important in determining the length of their unbudded

period. Birth size is important for daughter cells, the slope of the line being −0·12. However, since the correlation coefficient is only 0·55, the size effect is only a loose one.

Wiemken, Matile & Moor (1970) have reported on the dynamic behaviour of the vacuole during the cell cycle of *S. cerevisiae*. We have seen this behaviour only in glucose-grown cells. Small vacuoles appeared at about the time the nucleus divided. The small vacuoles fused to form a large vacuole, which broke down after a few minutes into several small vacuoles. Shortly afterwards these vacuoles disappeared. The length of time between appearance and disappearance of the vacuoles seemed to depend on the genealogical age of the cell. The vacuoles of cells budding for the first time (A and B in Fig. 2) disappeared about 8 min before cell separation. Disappearance of the vacuoles occurred at about the same time as cell separation in the older, parent cells. Unlike Wiemken *et al.* (1970), we did not see vacuoles in the buds.

DISCUSSION

In all of the models describing yeast cell-cycle kinetics traverse of start is the rate-limiting step in cell proliferation. Once initiated, the cell is committed to a cell-division sequence leading to the birth of 2 cells. There is some controversy surrounding the nature of the role of size in governing traverse of start.

The simple deterministic model (Hartwell & Unger, 1977) cannot account for Fig. 4, since daughter cells at bud emergence should be homogeneous in size whereas they are as variable as at birth. The transition probability model, in its original and modified form (Brooks, Bennett & Smith, 1980; Smith & Martin, 1973), is also inadequate to account for Figs. 3 and 5. That the rate at which cells traverse start is dependent (albeit loosely) upon birth size is evident in Fig. 5. Fig. 3 shows that the quasi-exponential portions of the daughter and parent curves are not parallel even when they are passing the same rate-controlling step, i.e. start.

A model has been suggested (Shilo *et al.* 1977) and elaborated (Wheals, 1981*b*) that attempts to combine the probabilistic and deterministic elements in tandem. Although this model qualitatively accounts for a size control and a random element, there are 2 pieces of evidence against it. Firstly, the model predicts that, after daughter cells have completed the requirement of growth to a critical size, they should exhibit the same kinetics of entry to the division sequence as parent cells. That is, the straight line portions of the α curves in Fig. 3 should be parallel, which they clearly are not. Secondly, since daughter cells grow throughout the unbudded phase, after attaining the critical size daughter cells should have an approximately constant probability of traversing start (and consequently of budding) per unit increase in size. A representative γ plot (Wheals, 1981*a*), i.e. the percentage of unbudded daughter cells (on a logarithmic scale) against cell size, is shown for galactose-grown cells in Fig. 6. The model predicts a straight line slope after attainment of the critical size. The best fit to the data is a curve of increasing slope, which

could only be accommodated in the tandem model by the additional *ad hoc* assumption of very large variance in the critical cell size.

A simpler model that fuses the probabilistic and deterministic elements into a single scheme is the sloppy size control (SSC) model (Wheals, 1981*a*). This model suggests that a cell has an increasing probability of traversing start the larger it is. The important difference between this and the 3 previous models can be seen in Fig. 7, which gives the theoretical relationship between the probability of traversing

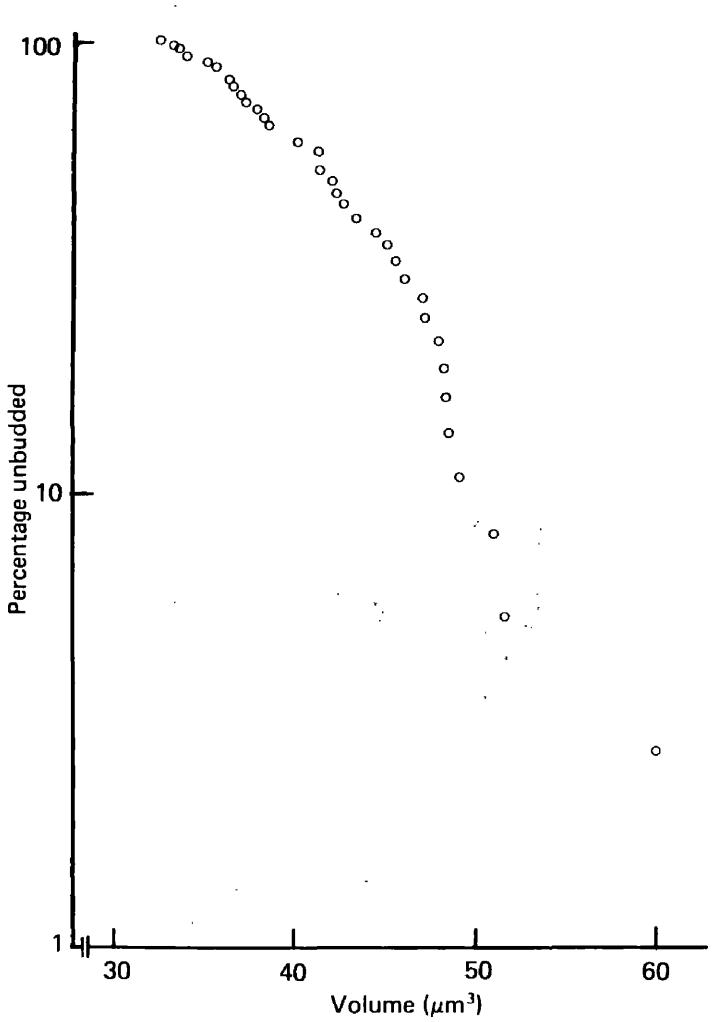

Fig. 6. γ plot of data from galactose-grown cells. A γ plot is the percentage of cells remaining unbudded (on a logarithmic scale) plotted against size at bud emergence.

start and cell size. For the deterministic model (Fig. 7A), all cells below critical size have zero probability and all cells at or above critical size have a probability of unity. For the probabilistic model (Fig. 7B), all cells have the same probability, regardless of size. For the tandem model (Fig. 7C), all cells below critical size have zero probability and all cells at or above critical size have a high probability (not unity). In the case of the SSC model (Fig. 7D) the probability increases smoothly with size to a high plateau value. From the data in Fig. 4 we have calculated the frequency of bud emergence in each size-interval. The frequency of bud emergence in a particular size-interval is the number of cells with newly emerged buds in that interval

divided by the number of cells competent to bud (i.e. the number of cells in that interval plus the number of cells in the preceding intervals that have not budded). Since size at bud emergence is a measure of size at start, we can take the frequency of bud emergence to be a good estimate of the probability of traversing start. Fig. 8 therefore shows the experimentally derived relationship between probability of traversing start and cell size. A comparison of Fig. 8 with Fig. 7 reveals that neither the deterministic, the probabilistic nor the tandem model predict the relationship obtained, whereas there is good agreement between the predicted and the experimentally derived relationship between probability and size in the case of the SSC

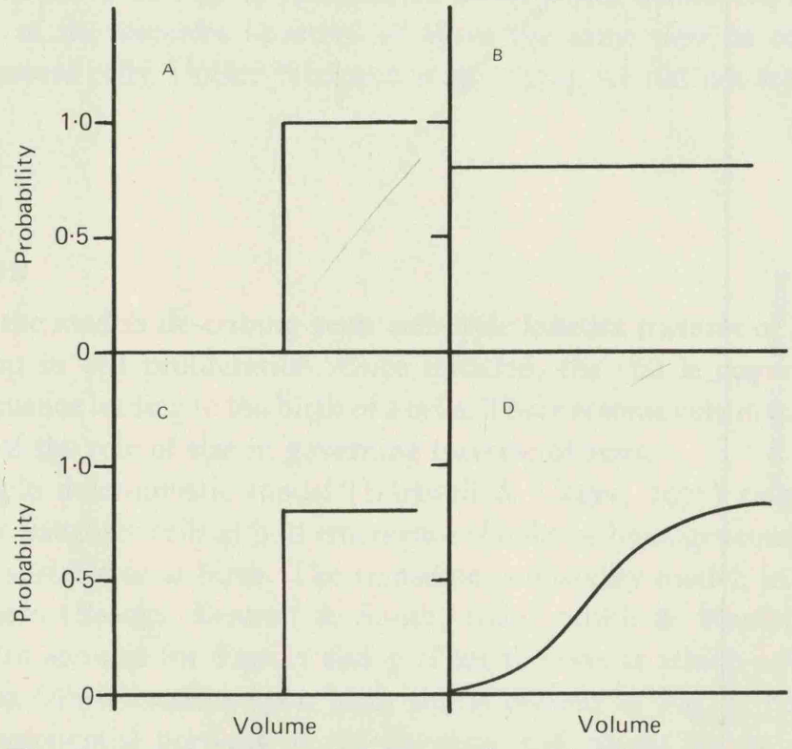

Fig. 7. The theoretical relationship between the probability of traversing start and cell size. A, the simple deterministic model; B, the simple probabilistic model; C, the tandem model; and D, the sloppy size control model.

model. A consequence of the SSC model is that the pre-start (unbudded) period should be, on average, proportional to birth size. The model can thus provide an explanation of the distribution in Fig. 5. Cells that are small at birth (most daughter cells) have long but very variable times to bud emergence. Larger daughter cells have shorter unbudded periods with less variance. The largest cells (all parent cells) have a short and relatively invariant unbudded period since they have a high probability of traversing start after division.

We conclude that any model without a size-related component is incompatible with our data set, so we reject the transition probability hypothesis completely. We also conclude that any model that does not include a variable component must also be rejected. The critical-size hypothesis would therefore have to be modified to include a large variance in the value of the critical size within a population. The

model still retains the somewhat implausible assumption of a step-function-like response of the cell as it reaches critical size. Although the tandem model comprises both probabilistic and deterministic elements it would still need further arbitrary modification (i.e. variance in critical size and different transition probability values for parent and daughter cells) to account quantitatively for our data. The SSC model is an intrinsically simpler model in good agreement with all the data, whose mechanistic basis can be easily modelled using properties of known control systems (Wheals, 1981*a*). Nevertheless there are 2 important assumptions of this model

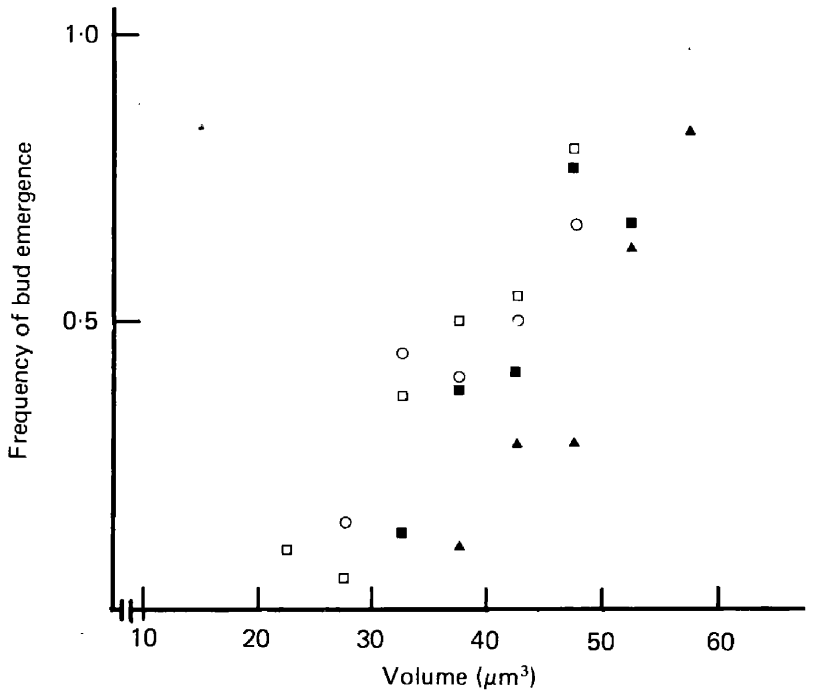

Fig. 8. The frequency of bud emergence as a function of size for each growth rate. This was calculated from the data in Fig. 4 by dividing the number of cells with newly emerged buds in a size-interval by the number of cells competent to bud, the number of cells in that size-interval plus the number of cells in preceding intervals that have not produced buds. Glucose-grown cells (▲); raffinose-grown cells (□); sorbitol-grown cells; (○); and galactose-grown cells (■).

that deserve mention. (1) We have assumed that bud emergence is a good marker for start, although detailed evidence on this point is lacking. Some of the variation we see could be occurring between start and bud emergence. (2) We have assumed that cell volume is a good measure of what the cell actually monitors. There is already evidence to show that this is not necessarily so, and thus a part of the observed 'sloppiness' could be due to a loose correlation between cell volume and what the cell monitors rather than due to an intrinsic property of the control mechanism.

It has been suggested that, for both mammalian cells and budding yeasts (Smith & Martin, 1973; Shilo, Simchen & Pardee, 1978), the rate of cell proliferation varies with growth rate solely due to alterations in the average duration of the pre-start period (as a consequence of an altered transition probability) rather than alterations in the duration of the post-start period (B phase). The yeast data have

been obtained from cells released from a block at start, using α factor or temperature-sensitive mutants, into media containing different nutrients, cycloheximide at different concentrations or rate-limiting concentrations of auxotrophic supplements (Shilo *et al.* 1976, 1977, 1978; Shilo, Riddle & Pardee, 1979). Our data from steady-state cultures give a quite different picture (Fig. 3). At slower growth rates the post-start period (initial horizontal portion of the α curves) elongates in addition to a decrease in the rate of traverse of start (a decrease in the slope of the α curves), especially for daughter cells.

A feature of Fig. 5 that is not predicted by any of the models is the observation that no daughter cells have an unbudded period less than 25 min even though some daughter cells are born at about the same size as the smallest parent cells. We

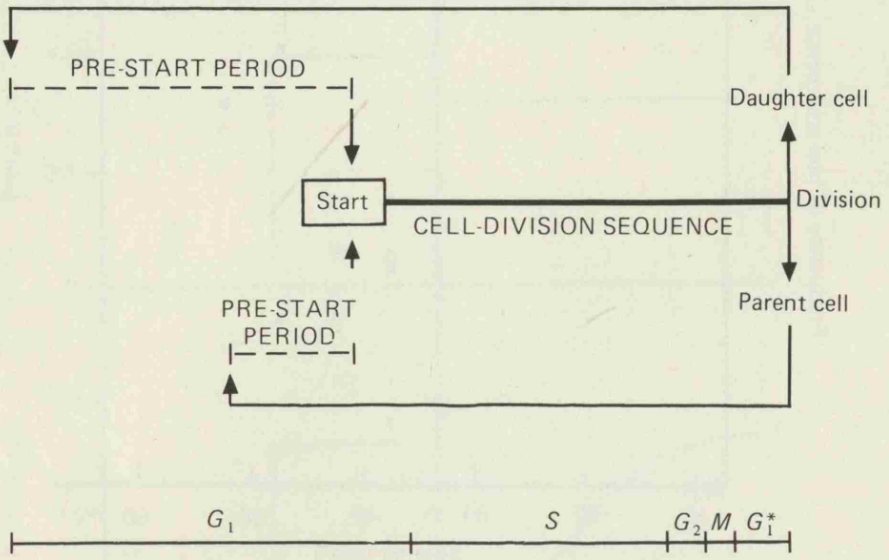

Fig. 9. Diagram of the yeast cell cycle. Illustrated are the variable phase (---); and the relatively constant phase (——) in relation to G_1, S, G_2, M and G_1* (that part of G_1 prior to cell division).

believe this represents an additional, refractory, period in the daughter cycle, so that whereas the minimum parent-cycle time is the budded period plus 2 min the minimum daughter-cycle time is the budded period plus 25 min. We have called this period G_w (for gee whizz) and it has values for glucose, sorbitol and galactose of 14, 38 and 23 min, respectively, suggesting that G_w may also be proportional to growth rate. The G_w period may be pre-start; for example, a function (possibly associated with the sizing mechanism) may have to be carried out before the sizing mechanism can operate. Alternatively it may be post-start, in which case, for example, although start has been traversed the cell has not had adequate time to synthesize enough of the enzymes necessary for post-start functions.

Although previous estimates have suggested that the budded period is of the same duration in parent and daughter cycles (Hartwell & Unger, 1977), this study clearly shows a shorter parental budded period. Since the time from nuclear migration through to cell separation is identical for both parent and daughter cells, this

indicates that bud emergence is delayed in parent cells. We suggest that this is because the previous bud has to separate from the parent cell before a new one can emerge. The signal to form a bud may have occurred but the timing is dependent on the completion of previous events. Further to this, we believe it is unreasonable to suppose that the time from start to bud emergence could be as little as 1 min (the shortest unbudded period of galactose-grown cells). Rather, a parent cell is competent to traverse start when it has separated physiologically from the daughter cell (directly analogous to the situation in *Schizosaccharomyces pombe* (Nasmyth, Nurse & Fraser, 1979; Nurse & Thuriaux, 1977). Since the onset of cytokinesis occurs about 10 min before cell separation, and membrane separation has occurred by this stage (Cabib, 1975), traverse of start could be occurring 10–20 min before bud emergence.

Smith & Martin (1973) suggested that the mammalian cell cycle comprised 2 periods. One period, the A state, is randomly variable, whereas the other period, the B phase, is relatively constant. Our data agree with this proposal, as shown in Fig. 9 (for simplicity we have omitted the G_w period since we do not as yet know its precise location). After traversing start, cells enter the cell-division sequence in which DNA synthesis, bud emergence, nuclear migration, nuclear division, cytokinesis and, ultimately, cell separation occur. This sequence is equivalent to the B phase of Smith & Martin (1973) in that it is of relatively constant duration. After division parent and daughter cells enter a variable pre-start period. The extent of the variability is different between parent and daughter cells since it is dependent on the sizes of the cells after division. Parent cells after division are of such a size that the probability of their traversing start is high. Daughter cells after division are smaller than parent cells. The smallest daughter cells have a low probability of traversing start and consequently have, on average, a long pre-start period. The largest daughter cells have a high probability so their pre-start period is, on average, short. The extent of the variability of the daughter pre-start period is thus determined by the smallest daughter cells. Exit from the pre-start period is probabilistic, as is exit from the A state of mammalian cells, but the rate (probability) of exit is determined by cell size.

REFERENCES

Brooks, R. E., Bennett, D. C. & Smith, J. A. (1980). Mammalian cell cycles need two random transitions. *Cell* **19**, 493–504.

Cabib, E. (1975). Molecular aspects of yeast morphogenesis. *A. Rev. Microbiol.* **29**, 191–214.

Donachie, W. D. (1968). Relationship between cell size and time of initiation of DNA replication. *Nature, Lond.* **219**, 1077–1079.

Fantes, P. A. (1977). Control of cell size and cycle time in *Schizosaccharomyces pombe*. *J. Cell Sci.* **24**, 51–67.

Fantes, P. A., Grant, W. D., Pritchard, R. H., Sudbery, P. E. & Wheals, A. E. (1975). Regulation of cell size and the control of mitosis. *J. theor. Biol.* **50**, 213–244.

Hartwell, L. H. (1967). Macromolecule synthesis in temperature sensitive mutants of yeast. *J. Bact.* **93**, 1662–1670.

HARTWELL, L. H., CULOTTI, J., PRINGLE, J. R. & REID, B. J. (1974). Genetic control of the cell division cycle in yeast. *Science, N.Y.* **183**, 46–51.

HARTWELL, L. H. & UNGER, M. W. (1977). Unequal division in *Saccharomyces cerevisiae* and its implications for the control of cell division. *J. Cell Biol.* **75**, 422–435.

HEREFORD, L. M. & HARTWELL, L. H. (1974). Sequential gene function in the initiation of *Saccharomyces cerevisiae* DNA synthesis. *J. molec. Biol.* **84**, 445–461.

JOHNSTON, G. C., PRINGLE, J. R. & HARTWELL, L. H. (1977). Co-ordination of growth with cell division in the yeast *Saccharomyces cerevisiae*. *Expl Cell Res.* **105**, 79–98.

KAUFFMAN, S. & WILLE, J. J. (1975). The mitotic oscillator in *Physarum polycephalum*. *J. theor. Biol.* **55**, 47–93.

KUBITSCHEK, H. E. (1971). The distribution of cell generation times. *Cell Tiss. Kinet.* **4**, 113–122.

NASMYTH, K., NURSE, P. & FRASER, R. S. S. (1979). The effect of cell mass on the cell-cycle timing and duration of *S* phase in fission yeast. *J. Cell Sci.* **39**, 215–233.

NURSE, P. & THURIAUX, P. (1977). Controls over the timing of DNA replication during the cell cycle of fission yeast. *Expl Cell Res.* **107**, 365–375.

POWELL, E. O. (1955). Some features of the generation times of individual bacteria. *Biometrika* **42**, 16–44.

PRITCHARD, R. H., BARTH, P. T. & COLLINS, J. (1969). Control of DNA synthesis in bacteria. *Symp. Soc. gen. Microbiol.* **19**, 263–297.

ROBINOW, C. F. (1975). The preparation of yeasts for light microscopy. In *Methods in Cell Biology*, vol. 11 (ed. D. M. Prescott), pp. 1–22. New York, London: Academic Press.

SHILO, B., RIDDLE, V. G. H. & PARDEE, A. B. (1979). Protein turnover and cell cycle initiation in yeast. *Expl Cell Res.* **123**, 221–227.

SHILO, B., SHILO, V. & SIMCHEN, G. (1976). Cell cycle initiation in yeast follows first order kinetics. *Nature, Lond.* **264**, 767–769.

SHILO, B., SHILO, V. & SIMCHEN, G. (1977). Transition probability and cell cycle initiation in yeast. *Nature, Lond.* **267**, 648–649.

SHILO, B., SIMCHEN, G. PARDEE, B. (1978). Regulation of cell cycle initiation in yeast by nutrients and protein synthesis. *J. cell. Physiol.* **97**, 177–188.

SMITH, J. A. & MARTIN, L. (1973). Do cells cycle? *Proc. natn. Acad. Sci. U.S.A.* **70**, 1263–1267.

WHEALS, A. E. (1981*a*). Sloppy size control of the *Saccharomyces cerevisiae* cell cycle. *Molec. cell. Biol.* (In Press.)

WHEALS, A. E. (1981*b*). The timing of events in the *Saccharomyces cerevisiae* cell cycle. In *Proc.* Vth *Int. Symp. Yeasts* (ed. G. G. Stewart). (In Press.)

WIEMKEN, A., MATILE, P. & MOOR, H. (1970). Vacuolar dynamics in synchronously budding yeast. *Arch. Mikrobiol.* **70**, 89–103.

(*Received* 3 *February* 1981)